Spring 2012

Formation of amyloid fibrils by diblock peptides

Kunal Mukesh Naik

Department:

FORMATION OF AMYLOID FIBRILS BY DIBLOCK PEPTIDES

by

KUNAL MUKESH NAIK

A THESIS

Presented to the Faculty of the Graduate School of the

MISSOURI UNIVERSITY OF SCIENCE AND TECHNOLOGY

In Partial Fulfillment of the Requirements for the Degree

MASTER OF SCIENCE IN CHEMICAL ENGINEERING

2012

Approved by

Dr. Daniel Forciniti, Advisor
Dr. Muthanna H. Al-Dahhan
Dr. Parthasakha Neogi

ABSTRACT

The objective of this study was to identify and then synthesize a series of peptides which were able to form fibrils rich in β-sheet structure and to study the effect of the presence of surfaces on their formation. We decided to focus our experimental work on a family of peptides containing one “beta-sheet forming amino acid” and one ‘alpha-helix forming amino acid'. This selection covers a wide range of hydrophillicites and charges and, by avoiding highly hydrophobic amino acids we can assure that the diblock peptides are soluble in a wide range of concentrations and solvent conditions. Three different diblocks (20:80; 50:50 and 80:20) were synthesized. The aggregation studies were done in the absence and in the presence of solid/liquid interfaces. Two types of surfaces were used: polystyrene latexes with different surface chemistry and liposomes. The rate and extent of aggregation was followed by dynamic light scattering, which was used to monitor the size of the aggregates as a function of time. Congo Red assays were performed to confirm if the aggregates were amyloidic and selected samples were inspected by optical, scanning and atomic force microscopy. Secondary structure of the fibrils was studied using FT-IR.

ACKNOWLEDGEMENTS

First, I would like to thank and express my sincere gratitude to my advisor, Dr. Daniel Forciniti, for his advice, guidance and encouragement throughout my graduate studies and particularly during this research. I dedicate this thesis to him.

I would also like to express my deepest gratitude and thank Dr. Muthanna Al-Dahhan and Dr. Parthasakha Neogi for their time and effort in serving as committee members and reviewing this thesis. Special thanks go to my colleagues for their wonderful support. This material is based upon work supported by the National Science Foundation under Grant No. 0933468.

Finally, I am very thankful to my parents for their continuous love and support.

TABLE OF CONTENTS

Page

LIST OF FIGURES

LIST OF TABLES

NOMENCLATURE

SYMBOL	DESCRIPTION
PC	Phosphatidylcholine
PS	Phosphatidylserine
C	Cholesterol
PG	Phosphatidylglycerol
PE	Phosphatidylethanolamine
Ile	Isoleucine
Lys	Lysine
Glu	Glutamic acid
Leu	Leucine
PS	Polystyrene
PS-NH_2	Polystyrene amino
PS-OH	Polystyrene hydroxylate
PS-COOH	Polystyrene carboxylate
FT-IR	Fourier Transform Infrared Spectroscopy
DLS	Dynamic Light Scattering

1. INTRODUCTION

Amyloid fibrils are proteinaceous deposits associated with a variety of human diseases like Alzheimer (AD), islet amyloidosis, type two diabetes, systemic amyloidosis, transmissible spongiform encephalopathy, Parkinson disease, familial amyloid polyneuropathy etc. (Sousa and Saraiva, 2003) The impact of amyloid fibrils on human health is yet to be fully recognized (Dentchev *et al.*, 2003). Amyloid diseases are apparently unconnected; however, intermolecular secondary structure (mostly β-sheets) is present in all amyloid aggregates. Although the proteins involved in the different types of fibrils lack homology, the morphology of the deposits is remarkable similar (Sunde and Blake, 1997, Blake *et al.*, 1996, Blake and Serpell, 1996). Some experimental findings support the universality of amyloid fibrils formation (Koga *et al.*, 2003, Sunde *et al.* 1998) whereas others contradict it (Kirschner, 1996, Inouye *et al.*, 1993, Come *et al.*, 1993).

Amyloid deposits associated with Alzheimer disease, AD, are well studied. Amyloid β protein residue 1-42 is the most abundant peptide found in these deposits. An AMF micrograph of fibrils produced by amyloid β 1-42 obtained in this laboratory is shown in Figure 1.1.

AD plaque contains advanced glycosylation end products (Muench *et al.*, 2003ab, Deuther-Conrad, 2001, Loske *et al.*, 2000, Munch *et al.*, 1998) cooper iron (Munch *et al.*, 1998), amyloid Aβ(1-40), τ-protein, neuronal thread proteins, apolipoprotein E, glycosylated acetylcholinesterase, serum amyloid P, etc. For a review, see Mulder *et al.* (2000). It has been suggested that some of the non-fibrillar components enhance local densities of fibril entanglements.(MacRaild *et al.*, 2004) There is a lack of correlation between the extent of plaque formation and the severity of AD symptoms. Current evidence suggests that precursors of the deposits such as oligomers and protofibrils are the toxic species (Chiti *et al.*, 2006). Most likely, toxicity is the result of a combination of effects (Hall, 2008).

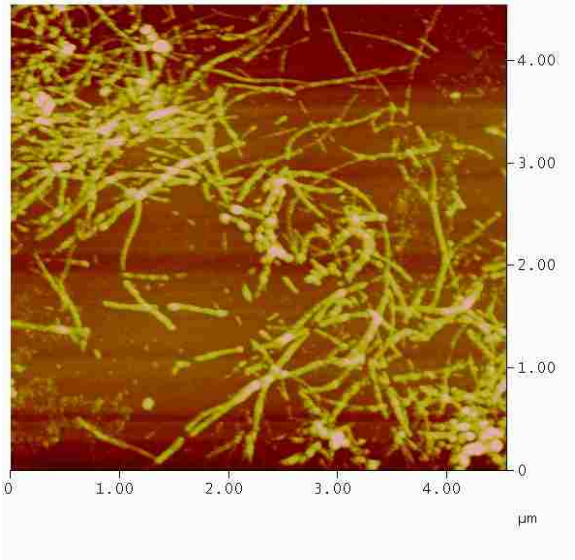

Figure 1.1. Atomic force microscope micrograph of fibrils formed by amyloid αβ 1-42. The concentration was 0.8 mg/mL at pH 7 incubated at room temperature for 4 days.

Model compounds have been used to study the formation of amyloid deposits in a controlled manner and to address the question: Are all proteins capable of forming amyloid deposits? There are several reports using peptides or peptides mimics. A few of examples are discussed in the following paragraphs.

Lashuel *et al.* (2000) used a peptidomimetic compound that self-assembles into polymorphic β-sheet quaternary structures, including protofilaments, filaments, fibrils, and ribbons that resemble the highly ordered structures displayed by the amyloidogenic peptides Aβ, calcitonin, and amylin. Another example is found in the work of Kortemme *et al.* (1998) who designed a 20-residue peptide that forms amyloid type of structures. Banerjee *et al.* (2004) designed several blocked tripeptides containing aminocaproic acid that also form amyloid fibrils. Koga *et al.* (2003) studied the self-assembly of poly(γ-methyl-L-glutamate) grafted polyallylamine(1) in water-222-trifluorethanol and found that at a particular pH, salt concentration, and solvent composition the peptide forms fibrils rich in β-sheets. They used this evidence to suggest that the formation of fibrils is a universal phenomenon (i.e., it is not associated with a particular sequence). Symmons *et al.* (1997) followed an interesting approach for the study of the structure of amyloid

fibrils. They first found that a 23 amino-acid-long peptide having a single Leu-rich repeat polymerizes in solution yielding a β-sheet structure but a variant in which an Asn residue was replaced by Asp does not form fibrils. Another variant in which Asn are replaced by Gln yields the β structure. They argued that hydrogen bonding can be used to explain their findings. They concluded that the tendency to forming fibrils (and β structure) goes beyond the known "pathogenic" proteins and extent to protein domains (in general). Janek *et al.* (1999) used model peptides to study the influence of peptide length and concentration and D/L-amino acid substitution on fibril formation. The problem with their approach is that all of their peptides have a central β-sheet forming domain; therefore, these results, because of the "bias" included in their model compounds, cannot be used to prove that the formation of amyloid deposits is a universal phenomenon. Most of the model peptides used are reasonable small (less than 30 residues). This has important practical consequences for this work. The peptides to be used in this work will be prepared by solid-state synthesis whose yield decreases and the polydispersity of the product increases as the length of the peptide increases.

Different chemistries and a variety of incubation conditions have been used for the production of fibrils using polypeptides. For example, Hong *et al.* (2003) used 16-residues peptides consisting of alternating hydrophobic (alanine) and hydrophilic (lysine and glutamic acid) amino acids. Peptide concentration was 0.1 mg/mL and the pH range was from 4 to 11. The rationale for the selection of peptides was that peptides made of polar and non-polar amino acids are capable of forming β sheets structures. Factors that affected self-assembly were amino acid sequence, concentration of peptides molecular size, pH, temperature and ionic strength. Giri *et al.* (2007) made fibrils using the homopeptides $Ala_{11,}$ Ala_7 and Ala_{17} at pH 11 and incubated at room temperature for a period of 20 days. Klunk *et al.* (1989) used poly-L-lysine at a concentration of 10μg/mL at ph 11 and temperature of 50 ^{o}C. The incubation time was only 10 min. They also used poly-L-serine at pH 7.4. Fandrich and Dobson (2002) made fibrils using a) poly lysine at 2.5mg/mL in water at pH 11.2 at 65C for 4 days; b) poly glutamic acid at 1 mg/mL in water at pH 4 at 65 C for 2 days; and c) poly threonine 10mg/mL in water at pH 9 at 65C for 4 days. The same peptides needed to be incubated at room temperature for period of six weeks to obtain fibrils. Tjernberg *et al.* (1998) made fibrils using a family of

multiblock peptides using lysine, leucine, valine, phenyl- alanine, glutamine, alanine, glutamic acid and aspartic acid. The peptides were dissolved in 50 mM tris buffer at pH 7.5 and incubated at 37C for 3 days. Use of high temperatures and extreme pHs (with some exceptions) has been common. The incubation time varies from a few hours to weeks. Peptide concentration ranges from μg/mL to several mg/mL. All these examples were taking into consideration in our experimental design.

The effect of surfaces on the formation of the deposits remains obscure in spite of the large amount of published material (Giacomelli and Norde, 2003, Moores, 2011, Ruschak and Miranker, 2007). It is generally accepted that the effect of the presence of a solid/liquid interface affects the ability of peptides to form amyloid deposits and the mechanism of amyloid formation, particularly the nature and concentration of surfaces (Gorbenko and Kinnunen, 2006). Surfaces that mimic cell membranes, tissue surfaces and charged surfaces seems to be preferred. Surfaces may provide nucleation sites for fibril formation. The concentration of amyloid peptides in healthy or sick tissue is of the order of a few nano-moles per liter. Therefore, the presence of a liquid/solid interface may serve as a crowding agent that "catalyses" the formation of the aggregates affecting either the thermodynamics (equilibrium) or kinetic aspects of fibril formation. Absorption of the peptides on the solid surface may actually decrease their concentration in bulk inhibiting aggregation if the concentration of peptides is not high enough.

The primary objective of this work was to study the formation of fibrils by a family of diblock peptides in the presence and in the absence of solid/liquid interfaces. The choice of interfaces covers a range of inorganic surfaces with different surface chemistry and a family of liposomes with different charges and membrane fluidity. The formation of fibrils was followed by several methods simultaneously because it is know that the use of a single method may lead to false positives. The chosen techniques were a colorimetric assay, Congo Red, (Mahler *et al.* 200, Klunk *et al.*, 1989); FTIR (which is used to quantify the relative amounts of α helix and β sheets in proteins and protein aggregates); optical microscopy (to obtain some gross visual confirmation of the formation of fibrils); and either SEM, TEM or AFM to confirm some of the structures. The data is somehow fragmented because we tried to explore a very broad experimental data base.

2. MATERIALS AND METHODS

2.1 MATERIALS

Dimethylformamide (DMF) and trifluoracetic acid (TFA) were purchased from Acros organics, HBTU (O-Benzotriazole-N,N,N',N'-tetramethyl-uronium-hexafluoro-phosphate), the FMOC protected amino acids and the Wang resin were purchased from CS Bio, Menlo California, diisopropylethylamine (DIEA) was purchased from Fisher Scientific, ethyl ether, dichloromethane (DCM) peptide synthesis grade was purchased from Fisher Scientific. 99% piperidine, potassium bromide (KBr), Congo red dye, Calcein dye and Sephadex G-50 (bead size 20-50μm) were purchased from Sigma-Aldrich, Saint Louis. Calcium fluoride (CaF_2) Windows were purchased from (International Crystal Labs, Garfield, NJ). Polystyrene (PS) (diameter: 107 nm; concentration 2.64 w/v %), polystyrene amino ($PS\text{-}NH_2$) (diameter: 193 nm, concentration: 2.63 w/v %), polystyrene hydroxylate (PS-OH) (diameter: 193 nm, concentration: 2.63 w/v %) and polystyrene carboxylate (PS-COOH) (diameter: 107 nm, concentration: 2.57 w/v %) latexes were purchased from Polysciences Inc. Warrington, PA. L-α- Phosphatidylcholine (PC) from egg yolk (~99% pure), L-α- Phosphatidyl-L-serine (PS) from Glycine max (soybean), L-α-Phosphatidyl-DL-glycerol (PG), L-α-Phosphatidylethanolamine (PE) from egg yolk (~98% pure) and cholesterol (~99% pure) were purchased from Sigma (St. Louis, MO, USA). All chemicals were used as received without further purification.

2.2 METHODS

2.2.1 Peptide Synthesis. A CS Bio 336 peptide synthesizer was used for synthesizing peptides. A HBTU solution was prepared by dissolving 19 g of HBTU in 100 mL of DMF. 20% piperidine solution was prepared in DMF. 0.5 g of Wang resin was measured and added to the reactor. 1mmole of the desired amino acid was weighted and added to vials which were sealed and arranged as per required sequence into the wheel of the peptide synthesizer. The synthesis of a 10 residues peptide takes about 24 hr. whereas the synthesis of a 20 residues peptide takes 46 hours.

After the synthesis, the peptide was recovered from the reactor by adding generous amounts of DCM. The suspension was swirled and passed through a disposable

syringe having a filter at the other end. The residue was then dried under vacuum for 20 minutes. The peptide was cleaved from the dried resin using a 95% TFA / 5% water mixture and left in a sonicator for 40 min. Crushed ice was added to the sonicator to keep the temperature low; sonication increased the yield of peptide by 15 to 20 %.Then the cleaved mixture was passed through the same filter and the filtrate was directly precipitated in 30 mL of ice cold diethyl ether. The precipitate was centrifuged in a refrigerated centrifuge (RC-3B Refrigerated centrifuge, Soverall Instruments) at 4000 rpm, -5ºC for 30 min. The pellet was re-suspended in 20mL of fresh ether and centrifuged again. Then the supernatant ether was removed and the pellet was air dried under a laminar flow hood. The peptide was dissolved in 5mL of 0.010 M acetic acid and freeze-dried using a Labconco freeze dry system.

2.2.2 Liposome Preparation. The liposomes were prepared by freeze drying (Li and Deng, 2004) 20 mg total of lipid (must be lower than 30 mg/mL total) was dissolved in 1 mL of tert-ButylAlcohol (tBA). 150 mg of sucrose (must be 7.5 times the amount of lipid per weight. The addition of sucrose helps determining size) was dissolved in 1 mL of water. The two solutions were mixed at a volume ratio between 1:1 and 1:2. The mixture should be optically clear. To ensure proper mixing, the mixture was sonicated sometimes for 30 seconds. The solution was then filtered through a 0.22 µm filter into a 10 mL vial. The sample was then freeze-dried by freezing for 8 hours and drying for as long as it takes to dry. After drying the sample was stored in the freezer.

2.2.3 In Vitro Fibril Formation. Peptides solutions were prepared at a concentration of 0.1 % (1mg/mL). All buffers used were filtered with Whatman 0.22 µm filters. Bulk peptides and peptides in the presence of various surfaces were incubated at a temperature of 60º C for a period of up to 12 days (Hong *et al*, 2003, Giri *et al.*, 2007). The incubation of peptides was carried out at pH 4, 7 and 9. 0.1 % (1mg/mL) of peptide solutions at pH 4 and 7 were prepared and 2µL of 0.06 mg/mL of liposomes and 2.6mg/mL of polystyrene nanosphere surfaces were added to each cuvette. Dynamic light scattering readings were taken in a FOQELS particle size analyzer (Brookhaven Instruments Corporation, Holtsville, NY).

2.2.4 Congo Red Assay. A stock solution of Congo red dye was made by adding 7mg of dye to 1 mL of buffer Solution (150mM NaCl, 5mM KH_2PO_4, pH 7.40). A

Hitachi U2900 UV Spectrophotometer was used for wavelength scans. 1 mL of buffer was placed in a disposable cuvette and to it 5µL of Congo red dye from stock solution was added and the spectrum was recorded from 700nm to 300 nm. To the same cuvette 10µL of a peptide sample which has to be tested was added and the spectrum was recorded again. A red shift in the peak indicates the presence of amyloid fibrils.

2.2.5 Optical Microscopy. Samples which were found positive in Congo red tests were visually analyzed in a compound microscope. A 20µL sample was placed on top of a glass slide and covered with a cover slip. After 10 minutes it was viewed under an Olympus CKX-41 microscope. Images were taken using an Altra-20 camera. Some samples, which were found to be positive in Congo red, were centrifuged (Eppendorf 5810R centrifuge) at 4000 rpm for 20 min. The pellets formed were then suspended in 500µL of nanopure water and viewed under the microscope.

2.2.6 Atomic Force Microscopy and Scanning Electron Microscopy. Some samples were viewed using Scanning electron Microscopy (SEM) and Atomic Forced Microscopy (AFM). The SEM images were taken using a Hitachi S-4700 FESEM. Silicon wafers were cut using a diamond tipped cutter. The wafers were then cleaned thoroughly using the following protocol. 40 mL of 1% alconox solution was taken in a beaker the disks were each held & moved around 4-5 times in it with the help of sharp tweezers. The disks were then washed with deionised water. They were then dropped in 5% HF solution for 3 min. and then they were taken out and swirled around 4-5 times in a beaker containing deionised water. The disks were allowed to dry under a laminar flow hood. Approximately 15 µL of sample was dried on each silicon wafer under a laminar flow hood. Samples for SEM were dried on silicon wafers first and then coated with a carbon film to make the samples conducting. The scan size of the area ranged from 13.3µm to 1.75µm with a scan rate of 1.001 Hz. AFM imaging was carried out in tapping mode at room temperature.

2.2.7 FT-IR Analysis. Analysis of all the peptides and amyloid fibril samples was done in a Thermo Scientific Nicolet 6700 FTIR. IR scans of the peptides were done in solid state as well as in liquid state. In the solid state process 1mg of the sample to be analyzed was mixed with 50mg of KBr, the mixture was thoroughly crushed using a mortar and pestle. The powder was compressed using a press to form a pellet. The sample

chamber of the FTIR was purged with dry, CO_2 free, air for 5 minutes before and after loading the sample. 16 scans were taken at a resolution of 2 cm^{-1}. CaF_2 windows were used for liquid samples. Background was collected using only the CaF_2 windows. Approximately 20µL of sample was then dried on these windows and then IR scans was taken (Fandrich and Dobson, 2002; Kong and Yu, 2007; Nilsson, 2004)

2.2.8 Dye Leakage Experiments. Two buffers, A and B were prepared. Buffer A consisted of 1 mmol (142 mg) Na_2HPO_4 in 100 mL nanopure water and its pH was adjusted to 7 by adding 0.1M NaOH. Buffer B was made from 10 mmol (1.42 g) Na_2HPO^4 and 90 mmol (5.26 g) NaCl in 1L of nanopure water. 249 mg of calcein was dissolved in 10 mL of buffer A. 0.1 M NaOH was added drop by drop until calcein was completely dissolved and then the pH was adjusted to 7. Liposomes were hydrated in 1mL of calcein dye. The suspension was then stirred using a magnetic stirrer for 1 hour. Later the suspension was subjected to five freeze-thaw cycles. During each cycle freezing was done using a dry ice- acetone mixture and thawing with water at room temperature. Then the dye loaded liposome suspension was extruded twice using a 0.45 µm Whatman filter. The dye filled liposomes were separated from the excess dye using size exclusion chromatography. A BioLogic LP chromatography system (Bio-Rad Laboratories, Inc.) was used with a Sephadex G-50 column (length: 30 cm, diameter: 2cm) and 10 mmol phosphate buffer at pH 7 containing 90 mmol NaCl as eluent. Sample's size was 1 mL. 1 mL fractions were collected for the dye leakage experiments. Leakage induced by peptides was monitored by recording increased in intensity of calcein fluorescence.10µL each of peptide solution and dye filled liposomes were added to 200µL of buffer B in a 96 well plate (Fisher Scientific). Triton-X (20% in DMF) was added to liposomes to measure intensity for 100% leakage. Fluorescence intensity was measured in a Fulostar optima fluorescent plate reader with excitation wavelength 490nm and emission wavelength 520nm after 600 seconds.

3. RESULTS AND DISCUSSIONS

To identify and then synthesize a series of peptides that form aggregates rich in β-sheet structure will be like finding a needle in a haystack. How long the peptides should be? What amino acids should be used to build them? Although it is known that Ala, Leu, Met, Phe, Glu, Gln, Lys, Arg, and His have α-helix preference whereas Tyr, Trp, Ile, Val, Thr, and Cys have β-sheet preference, what sequence of amino acids is the appropriate one? Two approaches have been followed to solve this puzzle: 1) identification of a particular amino acid (Tartablia *et al.*, 2005) by the statistical analysis of protein sequences that form amyloid deposits (Tartablia *et al.*, 2005) and 2) the use of homo-peptides (Blondelle *et al.*, 1997). Although some particular sequences have been identified as β-sheet structure forming, it is impossible to say how many of those sequences exist. It has also been found that homopeptides of alanine (plus two terminal lysines) form amyloid type of aggregates. This in spite of the fact that alanine is an amino acid found preferentially in α-helices and whose presence in sequences associated with amyloid formation is rare (Tartablia *et al.*, 2005). The hypothesis of those using homopeptides is that all amino acids are able to form amyloid type of aggregates under the appropriate conditions. We have decided to take a pragmatic approach by using diblock polypeptides. We argue that diblock polypeptides resemble protein surface patches and thus they are better protein mimics than homopeptides or alternated block peptides. We decided to focus our experimental work on a family of peptides containing one "β-sheet forming amino acid" (Ile) and one 'α-helix forming amino acid' (Glu or Lys). In some experiments, Ile was replaced by leu that is an amino acid frequently found in α helices. This selection covers a wide range of hydrophillicites and charges and, by avoiding highly hydrophobic amino acids (tryptophan or phenylalanine) we can assure that the diblock peptides will be soluble in a wide range of concentrations and solvent conditions. Peptides were synthesized in two different lengths (10 and 20 amino acids) and different diblocks lengths.

Experiments aimed at the formation of fibrils were conducted with bulk peptides and with peptides near solid/liquid interfaces. A list of peptides used in this work is

shown in Table 1. More than one type of test was performed to assess the formation of amyloid type of fibrils.

Table 3.1. Peptides.

$(Ile)_{10}$-b-$(Lys)_{10}$	$(Ile)_7$-b-$(Lys)_3$	$(Ile)_7$-b-$(Glu)_3$	$(leu)_7$-b-$(Lys)_3$
$(Ile)_8$-b-$(Lys)_{12}$	$(Ile)_6$-b-$(Lys)_4$	$(Ile)_6$-b-$(Glu)_4$	$(Leu)_5$-b-$(Lys)_5$
$(Ile)_5$-b-$(Lys)_{15}$	$(Ile)_5$-b-$(Lys)_5$	$(Ile)_5$-b-$(Glu)_5$	
$(Ile)_9$-b-$(Lys)_1$	$(Ile)_4$-b-$(Lys)_6$	$(Leu)_9$-b-$(Lys)_1$	
$(Ile)_8$-b-$(Lys)_2$	$(Ile)_2$-b-$(Lys)_8$	$(Leu)_8$-b-$(Lys)_2$	

3.1 BULK PEPTIDES. A preliminary screening was done with 16 different peptides in the absence of solid/liquid interfaces. The peptides were all diblock peptides either 10 or 20 amino acids in length. The peptides were incubated at pH 4, 7 and 9 over a period of up to two weeks.

The ability of the peptides to form structures rich in β-sheet structure was determined by the Congo red assay. The Congo red dye binds specifically to β-sheets which results in a red wavelength shift of the scans (Klunk *et al.,* 1989*).* Samples incubated at pH 7 and 9 did not form amyloid fibrils but some incubated at pH 4 did (Table 2). The following peptides formed fibrils when incubated at pH 4: $(Ile)_{10}$-b-$(Lys)_{10}$, $(Ile)_5$-b-$(Lys)_5$, $(Ile)_8$-b-$(Lys)_{12}$, $(Ile)_7$-b-$(Lys)_3$ and $(Ile)_6$-b-$(Lys)_4$. A representative spectra-shift graph is shown in Figure 3.1. The remaining spectra are included in Appendix A.

Table 3.2. Preliminary screening of fibril formation by several peptides. The incubation time was 7 days.

Peptide	Fibril Formation	Peptide	Fibril Formation	Peptide	Fibril Formation
$(Ile)_{10}$-b-$(Lys)_{10}$	+				
$(Ile)_8$-b-$(Lys)_{12}$	+				
$(Ile)_5$-b-$(Lys)_{15}$	-				
$(Ile)_9$-b-$(Lys)_1$	-			$(Leu)_9$-b-$(Lys)_1$	-
$(Ile)_8$-b-$(Lys)_2$	-			$(Leu)_8$-b-$(Lys)_2$	-
$(Ile)_7$-b-$(Lys)_3$	+	$(Ile)_7$-b-$(Glu)_3$	-	$(leu)_7$-b-$(Lys)_3$	-
$(Ile)_6$-b-$(Lys)_4$	+	$(Ile)_6$-b-$(Glu)_4$	-		
$(Ile)_5$-b-$(Lys)_5$	+	$(Ile)_5$-b-$(Glu)_5$	-	$(Leu)_5$-b-$(Lys)_5$	-
$(Ile)_4$-b-$(Lys)_6$	-				
$(Ile)_2$-b-$(Lys)_8$	-				

Peptides containing less than 40% (mol %) or more than 70 % Ile did not form fibrils. Replacing of isoleucine by leucine (5^{th} column) and/or lysine by glutamic acid (3^{rd} column) inhibited the formation of fibrils. Isoleucine is a positional isomer of leucine, the branching at the β-carbon tends to increase its bulkiness and thus its hydrophobicity. Leucine is less hydrophobic (hydrophobic index: 2.2) than isoleucine (hydrophobic index: 3.1) and it shows a preference for being within α-helices more so than in β strands. Therefore (and in spite of their subtle structural differences), it is somehow expected that the replacement of isoleucine by leucine may inhibit the formation of fibrils, as observed. Lysine has an isoelectric point of 9 and glutamic acid an isoelectric point of 4 but they are both present in α helices. Peptides containing Lys form fibrils at pHs away from the isoelectric point (~ 9) of the amino acid. Therefore, we expected that peptides containing glutamic acid would form fibrils at basic pHs (the isoelectric point of the glutamic block would be ~ 4). We did not observe that. There is

some evidence (Fandrich and Dobson, 2002) that suggests that fibrils may be formed at pHs near the isoelectric point of homopeptides. It seems that the behavior of diblock peptides is quite different.

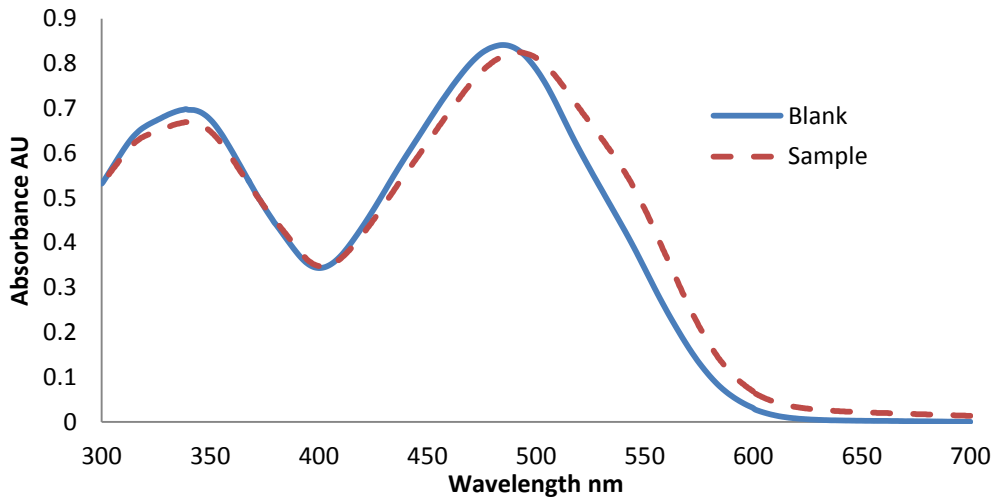

Figure 3.1. Congo red scan for $(Ile)_7$-b-$(Lys)_3$in bulk.

Table 3.3. Shorter incubation times for selected diblock peptides.

Time / Peptides	12 Hrs.	24 Hrs.	36 Hrs.	48 Hrs.	60 Hrs.	72 Hrs.
$(Ile)_{10}$-b-$(Lys)_{10}$	-	-	+	+	+	+
$(Ile)_5$-b-$(Lys)_5$	-	-	-	-	-	+
$(Ile)_6$-b-$(Lys)_4$	-	-	-	-	-	+
$(Ile)_7$-b-$(Lys)_3$	-	-	-	-	-	+
$(Ile)_8$-b-$(Lys)_{12}$	-	-	+	+	+	+

The experiments were extended to shorter incubation times in an attempt to capture kinetic differences between those peptides that yield fibrils after an incubation time of one week. Table 3.3 summarizes the results. For a given length, the fibrillation lag time seems to be constant. Fibrillation of longer peptides occurs faster than of shorter peptides (36 hrs. vs. 72 hrs. lag time). It is worth to notice that all experiments were done with the same peptide concentration on a mass base. Therefore, the concentration of the large peptides by mole is roughly one half the concentrations of the short peptides. Considering that aggregation is proportional to the number of moles of the species that aggregates this result is odd unless the formation of fibrils in the longer peptides is favored by a larger content of secondary structure. This was tested by FTIR.

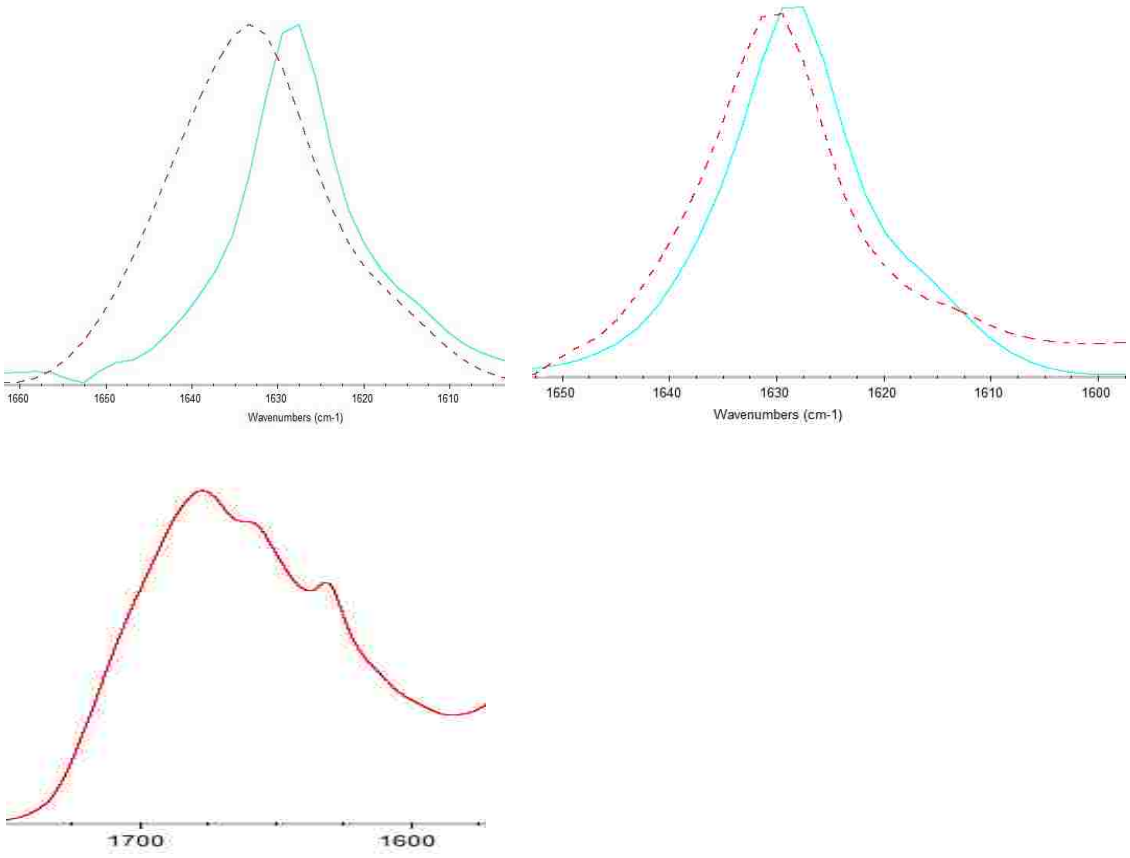

Figure 3.2. FTIR scans for upper left: $(Ile)_7$-b-$(Lys)_3$, upper right: $(Ile)_{10}$-b-$(Lys)_{10}$ lower left: $(Ile)_5$-b-$(Lys)_{15}$. In the upper panels the dotted line corresponds to the peptide before incubation and the solid lines to the peptide after incubation. The lower panel is for the peptide after incubation.

A single test is not sufficient to assess the formation of amyloid fibrils. FTIR spectroscopy may be used to determine the secondary structure of peptides. Characteristic bands found in the infrared spectra of proteins and polypeptides include the Amide I and Amide II. The wavelengths assignments for various secondary structures in the Amide l band are: (a) side chains: from 1600 to 1620 cm^{-1}, (b) β sheets: from 1620 to 1640 cm^{-1} , (c) α helices: from 1645 to 1660 cm^{-1} , (d) random coil: from 1660 to 1680 cm^{-1} , and (e) β turns from 1680 to1690 cm^{-1}.

Figure 3.2 shows the red shift of the amide I band, which is characteristic of β sheet structure. FTIR scans for peptide samples which did not show presence of amyloid fibrils have peaks at 1680 cm^{-1} and 1650 cm^{-1}, which correspond to α helices and β turns. Tables 3.4 and 3.5 below show the percentage of β sheets, α helices, random coils, β turns and side chains in the Amide I band of the spectra of several peptides.

Table 3.4. Secondary structure content of selected peptides before incubation.

Peptide	**% of β Sheets**	**% of α Helix**	**% of Random Coil**	**% of β turns**	**% of Side Chain**
$(Ile)_7$-b-$(Lys)_3$	49.5	3.3	5.4	32.5	9.3
$(Ile)_6$-b-$(Lys)_4$	45.7	12.5	10.9	20.0	10.9
$(Ile)_5$-b-$(Lys)_5$	40.6	18.0	-	37.2	4.3
$(Ile)_{10}$-b-$(Lys)_{10}$	38.5	5.6	14.2	24.8	16.8
$(Ile)_8$-b-$(Lys)_{12}$	38.1	4.0	18.4	22.6	16.1
$(Ile)_5$-b-$(Lys)_{15}$	21.0	35.1	-	36.5	7.4

Table 3.5. Secondary structure content of selected peptides after incubation for 12 days at 60 ^{o}C and a pH of 4.

Peptide	% of β Sheets	% of α Helix	% of Random Coil	% of β turns	% of Side Chain
$(Ile)_7$-b-$(Lys)_3$	65.7	3.9	10.0	11.8	8.5
$(Ile)_6$-b-$(Lys)_4$	63.4	4.9	9.2	13.0	9.4
$(Ile)_5$-b-$(Lys)_5$	73.5	-	9.0	9.9	7.6
$(Ile)_{10}$-b-$(Lys)_{10}$	73.4	1.7	-	15.4	9.4
$(Ile)_8$-b-$(Lys)_{12}$	46.7	2.9	14.6	25.6	9.9
$(Ile)_5$-b-$(Lys)_{15}$	29.4	19.7	22.5	19.1	9.3

There is a significant increase in β-sheet content after incubation. Also, samples that formed fibrils show significantly higher quantities of β sheets and β turns. For example, $(Ile)_{10}$-b-$(Lys)_{10}$ (a fibril forming peptide) contains approximately 80% β sheets and β turns whereas $(Ile)_5$-b-$(Lys)_{15}$ which was negative showed low content (approximately 50%) of β sheets and β turns. These findings were similar to those reported in (Krebs *et al.* 2004). Notice that $(Ile)_5$-b-$(Lys)_{15}$ before incubation has a very low β sheet and β turn content. Table 3.4 also shows that the shorter peptides have a higher β sheet and β turn but a lower random coil content than the longer peptides. It seems to suggest that more disorganized peptides form fibrils more readily. This is consistent with the fact that fibril formation is induced in native proteins by subjecting them to very harsh (denaturing) conditions.

3.2 PEPTIDES IN THE PRESENCE OF SOLID/LIQUID INTERFACES

Data in the presence of solid/liquid interfaces was taken after 5, 10 and 15 days. The pH was either 4 or 7 and the incubation temperature was 60 ^{o}C. Fibrillation did not take place at pH 7. The results at pH 4 are summarized in Table 3.6. We have included the bulk data as a reference.

Table 3. 6. Formation of fibrils in the presence of solid/liquid interfaces.

Peptides and incubation times / Surfaces		Bulk	Polystyrene	PS- COOH	PS- OH	PS- NH_2	80/20:PC/PS	80/20:PC/C	80/20:C/PC	2:2:1:1 C/PC/PG/PE	10:5:7.5:16 PC/PE/PS/C
$(Ile)_{10}$-b-$(Lys)_{10}$	5days	+	+	+	+	+	+	+	+	+	+
	10	+	+	+	+	+	+	+	+	+	+
	15	+	+	+	+	+	+	+	+	+	+
$(Ile)_5$-b-$(Lys)_5$	5days	+	-	-	-	-	-	-	-	-	-
	10	+	+	+	+	+	-	+	+	-	-
	15	+	+	+	+	+	-	+	+	-	-
$(Ile)_6$-b-$(Lys)_4$	5days	+	-	-	-	-	-	-	-	-	-
	10	+	+	+	+	+	-	+	+	-	-
	15	+	+	+	+	+	-	+	+	-	-
$(Ile)_7$-b-$(Lys)_3$	5days	+	-	-	-	-	-	-	-	-	-
	10	+	+	+	+	+	-	+	+	-	-
	15	+	+	+	+	+	-	+	+	-	-
$(Ile)_8$-b-$(Lys)_{12}$	5days	+	+	+	+	+	+	+	+	+	+
	10	+	+	+	+	+	+	+	+	+	+
	15	+	+	+	+	+	+	+	+	+	+
$(Ile)_8$-b-$(Lys)_2$	5days	-	-	-	-	-	-	-	-	-	-
	10	-	-	-	-	-	-	-	-	-	-
	15	-	-	-	-	-	-	-	-	-	-
$(Ile)_2$-b-$(Lys)_8$	5days	-	-	-	-	-	-	-	-	-	-
	10	-	-	-	-	-	-	-	-	-	-
	15	-	-	-	-	-	-	-	-	-	-

(PC=phosphatidylcholine; PS: phosphatidylserine; C: cholesterol; PG: phosphatidylglycerol; PE: phosphatidylethanolamine)

The presence of a solid/liquid interface does not affect the ability of large diblock peptides to form fibrils. Short peptides formation of fibrils is inhibited by both liposomes and latex. In the presence of surfaces, the twenty-residues peptides $(Ile)_{10}$-b-$(Lys)_{10}$ and $(Ile)_8$-b-$(Lys)_{12}$ were found to give positive Congo red test on the fifth day whereas 10

chain peptides $(Ile)_5$-b-$(Lys)_5$, $(Ile)_7$-b-$(Lys)_3$ and $(Ile)_6$-b-$(Lys)_4$gave positive results on tenth day. This is similar to the observed trend in bulk in which the shorter peptides showed a longer lag time. The effect of surface seems to be independent of surface chemistry and surface charge. The peptides are all positively charge at pH 4. The latex surface varies from a strong negative charge in the case of bare PS (isoelectric point ~ 2) to positively charged in the case of PS-NH_2. The only common feature of the latexes is the fact that all decrease the available volume causing an increase in the concentration of the peptides; particularly in the case in which the peptide and the latexes have the same type of charge. It is possible that different mechanisms are responsible for the apparent inhibitory effect of the latex. Liposomes containing phosphatidylethanolamine, phosphatidylglycerol, and phosphatidylserine inhibit the formation of fibrils. Our hypothesis in the case of those surfaces which inhibited fibril formation is that the peptides had infused into the liposomes and therefore they are not available for fibrillation. In order to conform this we carried out a series of dye leakage experiments in which liposomes were loaded with a fluorescent dye.

We attempted to follow the aggregation process by dynamic light scattering. Measurements were done immediately after sample preparation and after 4, 8 and 12 days. After 8 and 12 days most of the fibrils precipitate out and therefore the data is not very reliable. The complete data set is included in Appendix D. Each experiment has been done in duplicate; therefore, only data for which the correlation functions of both samples are comparable will be discussed below. We recognize that DLS has been used in the past (Mahler *et al., 2008*) for the monitoring of protein aggregation. However, we consider that most of that data may not be reliable because of intrinsic inconsistencies between duplicates caused by the somehow random aggregation processes. In the panels of Figures 3.3 through 3.6 we present time correlation functions for the peptides $(Ile)_{10}$-b-$(Lys)_{10}$ and $(Ile)_5$-b-$(Lys)_5$ after incubation in the presence of various liposomes and inorganic surfaces. Blanks are also included.

The bare latex was quite stable up to 8 days (Figure 3.3, panels e and f). Aggregates are present after four days for the larger peptide in PS-NH_2 (panel c). They are less evident for the shorter peptides (panel a). The sharp decay shown in panel (f) (blank) remains unaltered for the larger peptide (panel d). The decay is slower for the

smaller peptide in PS-OH (panel b). These results are somehow at odds with the results from Congo red that suggest that the presence of the latex prolongs the lag time for the formation of fibrils for the short peptide but has no effect on the aggregation of the longer peptide.

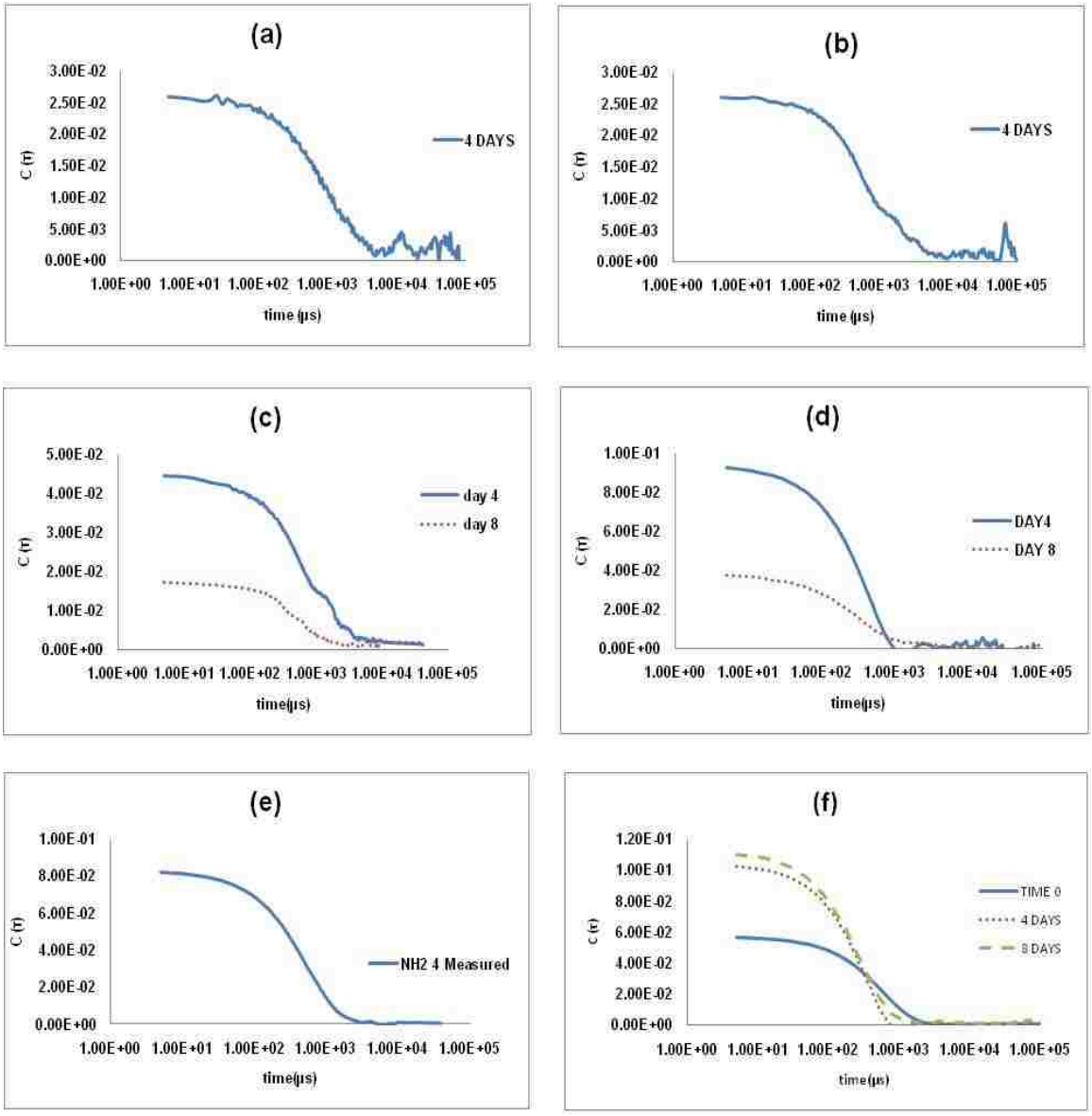

Figure 3.3. Aggregation of two peptides in the presence of two latexes. (a) $(Ile)_5$-b-$(Lys)_5$ in PS-NH_2. (b) $(Ile)_5$-b-$(Lys)_5$ in PS-OH. (c) $(Ile)_{10}$-b-$(Lys)_{10}$ in PS-NH_2 . (d) $(Ile)_{10}$-b-$(Lys)_{10}$ in PS-OH. (e) PS-NH_2. (f) PS-OH.

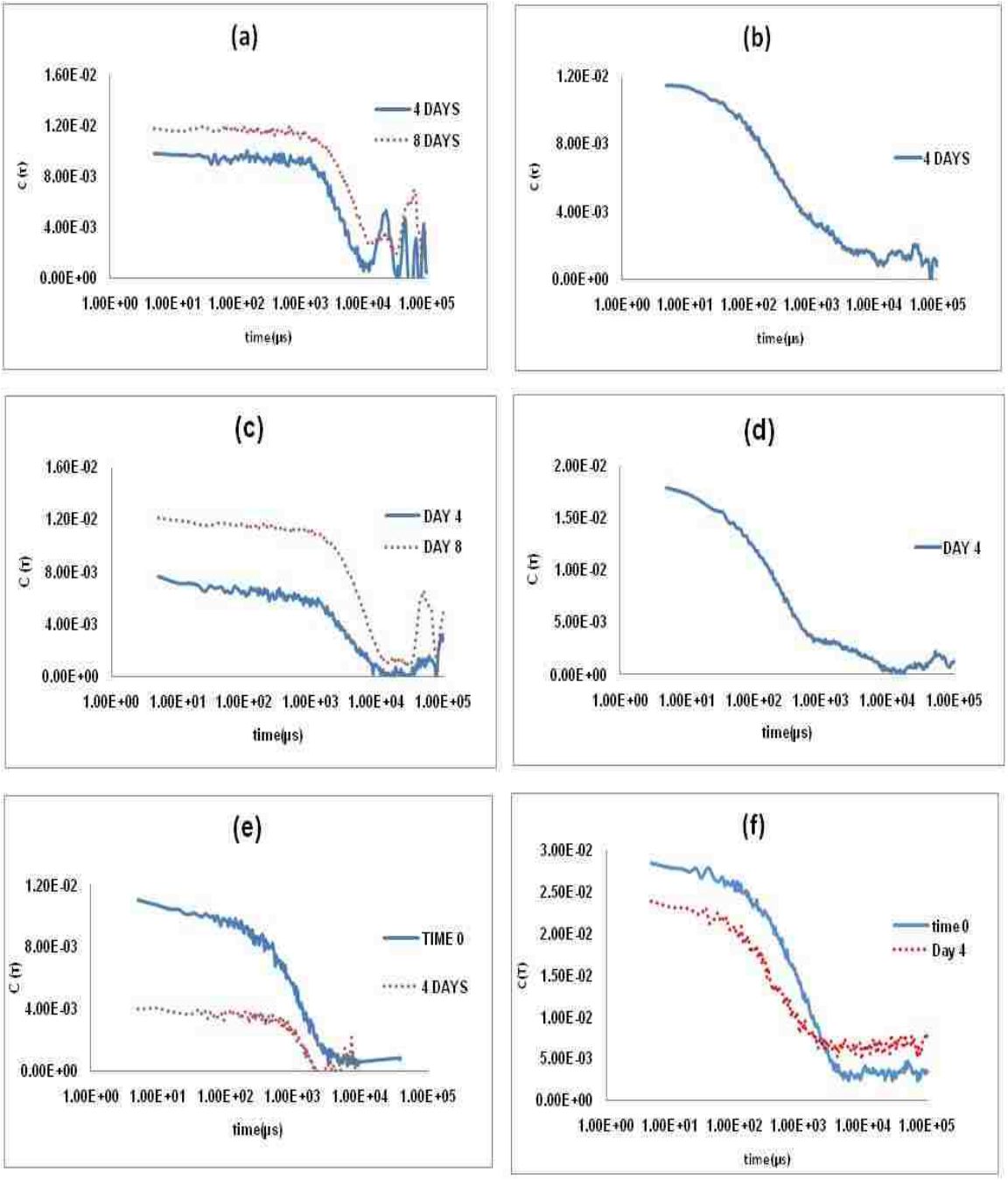

Figure 3.4. Dynamic light scattering results for $(Ile)_5$-b-$(Lys)_5$ and $(Ile)_{10}$-b-$(Lys)_{10}$ in the presence of PC/C liposomes at various times. The left panels are for PC/C 20%/80% and the right panels are for PC/C 80%/20%. a) b) $(Ile)_5$-b-$(Lys)_5$, c) d) $(Ile)_{10}$-b-$(Lys)_{10}$ e) and f) are blanks.

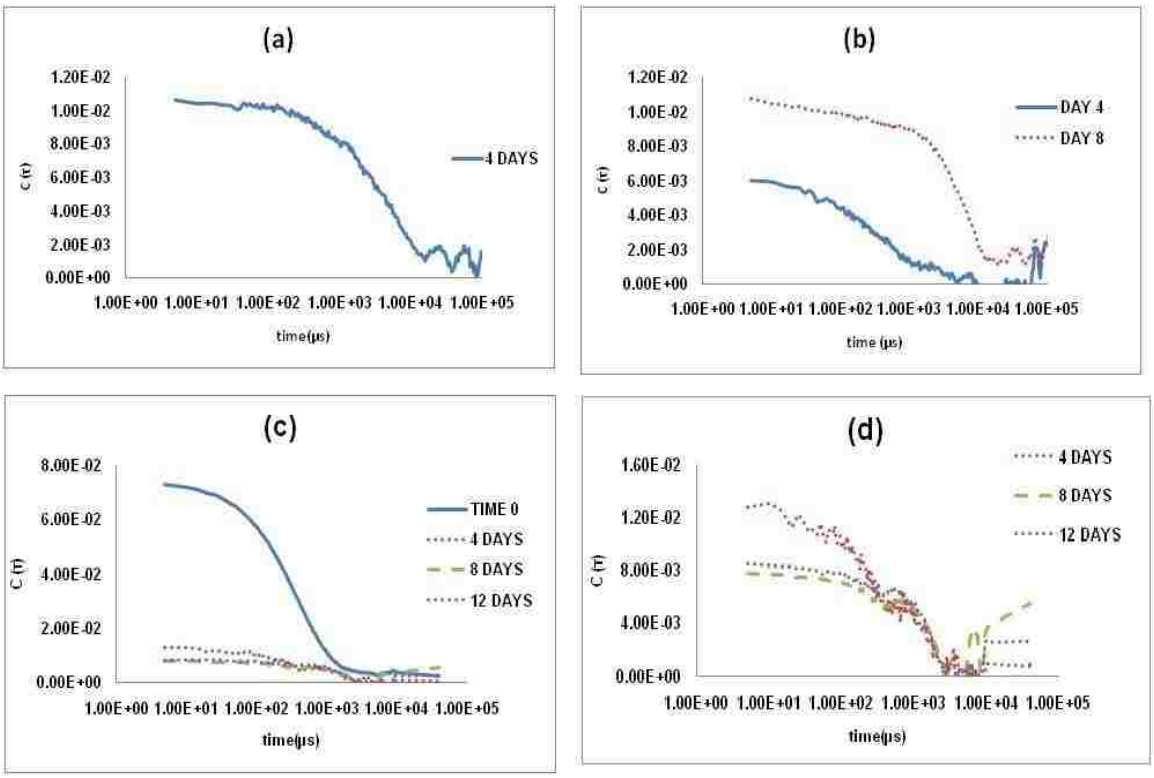

Figure 3.5. Dynamic light scattering results for (a) $(Ile)_5$-b-$(Lys)_5$ and (b) $(Ile)_{10}$-b-$(Lys)_{10}$ in the presence of PC/PS liposomes at various times. Panel (c) corresponds to liposome blanks. The blanks at 4, 8 and 12 days were replotted in panel (d) to highlight the changes.

Figure 3.4 shows that PC/C 20%/80% liposomes are not quite stable after four days whereas the PC/C 80%/20% remain reasonable unchanged after 4 days (panel f). Heavy aggregation is obvious for both peptides in 20%/80% liposomes. The data for 80%/20% liposomes seems to have a single population for the smaller peptide but two distinct populations for the larger peptide (panel (d)). Figure 3.5 shows that PC/PS liposomes aggregate after four days in the absence of peptides. Panel (d) clearly shows two populations with very distinct time constants. The small peptide shows aggregation after 4 days (Panel (a)). The large peptide shows small aggregates after 4 days and large aggregates after 8 days.

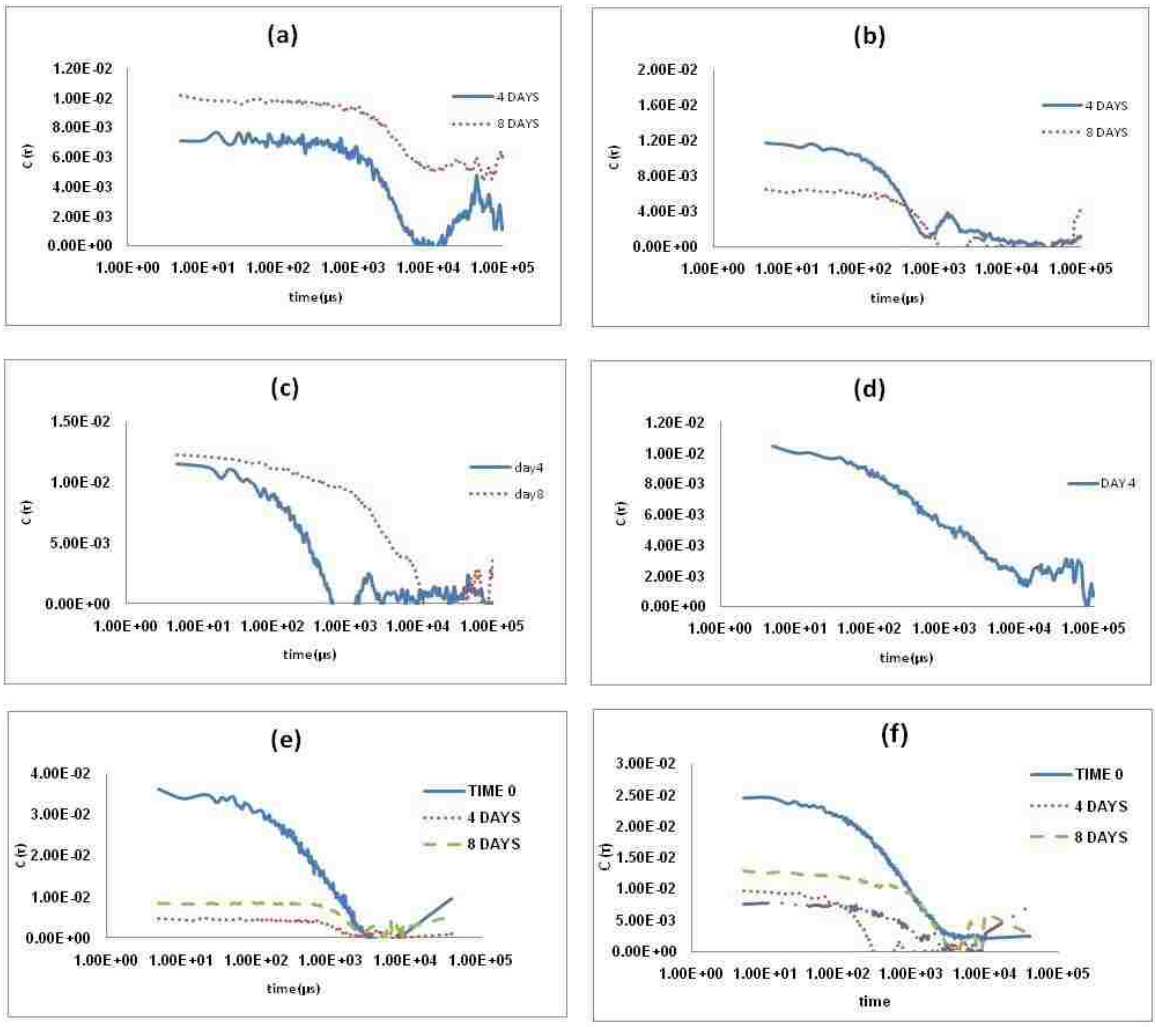

Figure 3.6. Dynamic light scattering results for $(Ile)_5$-b-$(Lys)_5$ and $(Ile)_{10}$-b-$(Lys)_{10}$ in the presence of PC/PE/PS/C and PC/PG/PE/C liposomes at various times. Left panels are for PC/PG/PE/C liposomes and right panels are for PC/PE/PS/C liposomes. (a) and (b) $(Ile)_5$-b-(Lys_5) ; (c) and (d) $(Ile)_{10}$-b-$(Lys)_{10}$; (e) and (f) are blanks.

Both PC/PG/PE/C and PC/PE/PS/C show signs of aggregations after four days (panels (e) and (f) in Figure 3.6). A comparison between panels (a) and (c) shows that the short peptide forms larger aggregates than that the larger peptide. The trend seems to reverse when PC/PG/PE/PC liposomes are used.

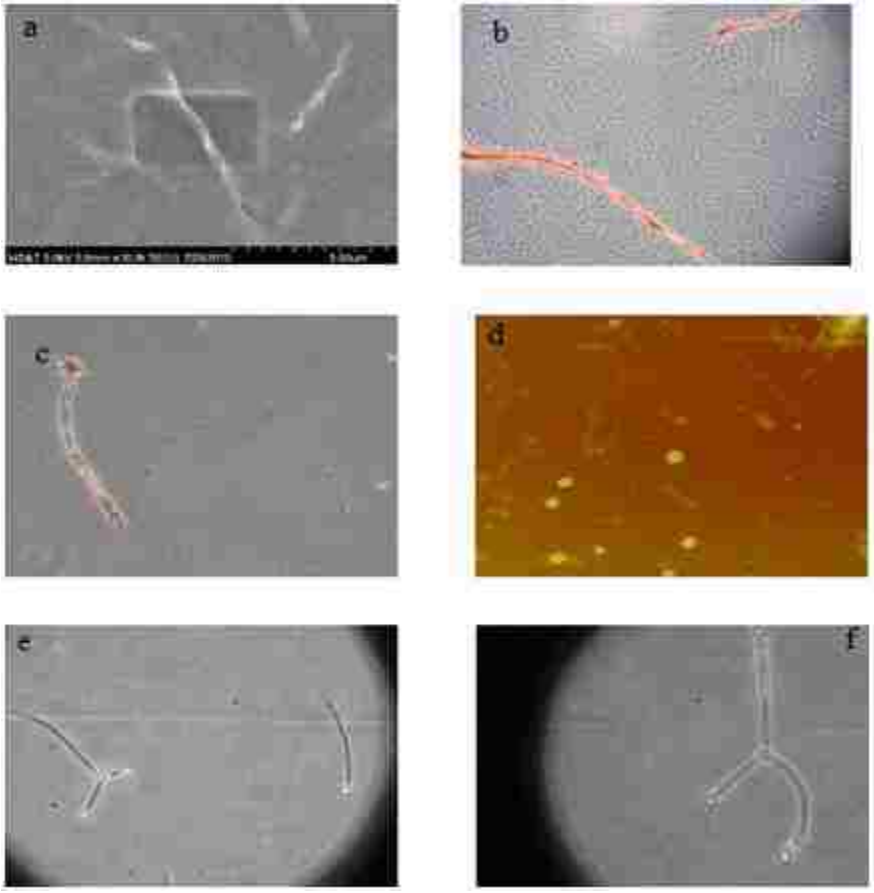

Figure 3.7. SEM micrograph of (a) $(Ile)_7$-b-$(Lys)_3$; (b) Optical microscope image of $(Ile)_6$-b-$(Lys)_4$ (c) Optical image of $(Ile)_7$-b-$(Lys)_3$ and polystyrene (d) AFM image of $(Ile)_7$-b-$(Lys)_3$ (e) $(Ile)_7$-b-$(Lys)_3$ and polystyrene; (f) $(Ile)_7$-b-$(Lys)_3$ and polystyrene.

SEM, TEM, AFM and an optical microscope were used to visualize the presence of fibrils. Representative pictures are shown in Figure 3.7 and a more comprehensive collection is included in Appendix C. The presence of Congo red bound to the fibrils is also evident in some images. Images of fibrils in presence of polystyrene beads appear to show that polystyrene spheres aggregate and serve as the nucleation sites for fibrils. Panels (e) and (f) shos images of amyloid fibrils in the presence of polystyrene and multiple fibrils attached from a single nucleation site are visible.

Four of the peptides that formed fibrils were checked for their ability to penetrate or induce leakage in all the liposomes that were used. It is worth to notice that this type of

test is commonly used to detect antimicrobial activity of synthetic peptides. All the peptides caused leakage in all but two (PC/C 80/20 and 20/80) of the liposomes (Figures 3.8 to 3.10).

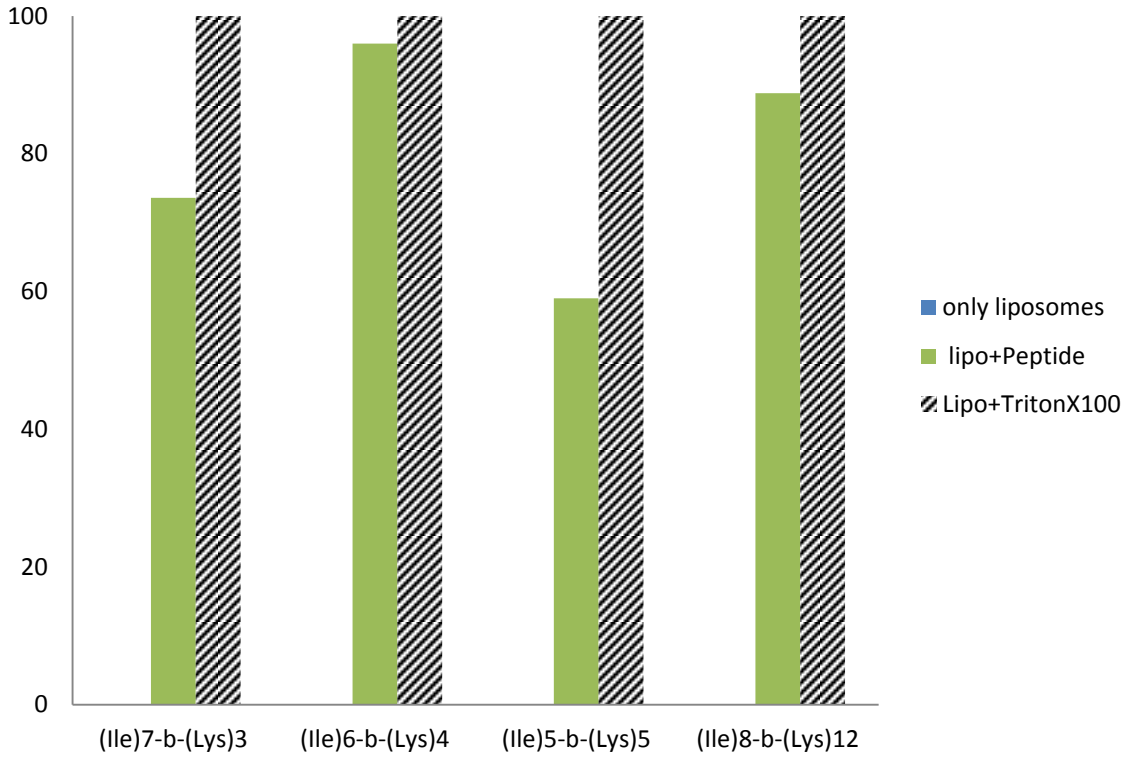

Figure 3.8. Percentage of leakage induced by four peptides to liposome 2:2:1:1(C/PC/PG/PE).

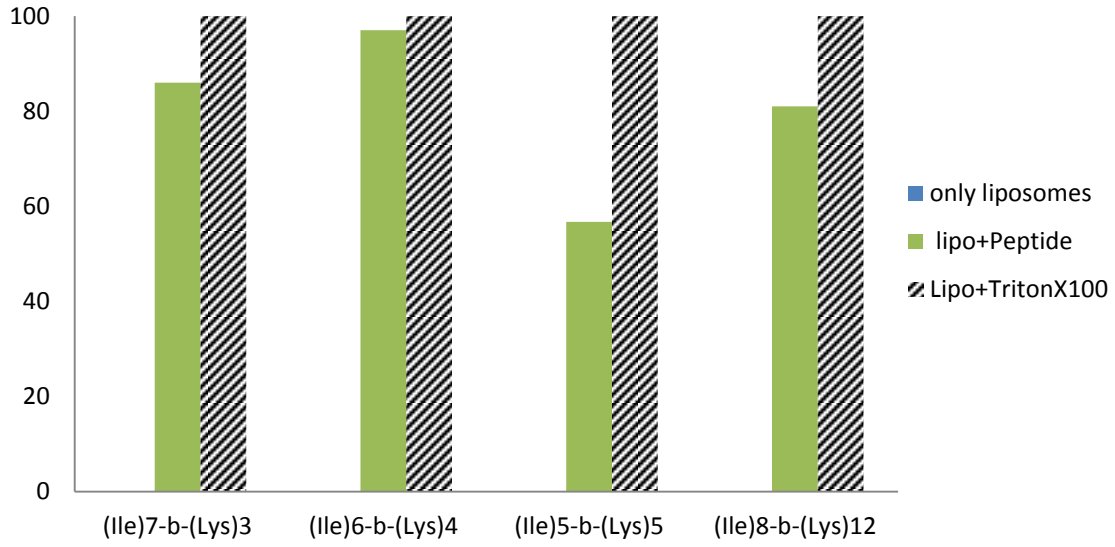

Figure 3.9. Percentage of leakage induced by four peptides to liposome 80%/20%(PC/PS).

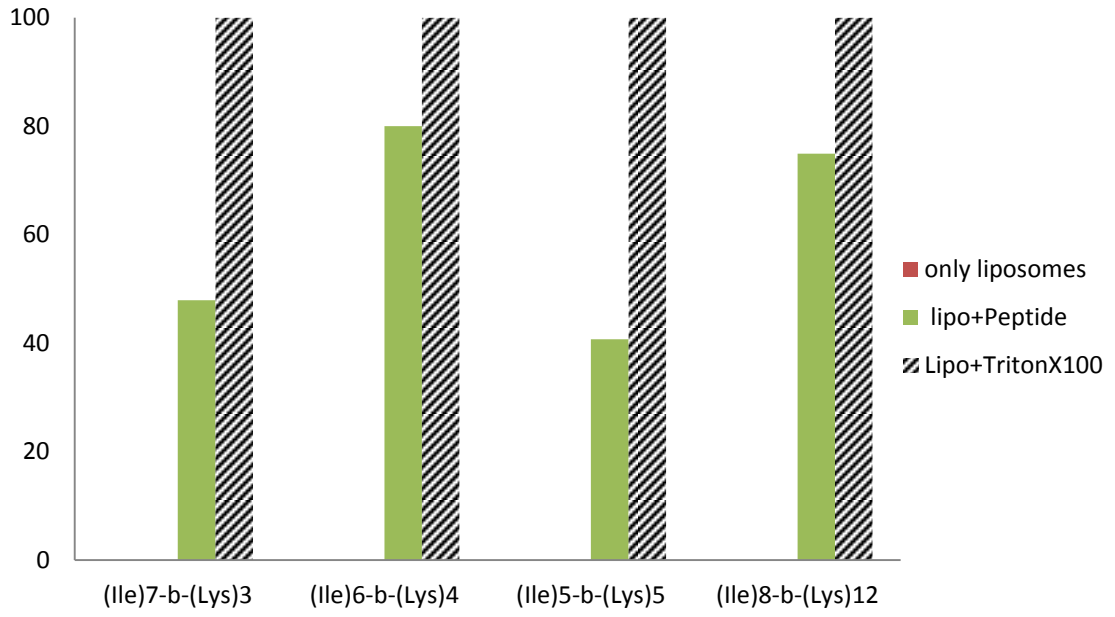

Figure 3.10. Percentage of leakage induced by four peptides into liposome 10:5:7.5:16(PC/PE/PS/C).

Readings were also taken after 24, 48 and 72 hours to determine if the amount of leakage increased after one day and if liposomes that were intact after 24 hrs show any leakage after further incubation. No changes were observed. Liposomes which did rupture in the presence of peptides resemble relatively complex biological membranes and have a more rigid surface because of the presence of cholesterol. It is striking that $(Ile)_5$-b-$(Lys)_5$, which has the higher helical content, is the peptide that causes the least leakage. It has been speculated that one of the features of antimicrobial peptides is that they exist as random coils in bulk but that they form helices near lipid bilayers. The other three liposomes which showed leakage in the presence of peptides are known to have a relative fluid membrane surface. Another hypothesis is that liposomes PC/C (80/20) and PC/C (20/80) did not show any leakage because of a lower surface charge. Haywood and Boyer (1984) found that charged lipids were needed for peptide fusion to take place.

4. CONCLUSIONS

We have identified a family of diblock peptides that forms amyloid fibrils at moderate conditions (pH 4 and 60 ^{o}C). The kinetics of fibril formation seems to be affected by the overall length of the peptide but not by their composition (beyond some critical block concentrations). Longer peptides form fibrils faster than shorter ones. The addition of a variety of surfaces does not positively affect the formation of fibrils. For example, the peptides are still unable to form fibrils in the presence of surfaces at neutral or basic pHs. As a matter of fact, some interfaces seem to inhibit the formation of fibrils. Our results suggest that some surfaces (liposomes) uptake the peptides and therefore the actual peptide concentration available for fibrillation maybe smaller than needed. Another plausible explanation for the seemingly inhibitory effect of some liposomes is that the presence of the peptides at the incubation conditions release free phospholipids into the bulk fluid and this affects the solvent conditions needed for the formation of fibrils.

It is obvious from this exploratory work that narrower kinetic explorations at shorter times are needed to elucidate the effect that surfaces have on the kinetics of fibrillation.

APPENDIX A

CONGO-RED SPECTRAL SHIFTS

$(Ile)_7$-b-$(Lys)_3$ in bulk

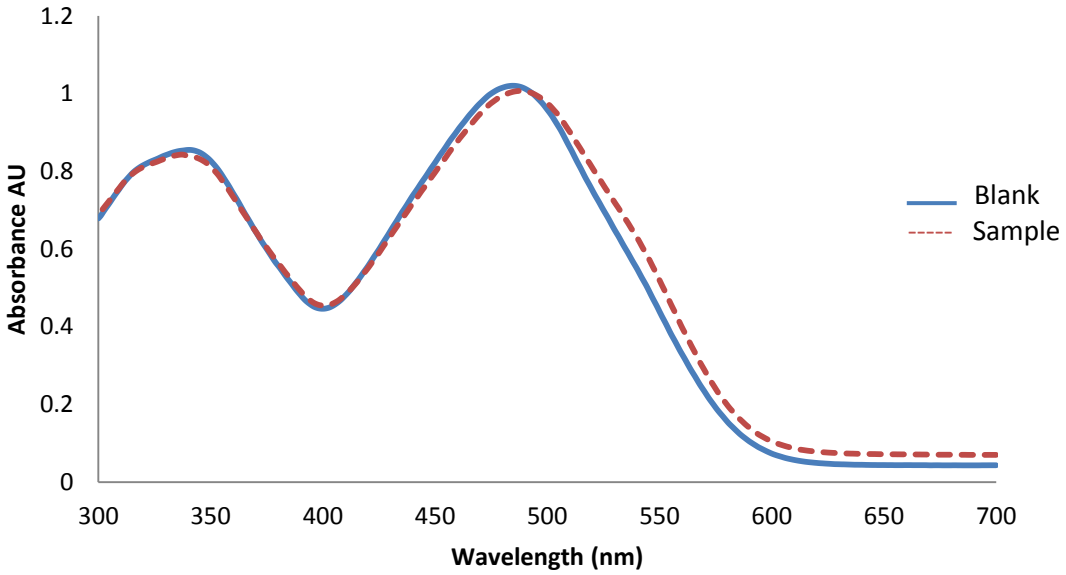

$(Lys)_{10}$-b-$(Ile)_{10}$ in PS-OH

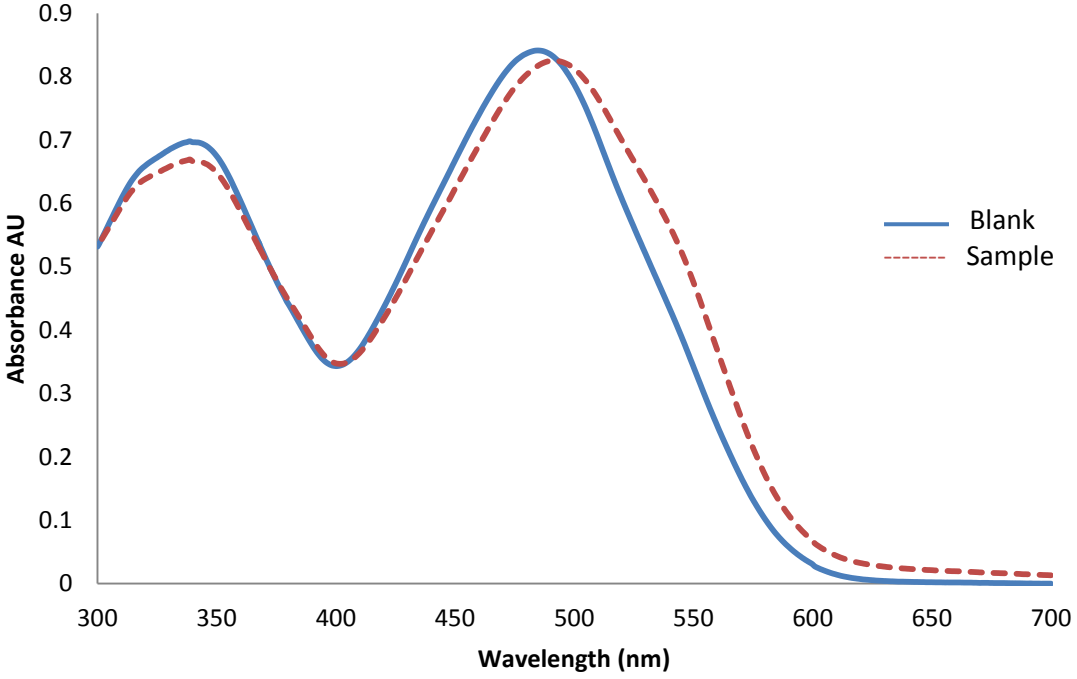

$(Lys)_{10}$-b-$(Ile)_{10}$ in PS-COOH

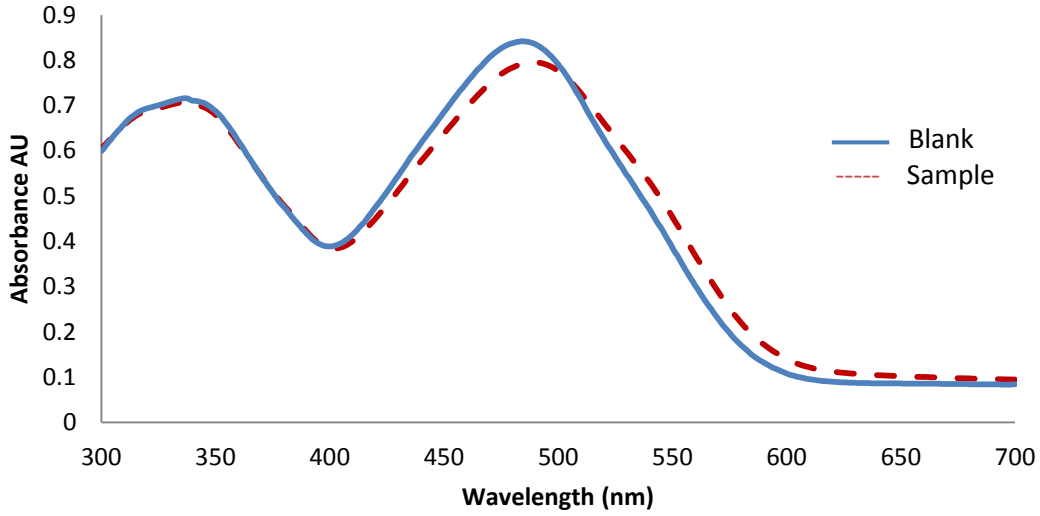

$(Lys)_{10}$-b-$(Ile)_{10}$ in PS-NH_2 (a)

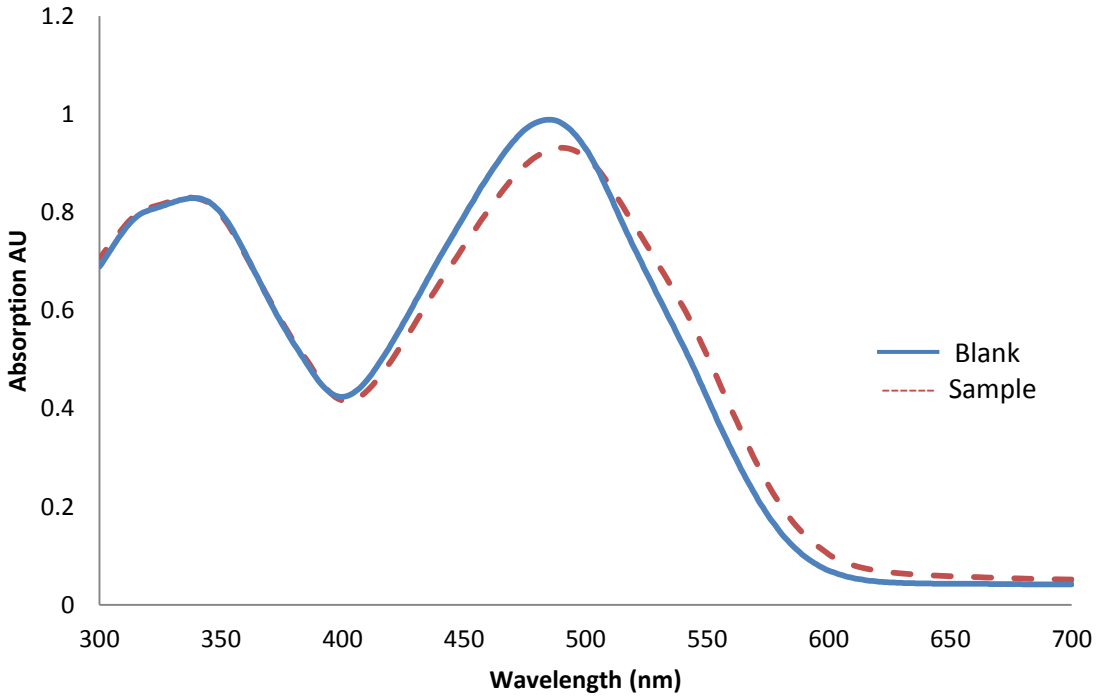

$(Lys)_{10}$-b-$(Ile)_{10}$ in PS-NH_2 (b)

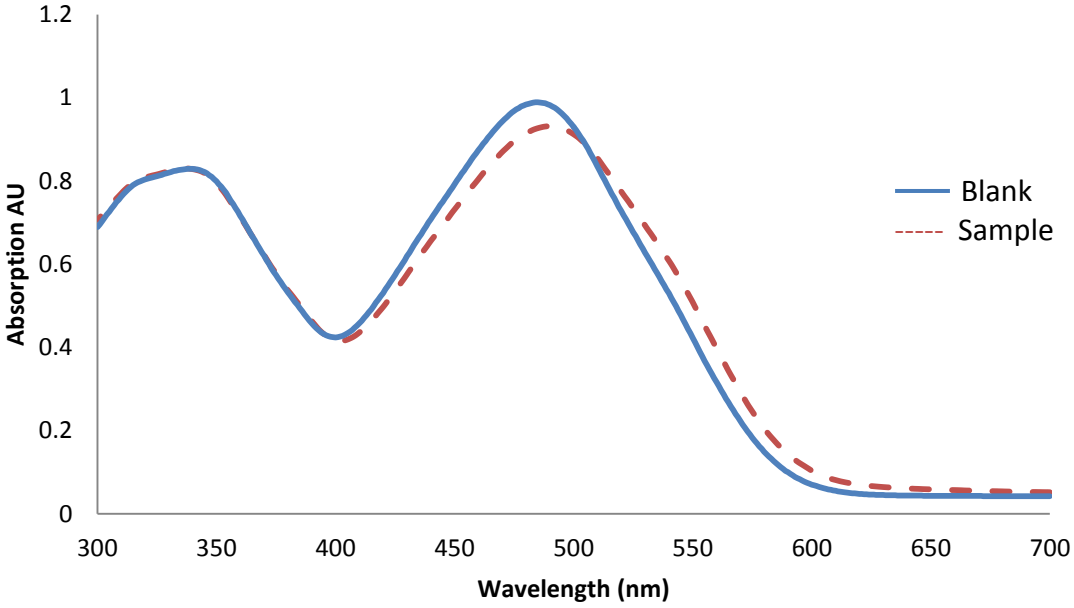

$(Lys)_{10}$-b-$(Ile)_{10}$ in PS (a)

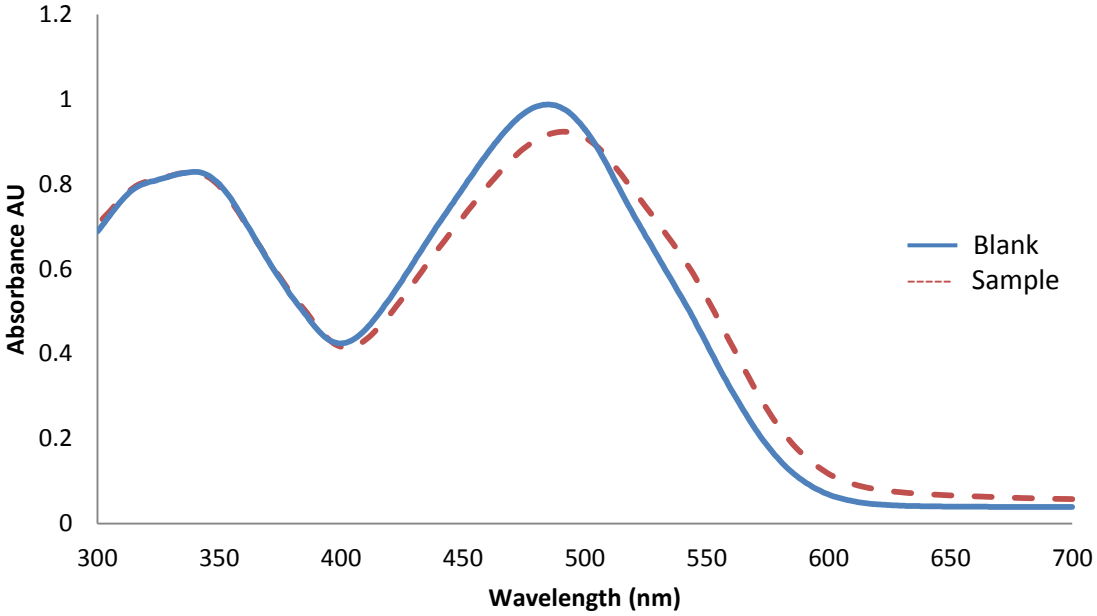

$(Lys)_{10}$-b-$(Ile)_{10}$ in 80/20:PC/PS (a)

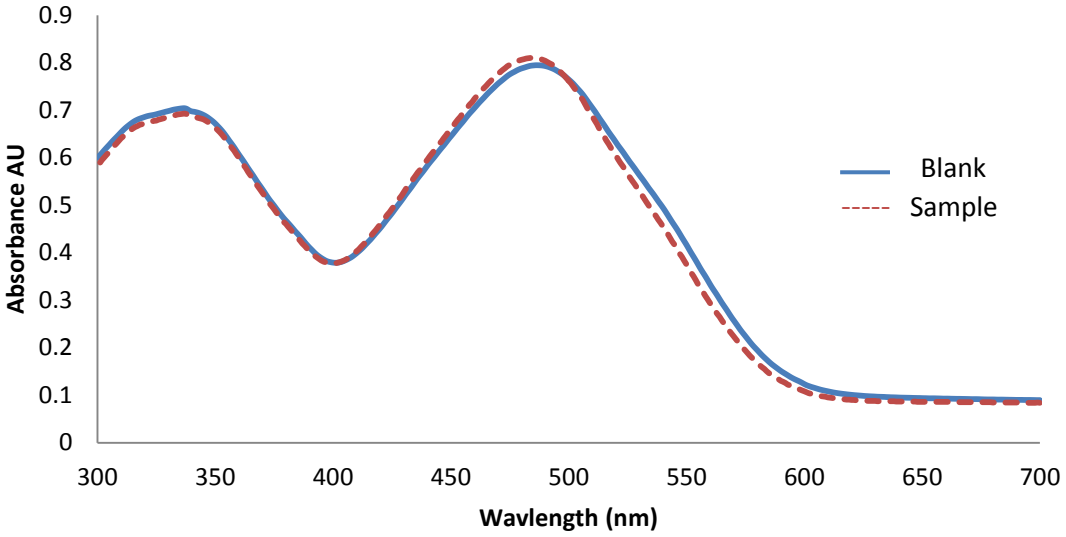

$(Lys)_{10}$-b-$(Ile)_{10}$ in 80/20:PC/C (a)

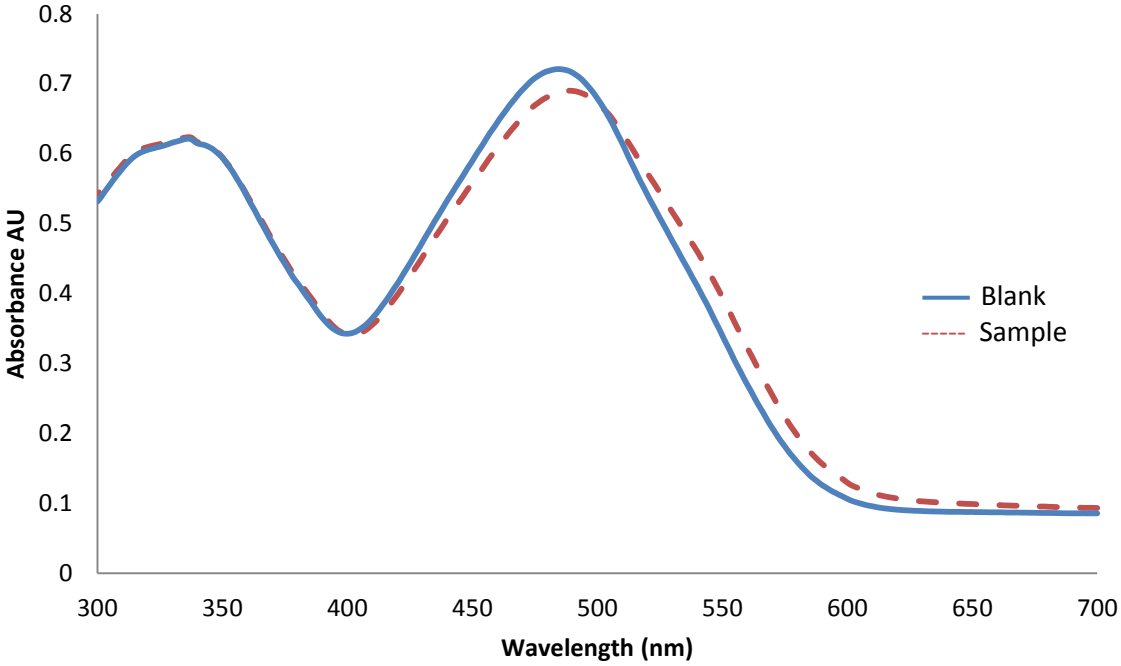

$(Lys)_{10}$-b-$(Ile)_{10}$ in 80/20:C/PC (a)

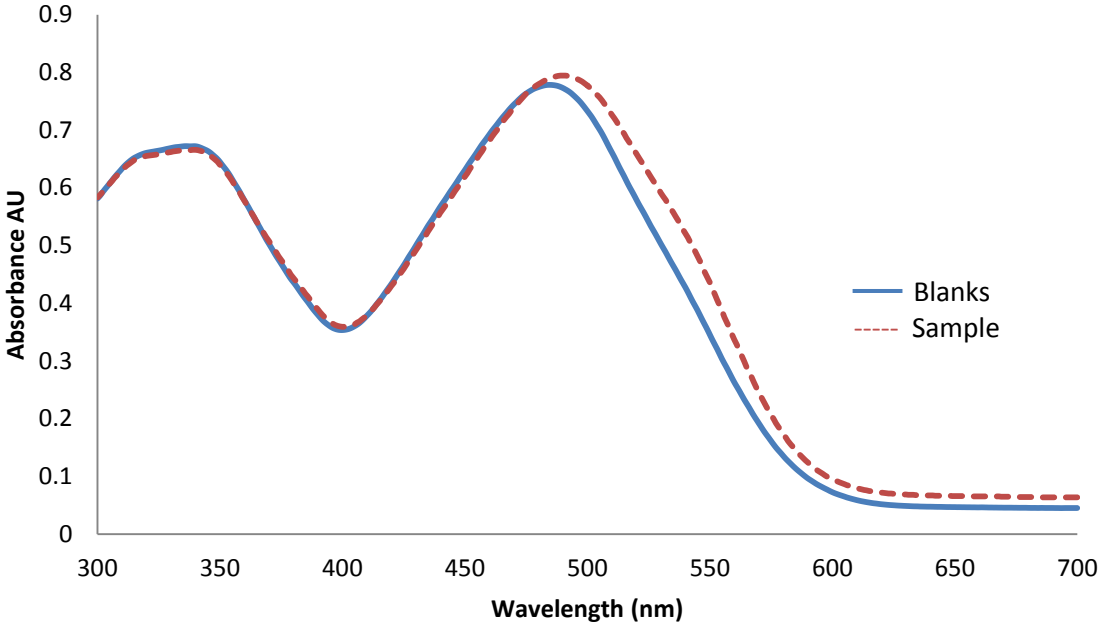

$(Ile)_{10}$-b-$(lys)_{10}$ in 2:2:1:1 C/PC/PG/PE (a)

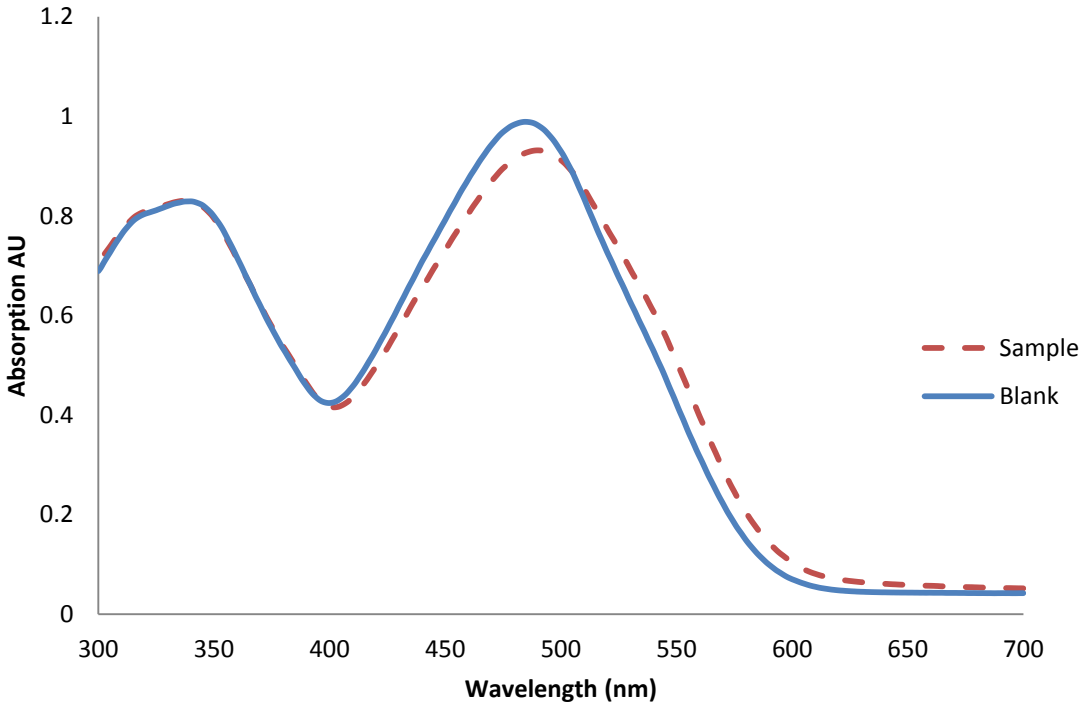

$(Lys)_{10}$-b-$(Ile)_{10}$ in 10:5:7.5:16 PC/PE/PS/C (a)

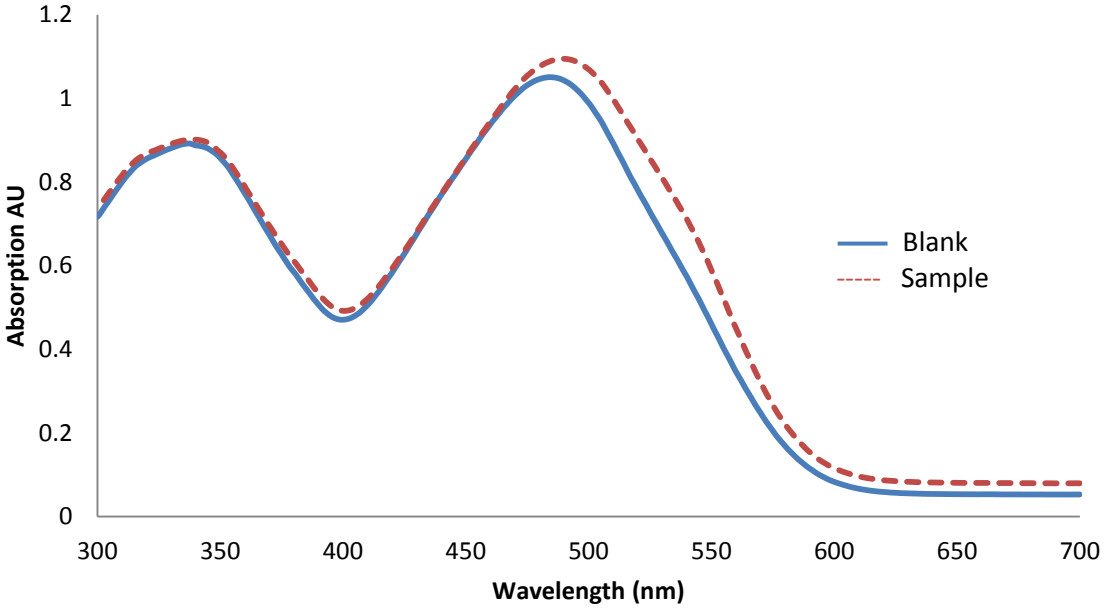

$(Lys)_{10}$-b-$(Ile)_{10}$ in PS (b)

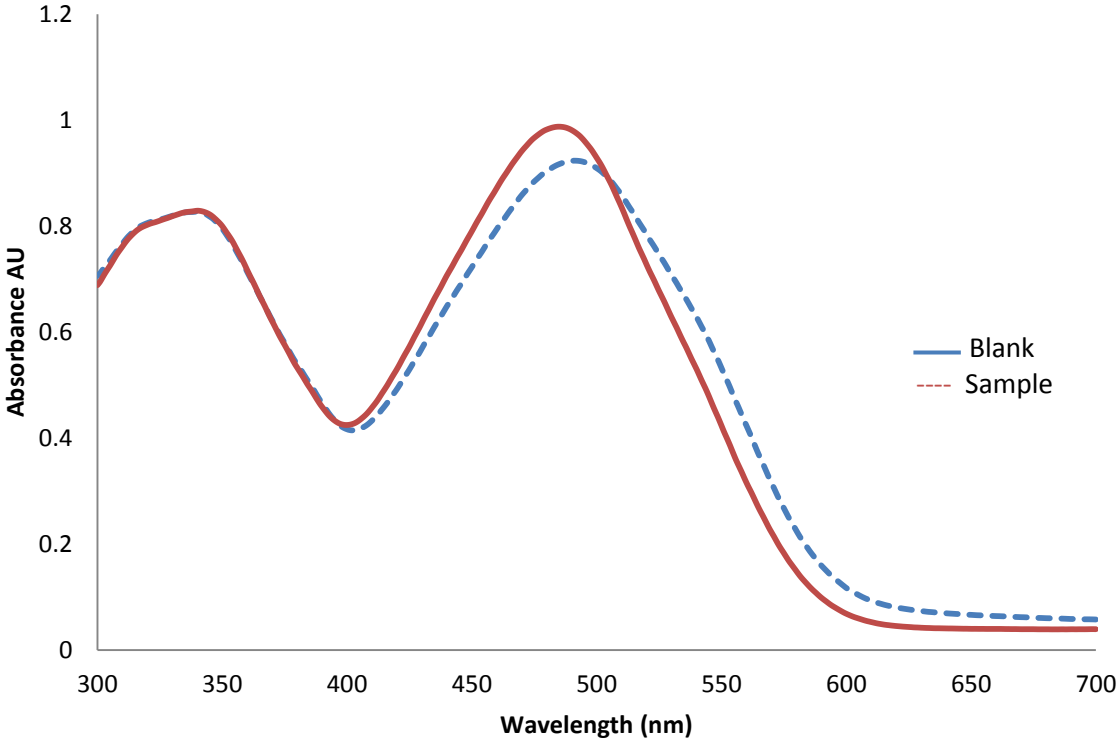

$(Lys)_{10}$-b-$(Ile)_{10}$ in PS-OH (b)

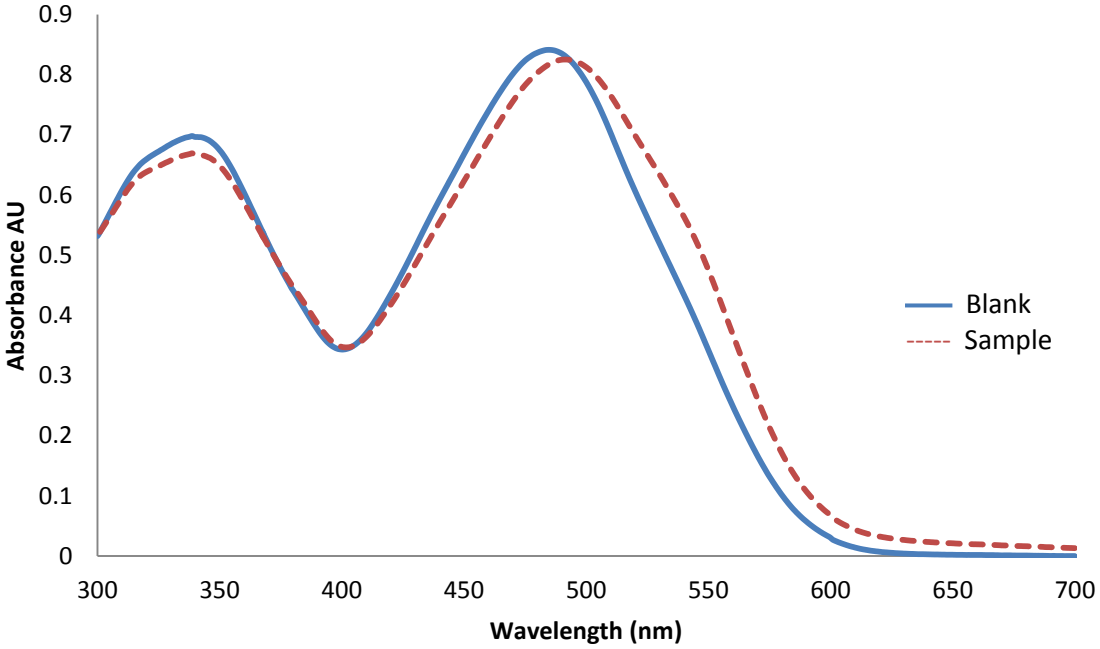

$(Ile)_7$-b-$(Lys)_3$ in PS-NH_2

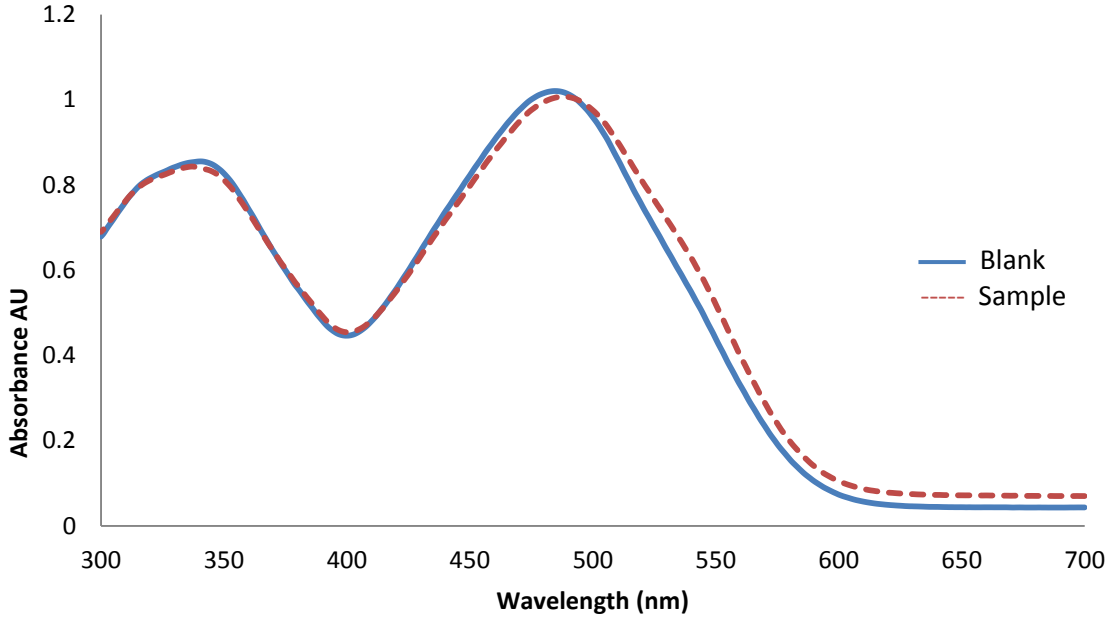

$(Lys)_{10}$-b-$(Ile)_{10}$ in PS-COOH (b)

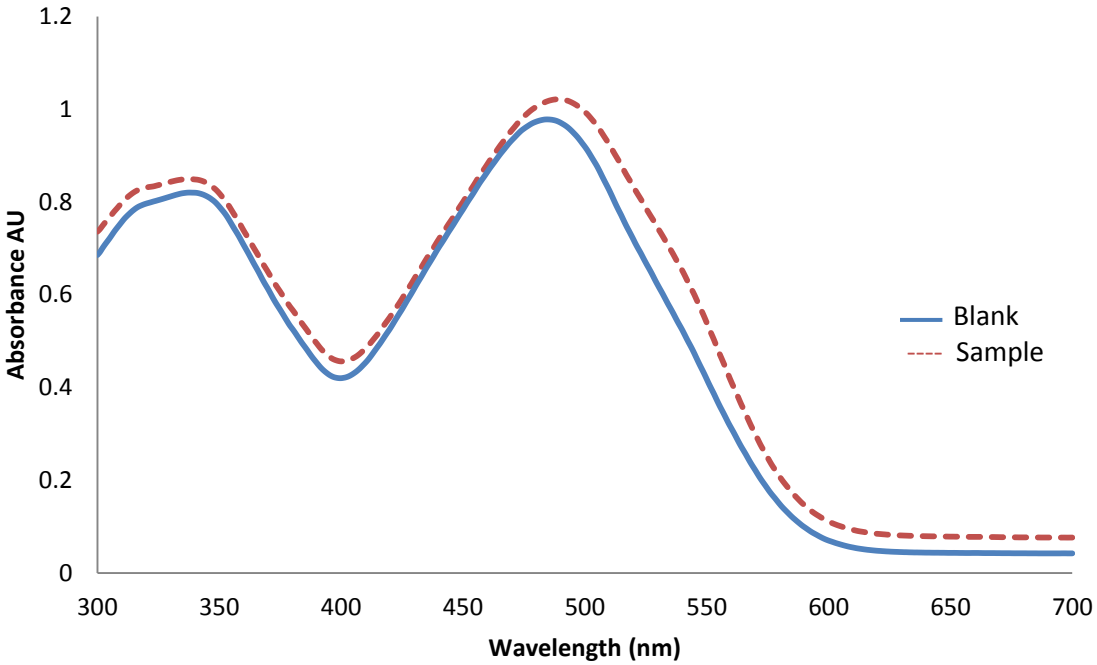

$(Lys)_{10}$-b-$(Ile)_{10}$ in 80/20:PC/PS (b)

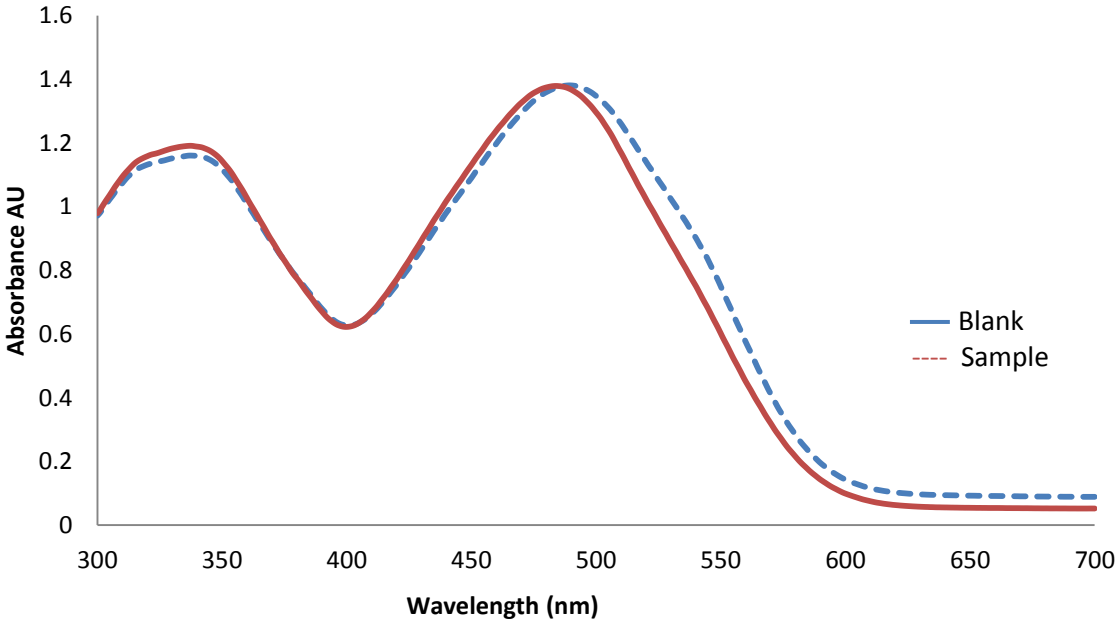

$(Lys)_{10}$-b-$(Ile)_{10}$ in 10:5:7.5:16 PC/PE/PS/C (b)

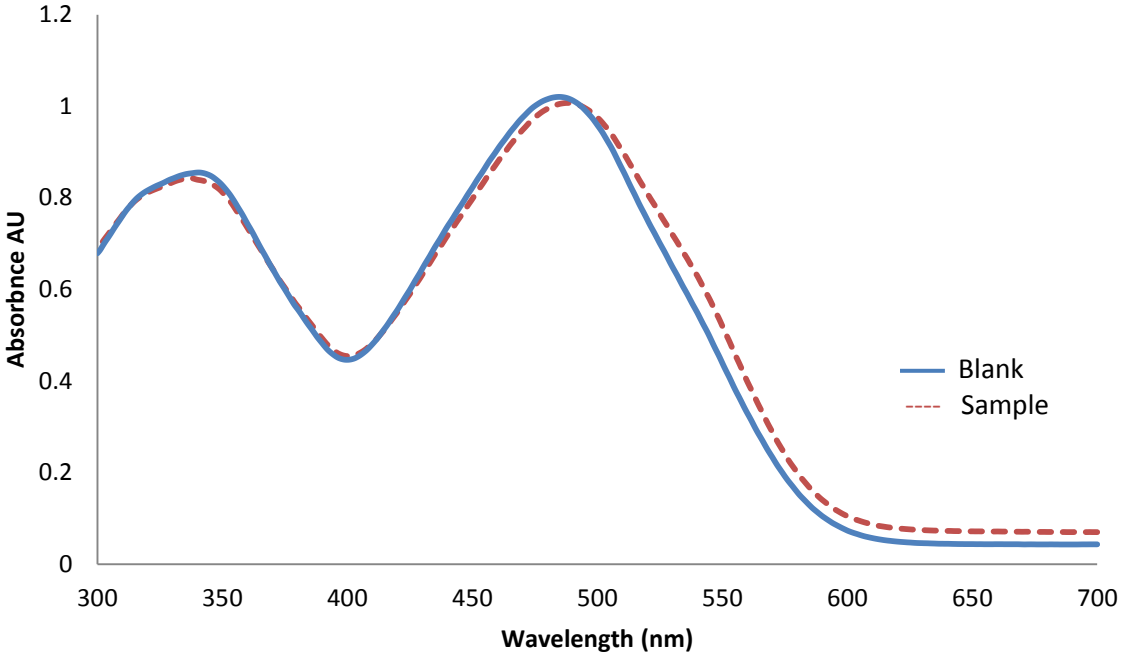

$(Ile)_5$-b-$(Lys)_5$ in bulk

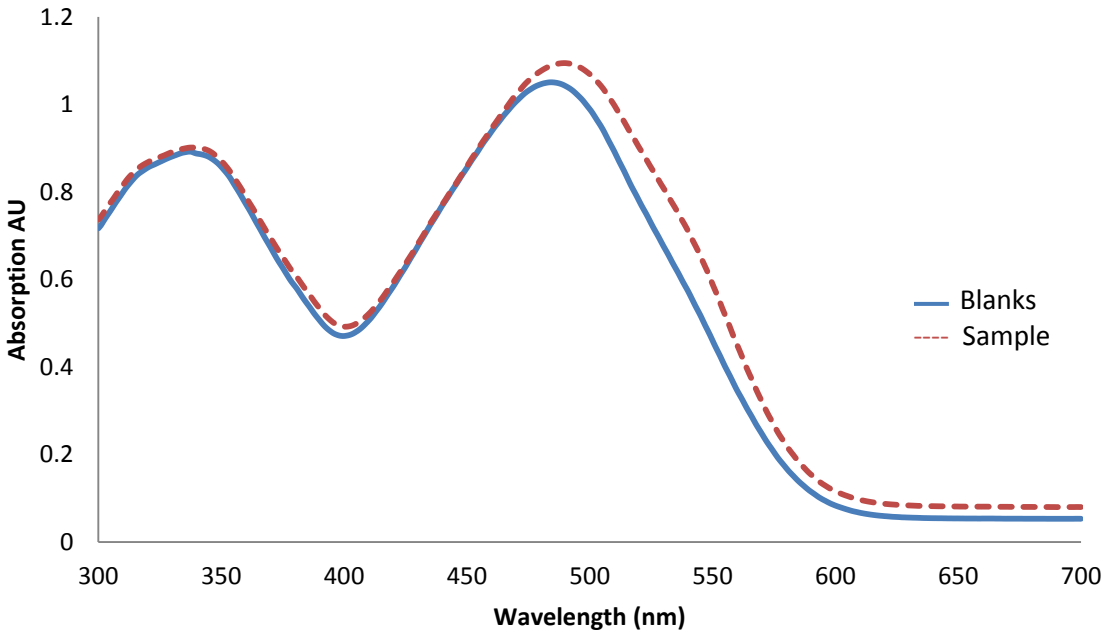

$(Ile)_7$-b-$(Lys)_3$ in bulk

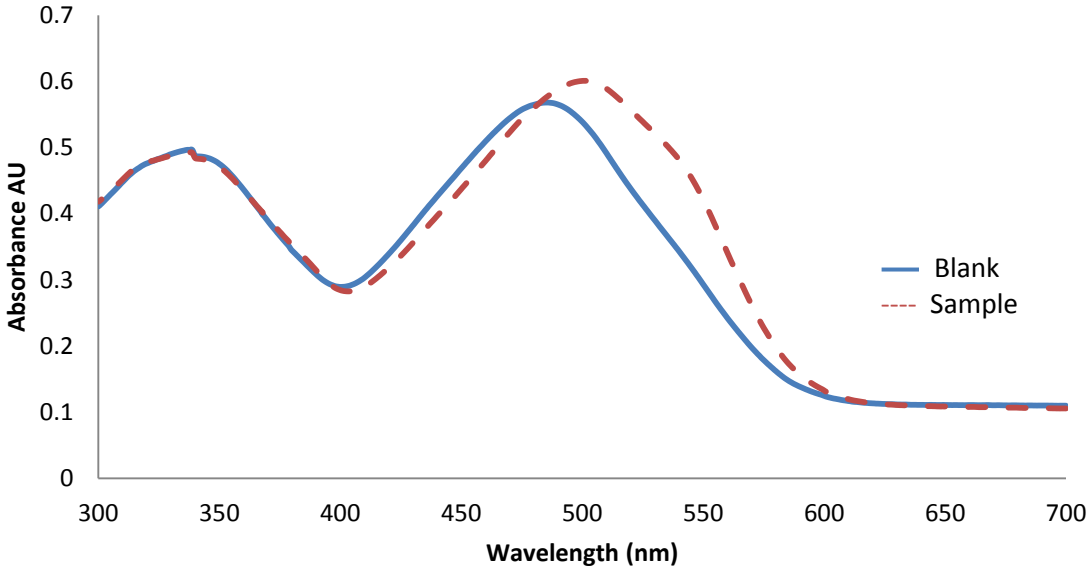

$(Ile)_{10}$-b-$(Lys)_{10}$ in bulk

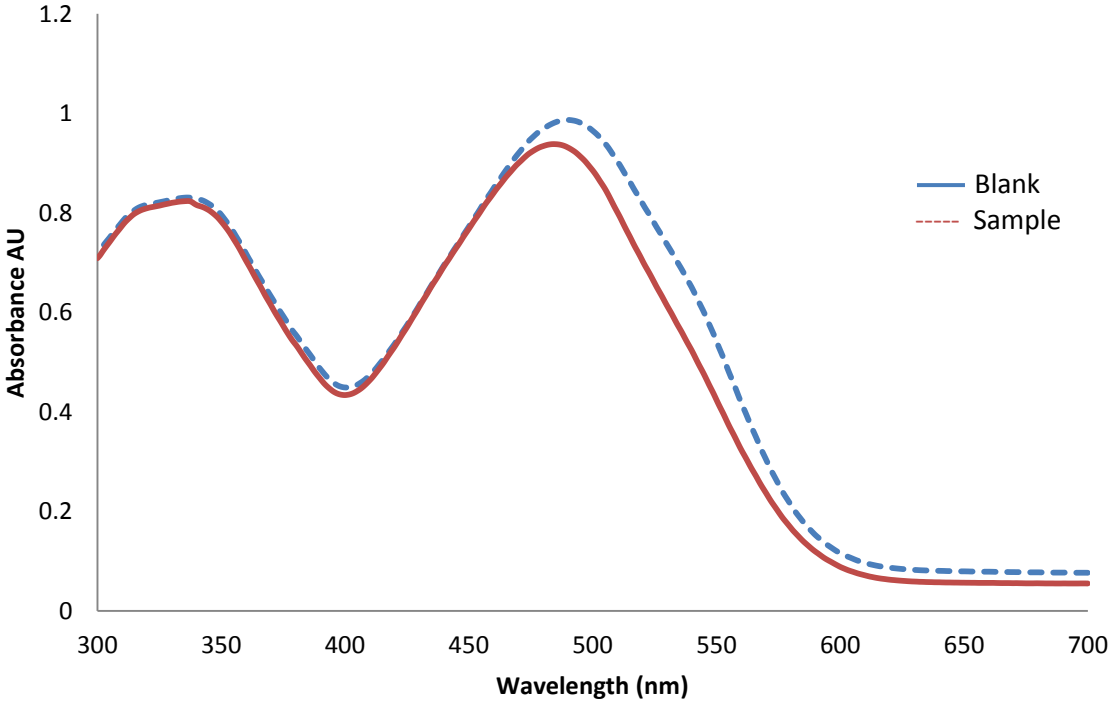

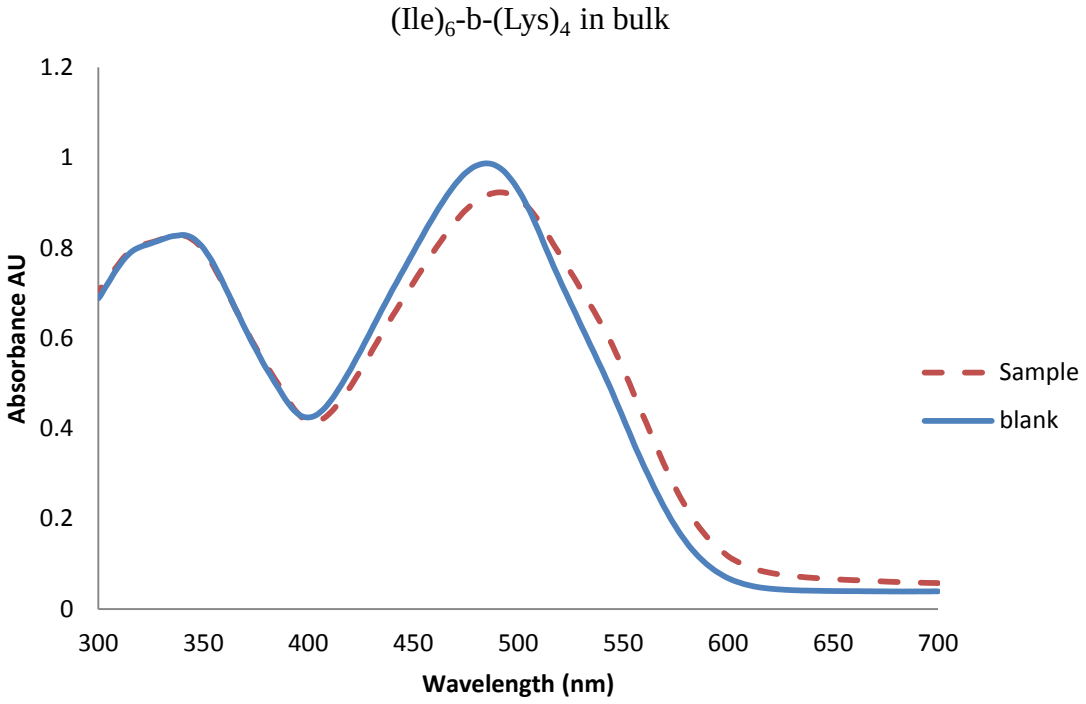
(Ile)6-b-(Lys)4 in bulk
1.2
1
0.8
0.6
0.4
0.2
0
Absorbance AU
300
350
400
450
500
550
600
650
700
Wavelength (nm)
Sample
blank

APPENDIX B
FT-IR RESULTS

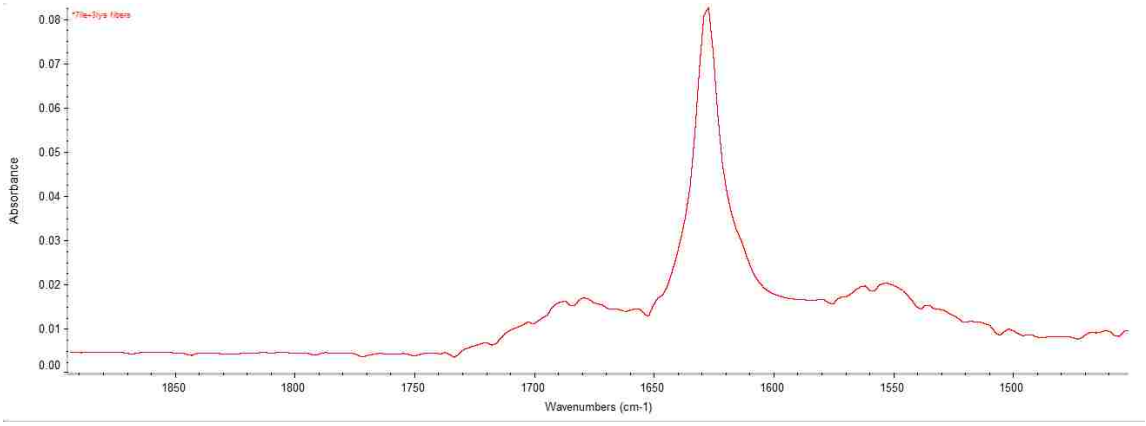

$(Ile)_7$-b-$(Lys)_3$

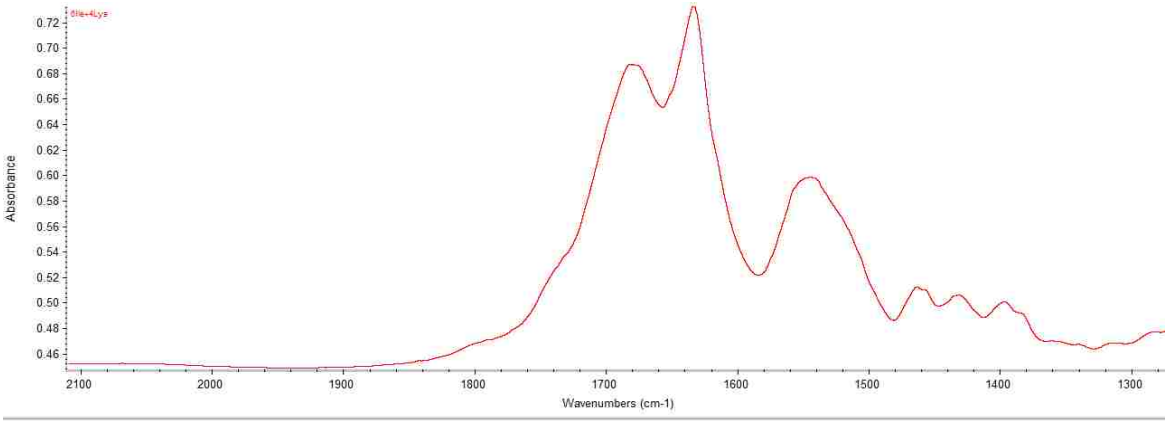

$(Ile)_6$-b-$(Lys)_4$

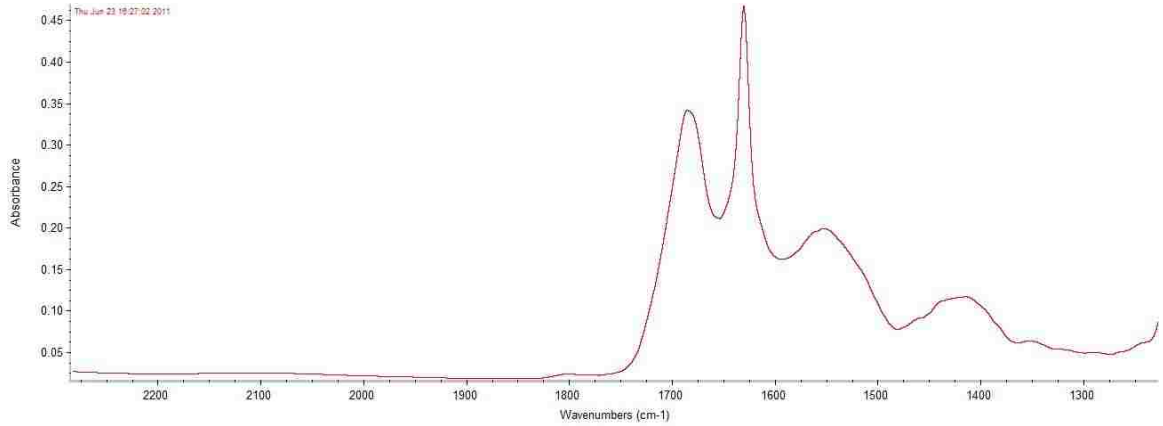

$(Ile)_5$-b-$(Lys)_5$ scans

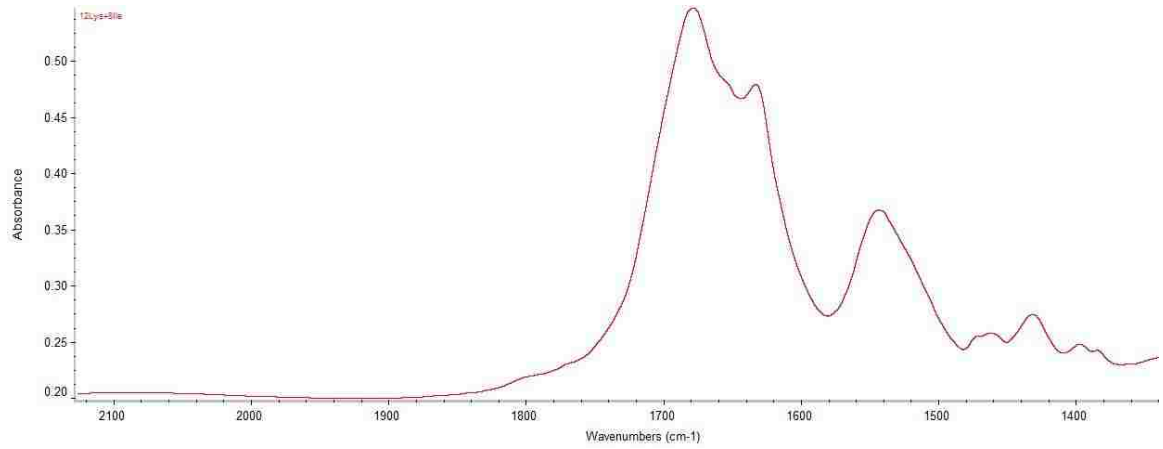

$(Lys)_{12}$-b-$(Ile)_8$

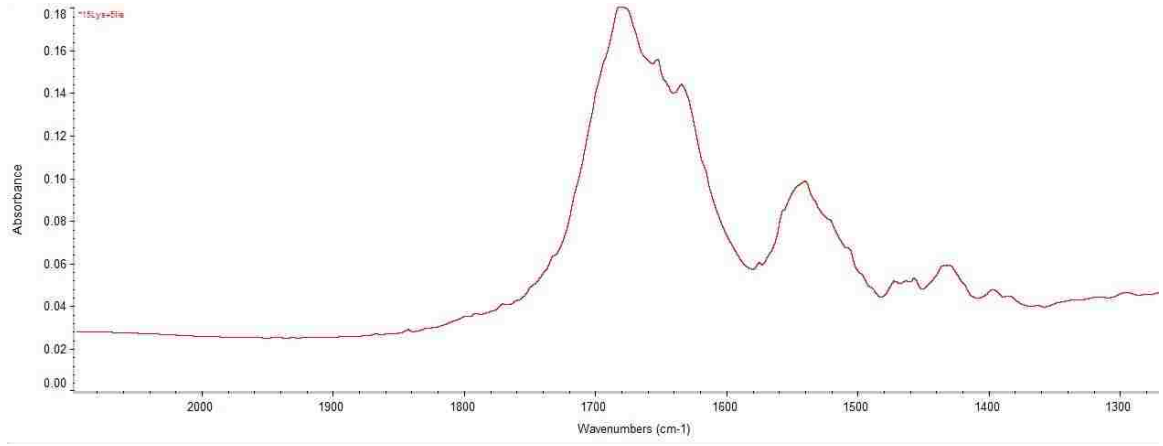

$(Lys)_{15}$-b-$(Ile)_5$

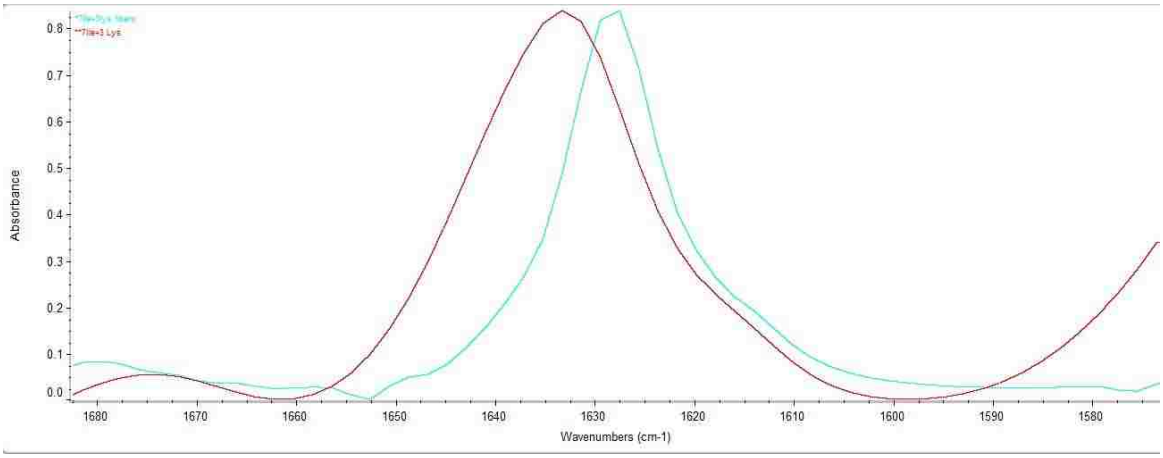

Overlapped scans of $(Ile)_{10}$-b-$(lys)_{10}$. Red: native, blue: fibrils.

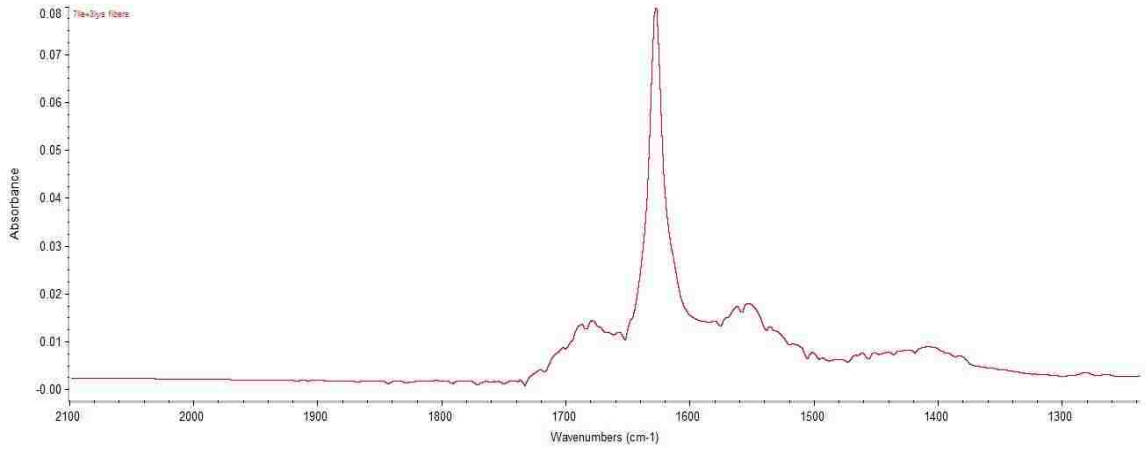

$(Ile)_7$-b-$(Lys)_3$. After incubation

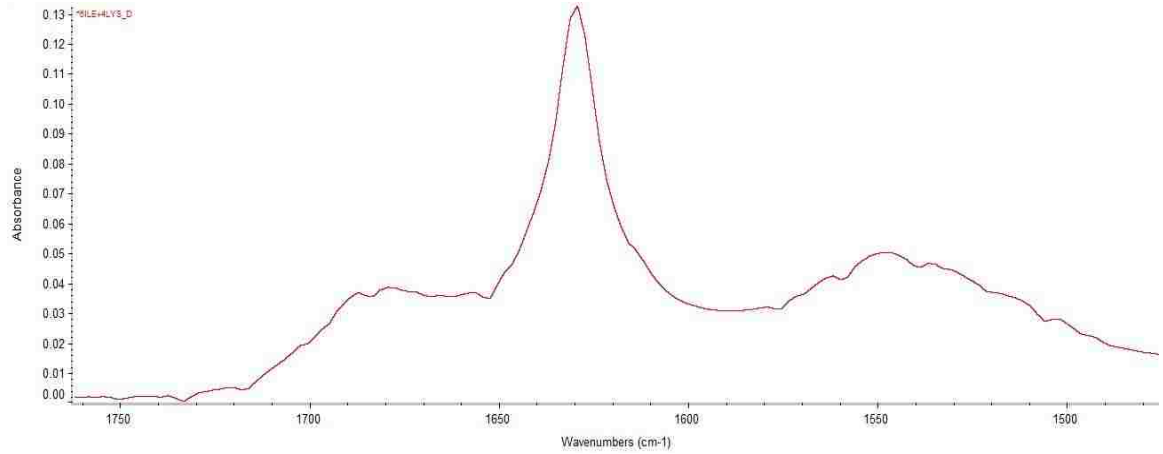

$(Ile)_6$-b-$(Lys)_4$. After incubation.

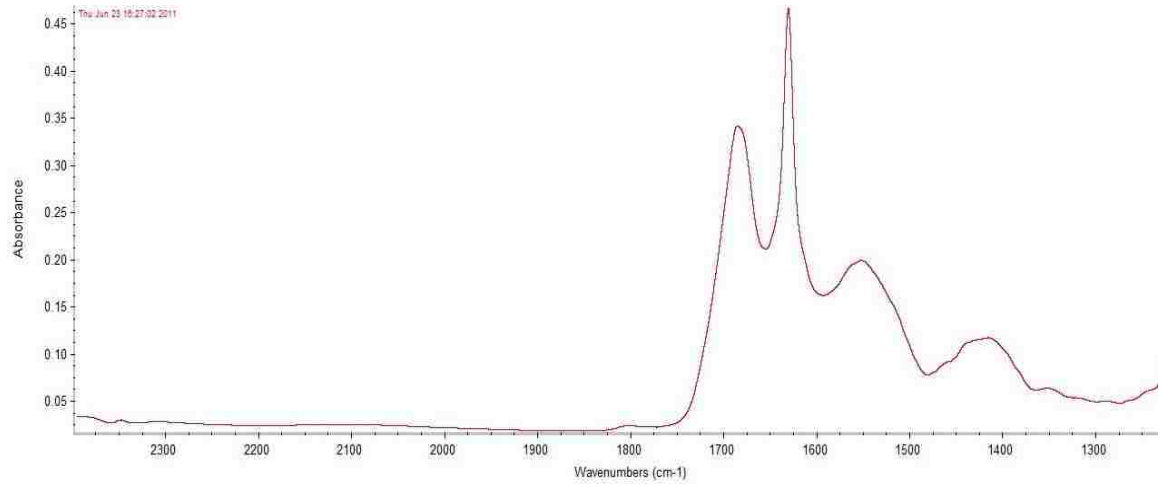

$(Ile)_5$-b-$(Lys)_5$. After incubation.

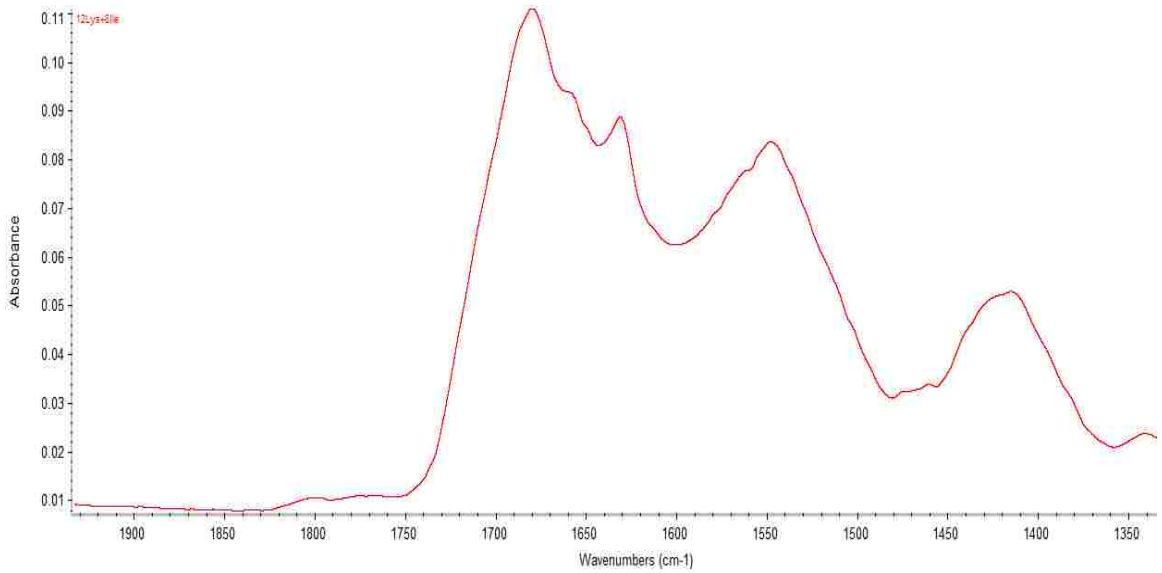

$(Lys)_{12}$-b-$(Ile)_8$. After incubation.

APPENDIX C
VISUAL EVIDENCE

$(Ile)_6$-b-$(Lys)_4$ in bulk

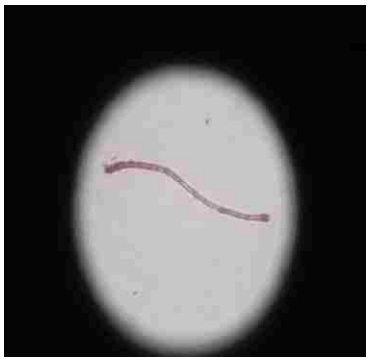

$(Ile)_6$-b-$(Lys)_4$ in PS

$(Ile)_6$-b-$(Lys)_4$ in PS-OH

$(Ile)_6$-b-$(Lys)_4$ in PS-COOH

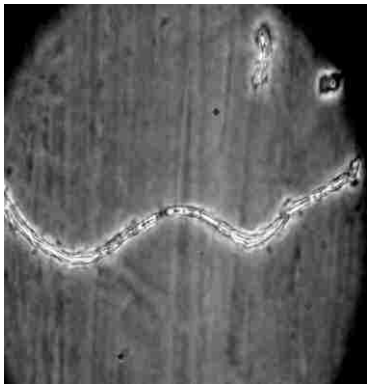

$(Ile)_{10}$-b-$(Lys)_{10}$ in bulk

$(Ile)_{10}$-b-$(Lys)_{10}$ in PS

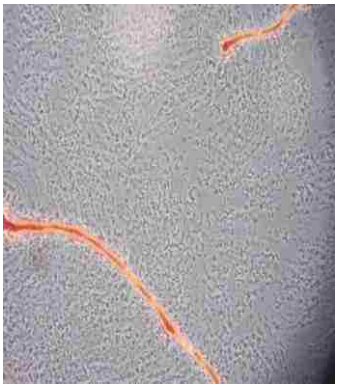

$(Ile)_{10}$-b-$(Lys)_{10}$ in PS

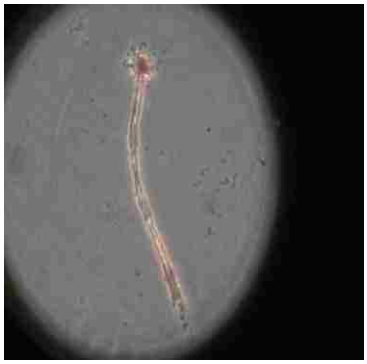

$(Ile)_{10}$-b-$(Lys)_{10}$ in PS

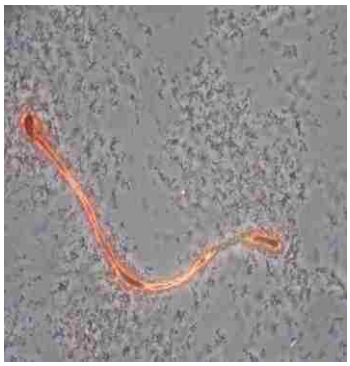

$(Ile)_{10}$-b-$(Lys)_{10}$ in PS-OH

$(Ile)_{10}$-b-$(Lys)_{10}$ in 80%/20%(PC/PS)

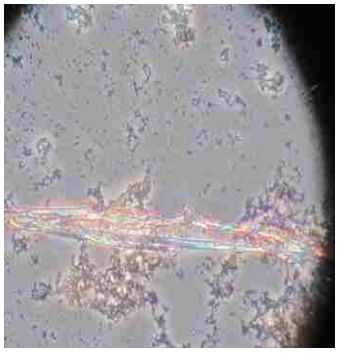

$(Ile)_{10}$-b-$(Lys)_{10}$ in 2:2:1:1C/PC/PG/PE

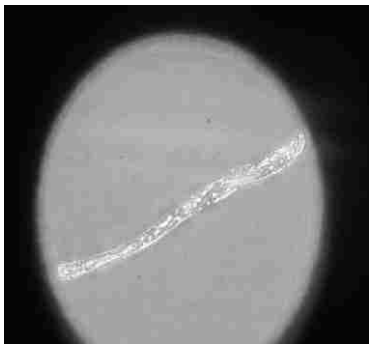

$(Ile)_5$-b-$(Lys)_5$ in bulk

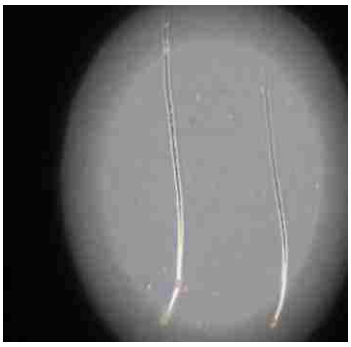

$(Ile)_5$-b-$(Lys)_5$ in PS

$(Ile)_5$-b-$(Lys)_5$ in PS-OH

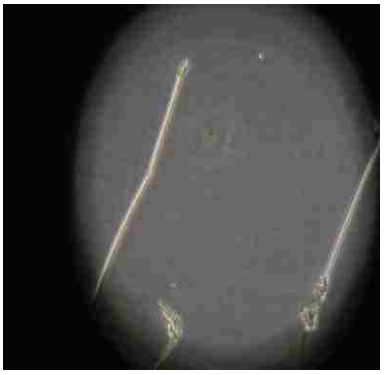

$(Ile)_5$-b-$(Lys)_5$ in bulk

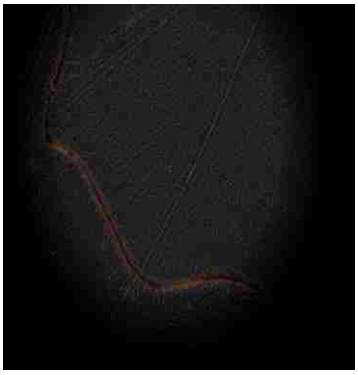

$(Ile)_5$-b-$(Lys)_5$ in 80%/20%(PC/C)

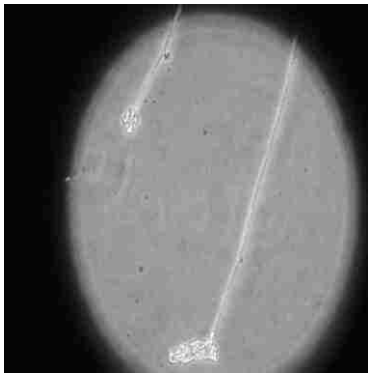

$(Ile)_5$-b-$(Lys)_5$ in 80%/20%(PC/C)

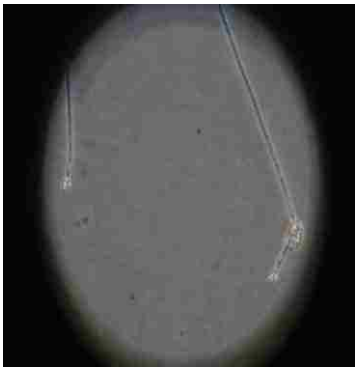

$(Ile)_7$-b-$(Lys)_3$ in bulk

$(Ile)_7$-b-$(Lys)_3$ in PS

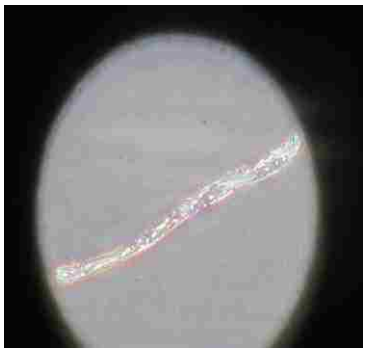

$(Ile)_7$-b-$(Lys)_3$ in PS

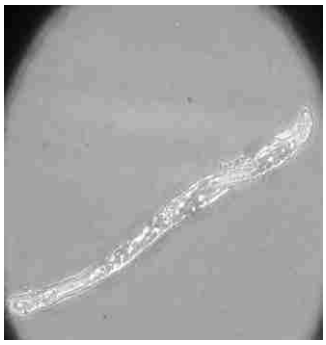

$(Ile)_7$-b-$(Lys)_3$ in 80%/20%(PC/C)

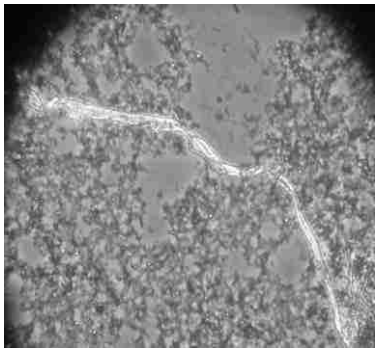

$(Ile)_7$-b-$(Lys)_3$ in 80%/20%(PC/C)

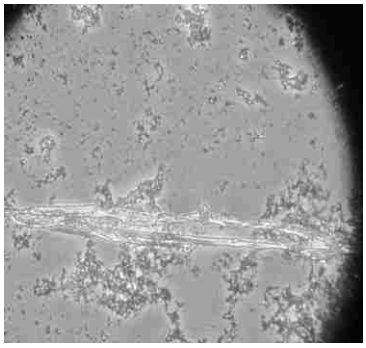

$(Ile)_7$-b-$(Lys)_3$ in PS-COOH

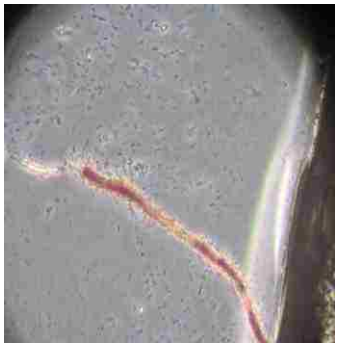

$(Ile)_7$-b-$(Lys)_3$ in PS-COOH

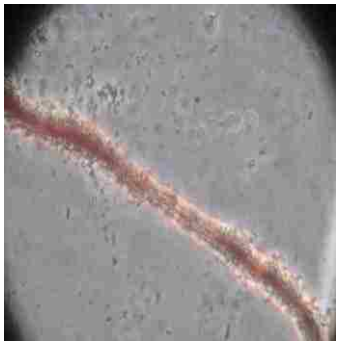

$(Ile)_7$-b-$(Lys)_3$ in bulk

$(Ile)_7$-b-$(Lys)_3$ in PS

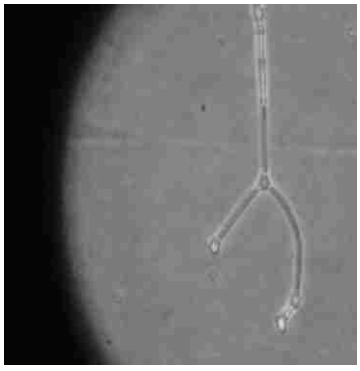

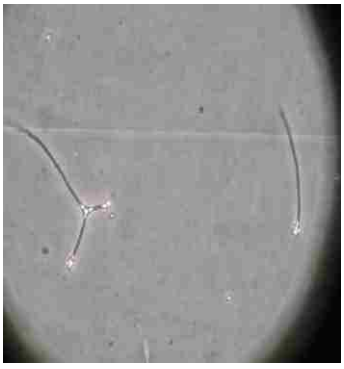

$(Ile)_7$-b-$(Lys)_3$ in bulk

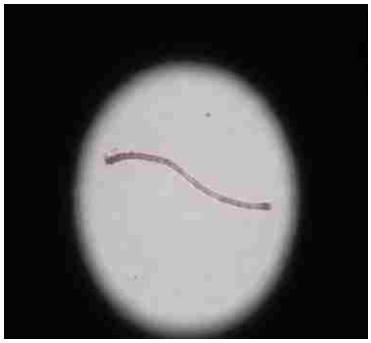

$(Ile)_7$-b-$(Lys)_3$ in PS-OH

$(Ile)_7$-b-$(Lys)_3$ in 80%/20%(C/PS)

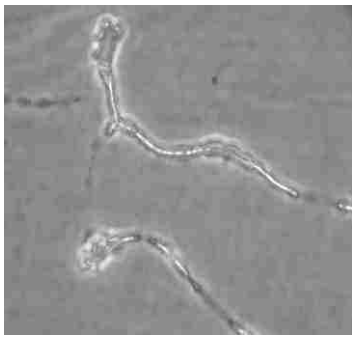

$(Ile)_7$-b-$(Lys)_3$ in 80%/20%(C/PS)

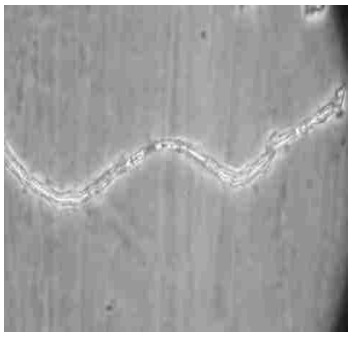

$(Ile)_7$-b-$(Lys)_3$ in PS-NH_2

$(Ile)_7$-b-$(Lys)_3$ in PS-NH_2

$(Ile)_7$-b-$(Lys)_3$ in PS-NH_2

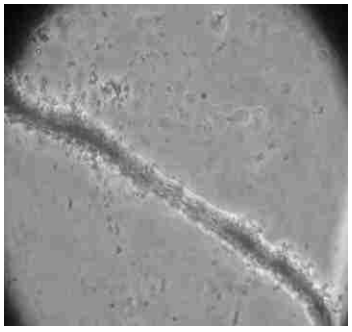

$(Ile)_7$-b-$(Lys)_3$ in bulk dried on slide

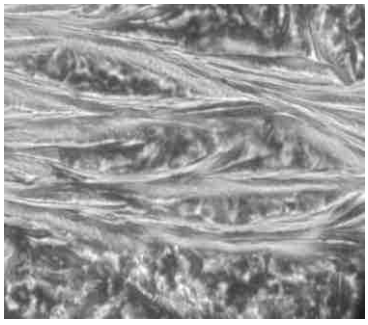

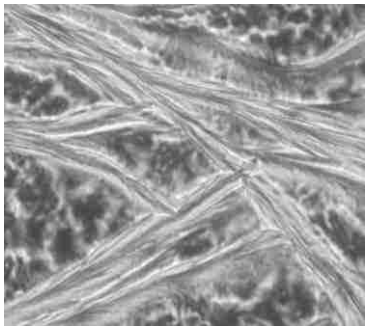

$(Ile)_7$-b-$(Lys)_3$ in bulk dried on slide

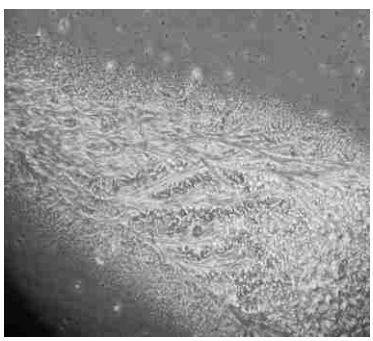
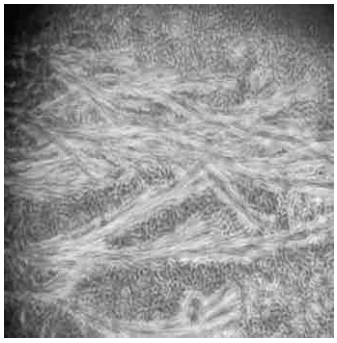
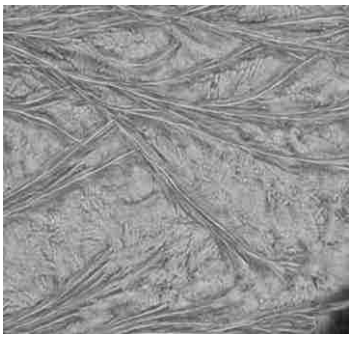

$(Ile)_8$-b-$(Lys)_{12}$ in bulk

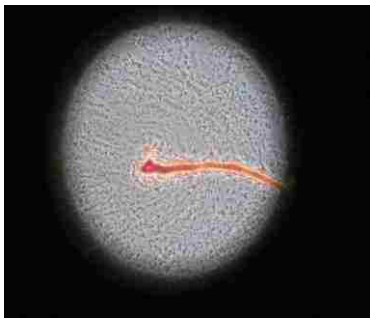

$(Ile)_8$-b-$(Lys)_{12}$ in 80%/20%(PC/C)

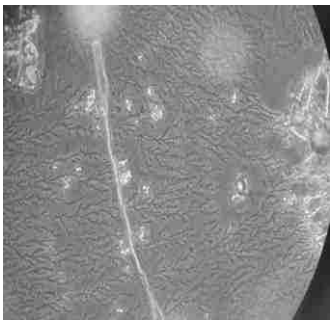

$(Ile)_8$-b-$(Lys)_{12}$in 80%/20%(PC/C)

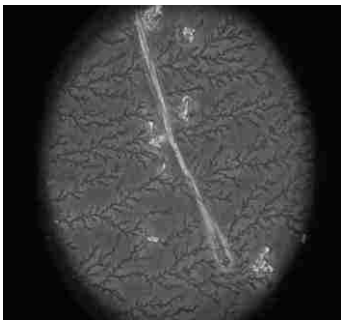

$(Ile)_8$-b-$(Lys)_{12}$ in bulk

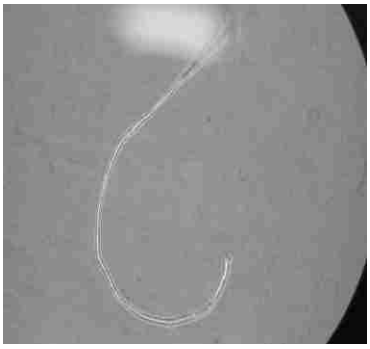

$(Ile)_8$-b-$(Lys)_{12}$ in 10:5:7.5:16PC/PE/PS/C

$(Ile)_8$-b-$(Lys)_{12}$ in PS

APPENDIX D

DYNAMIC LIGHT SCATTERING RESULTS

Note: The abscise is in units of µs for all following plots.

Blanks

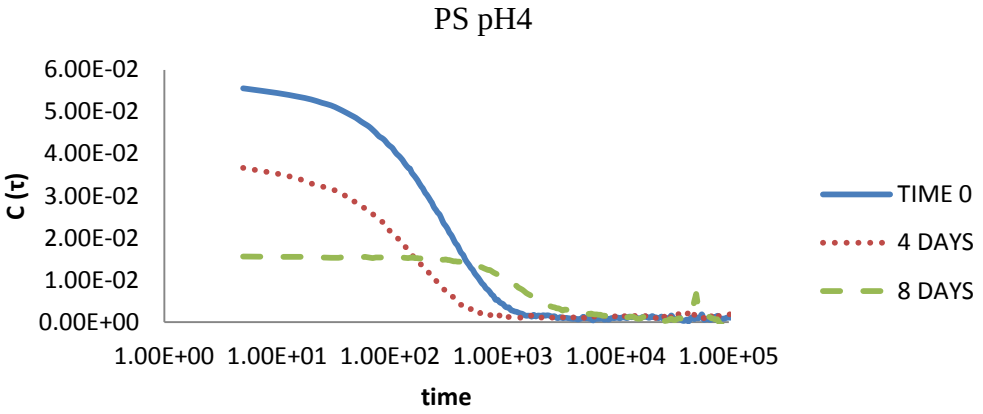

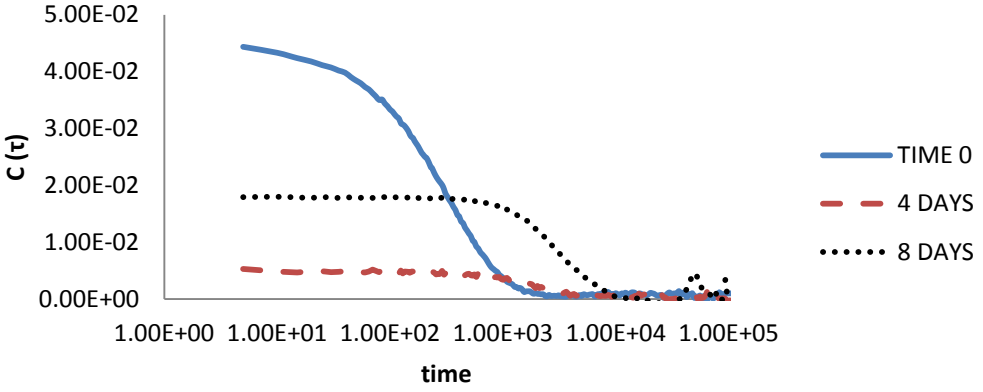

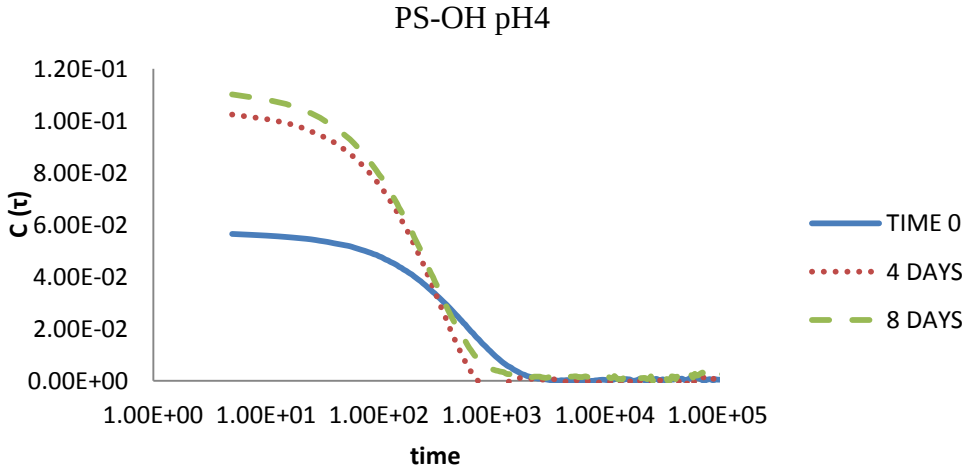

PS-OH pH 7

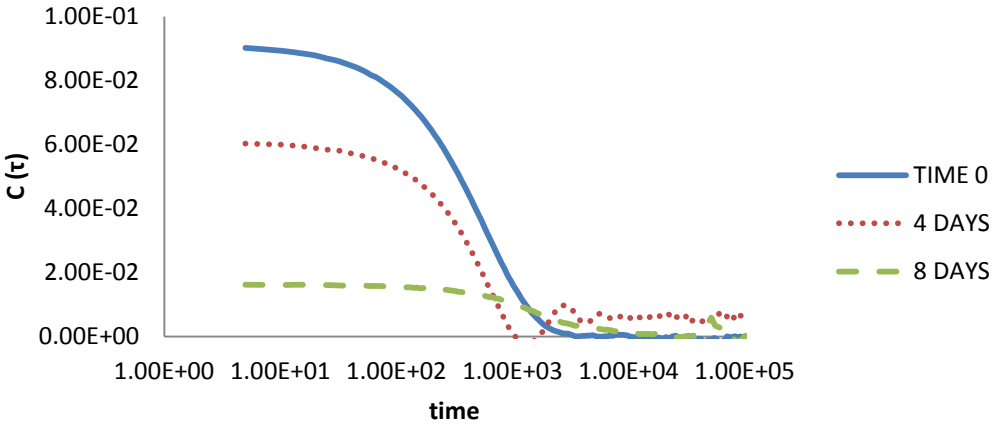

20%/80% (PC)/Cholesterol

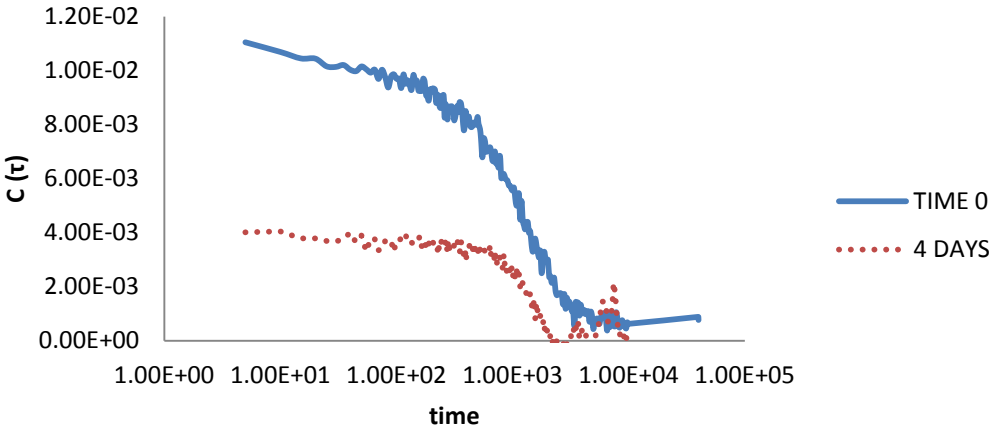

80%/20% PC /Cholesterol pH 7

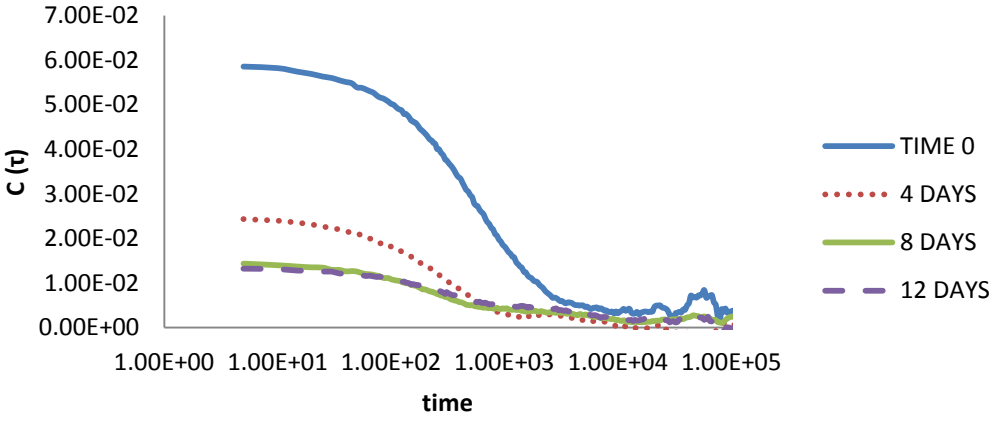

10/5/7.5/16 PC/PE/ PS/Cholesterol pH 7

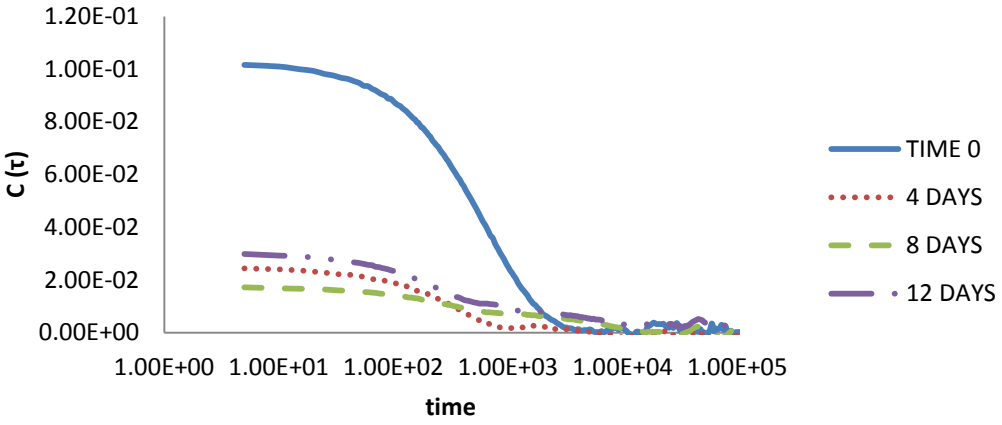

10/5/7.5/16 PC/PE/PS/Cholesterol pH4

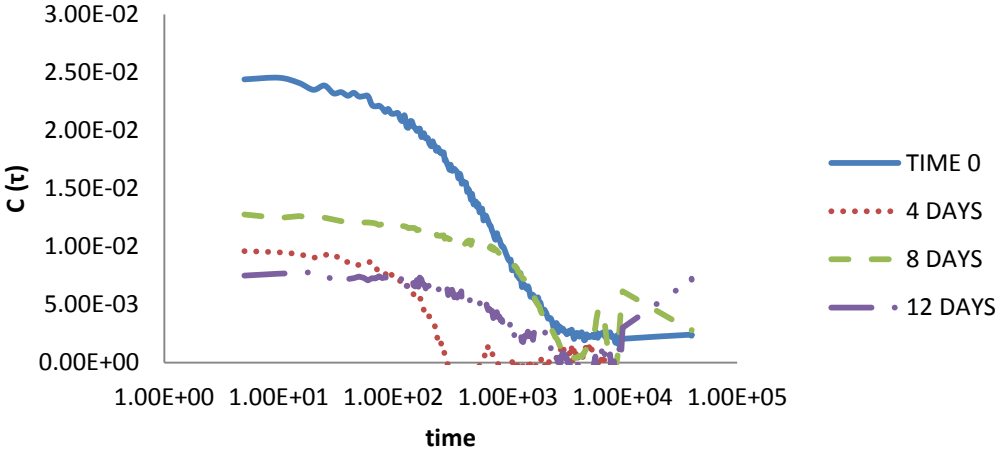

PS-COOH pH4

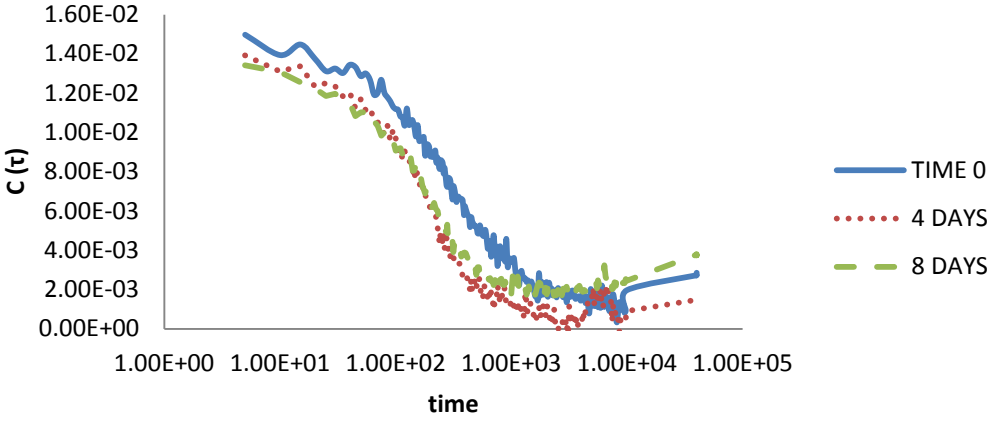

PS-COOH pH7

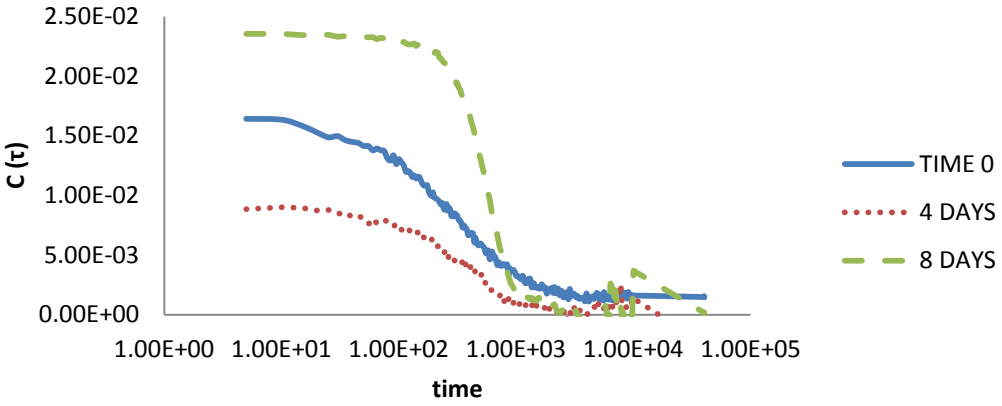

PS-NH_2 pH 7

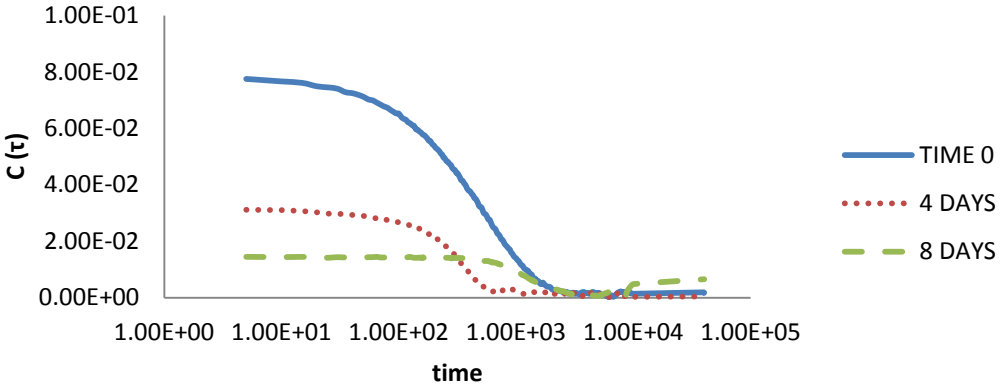

80%/20% PC /PS pH 7

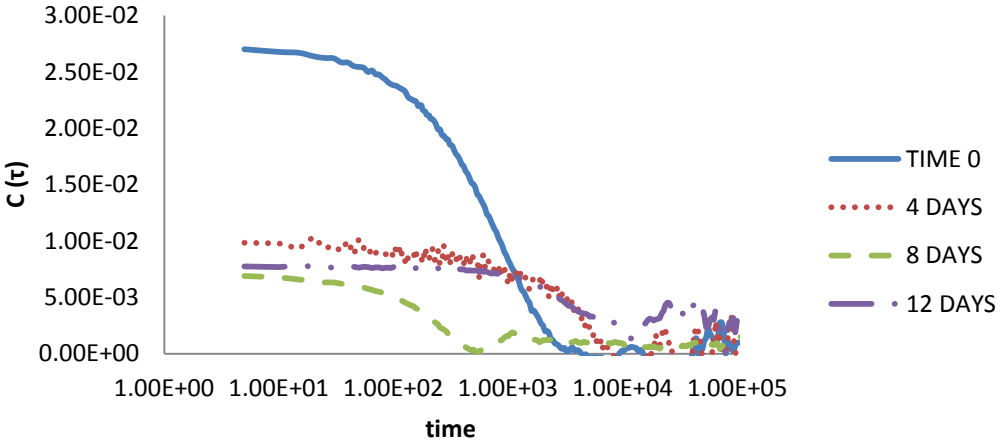

80%/20% PC /PS pH 4

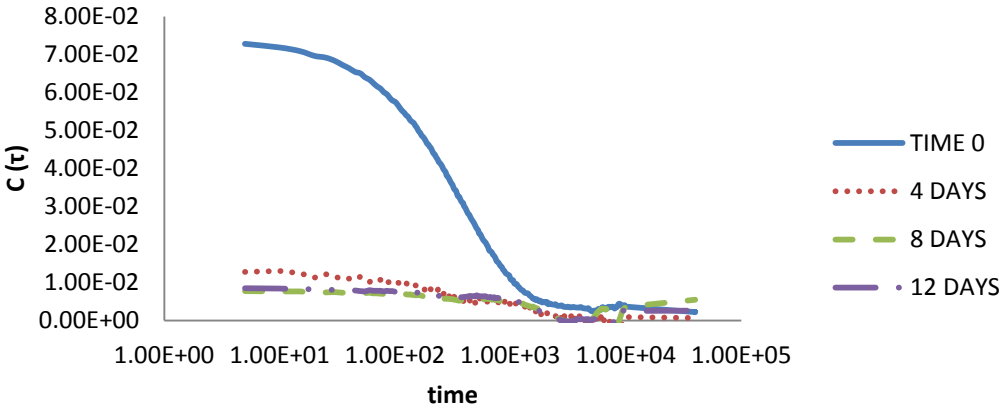

2:2:1:1 Cholesterol/PC/PG/PE
pH 7

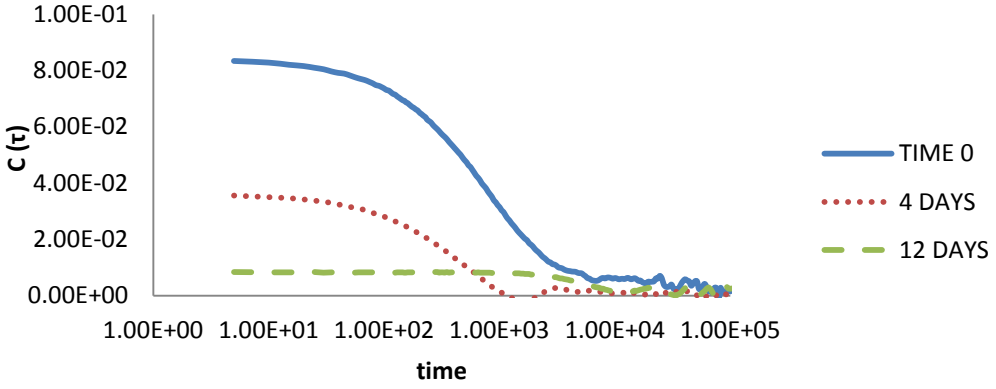

2:2:1:1 Cholesterol/PC/PG/PE
pH 4

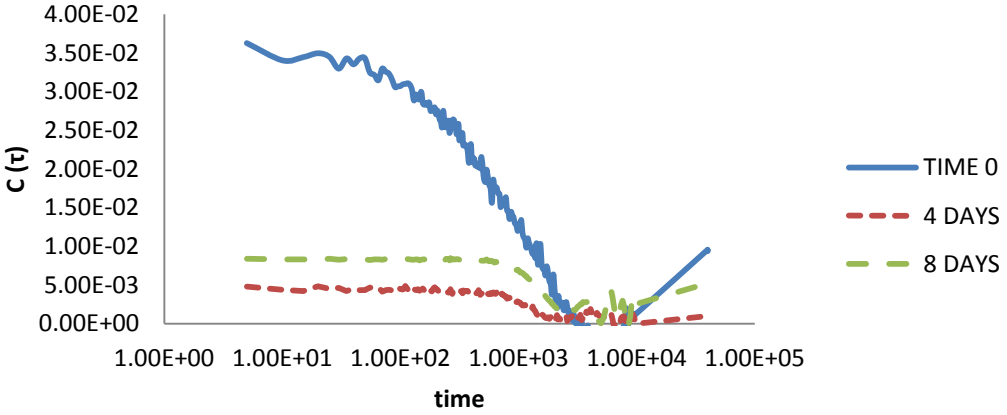

$(Lys)_{10}$-b-$(Ile)_{10}$

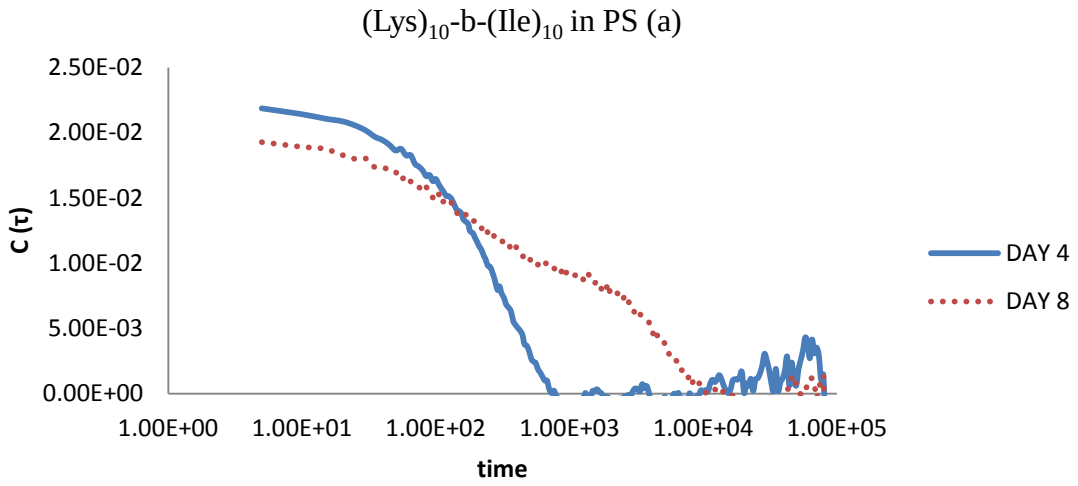

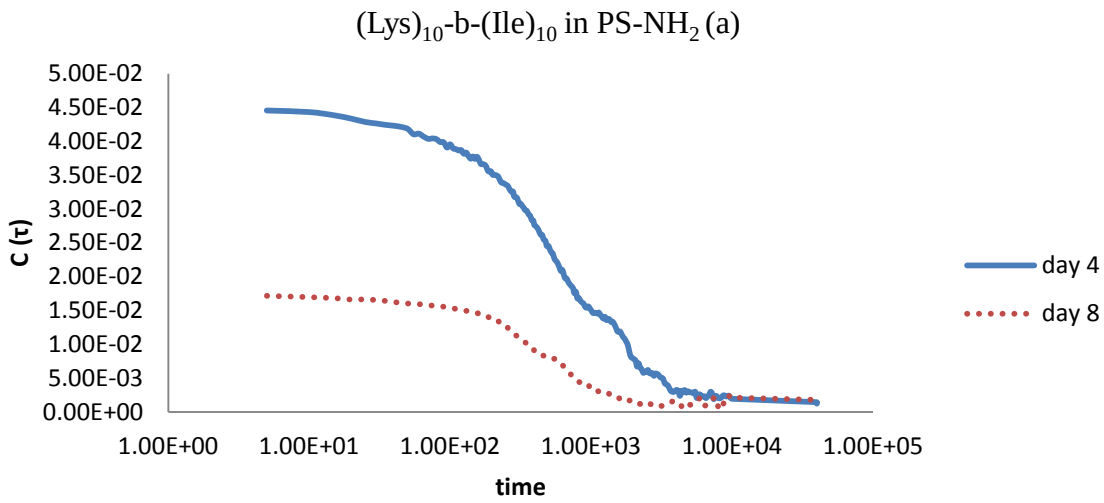

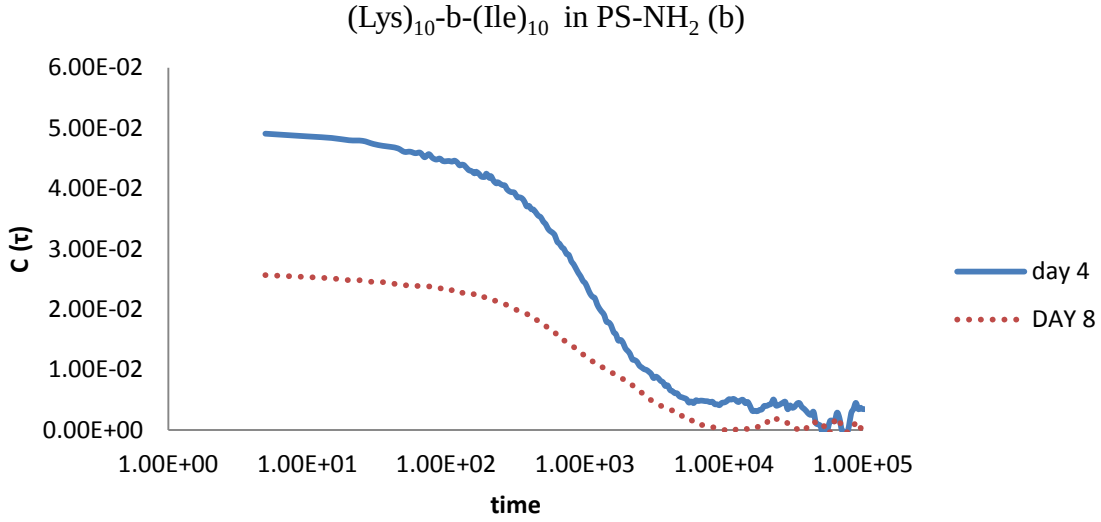

$(Lys)_{10}$-b-$(Ile)_{10}$ in PS-OH (a)

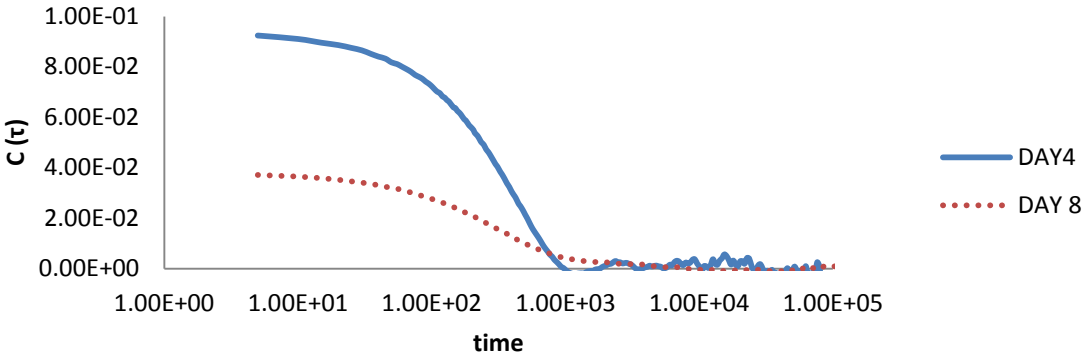

$(Lys)_{10}$-b-$(Ile)_{10}$ in PS-OH (b)

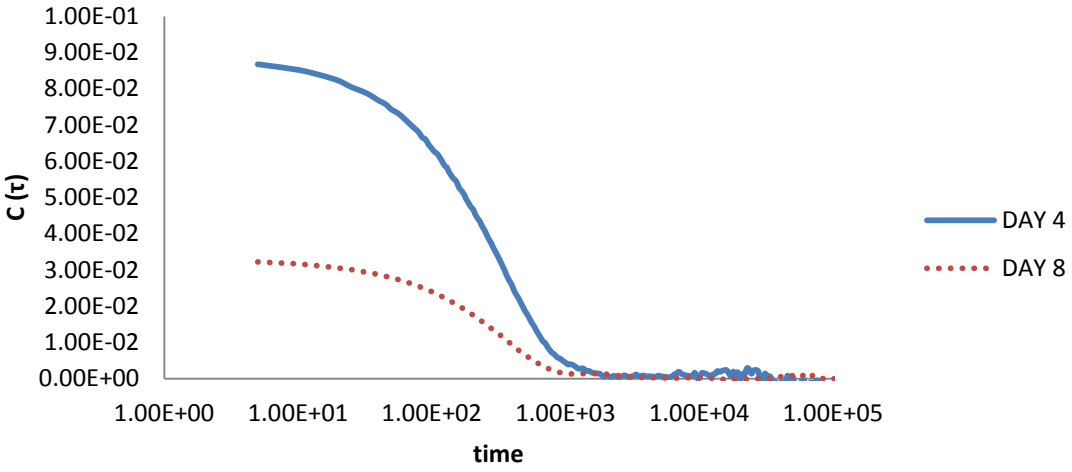

$(Lys)_{10}$-b-$(Ile)_{10}$ in PS (b)

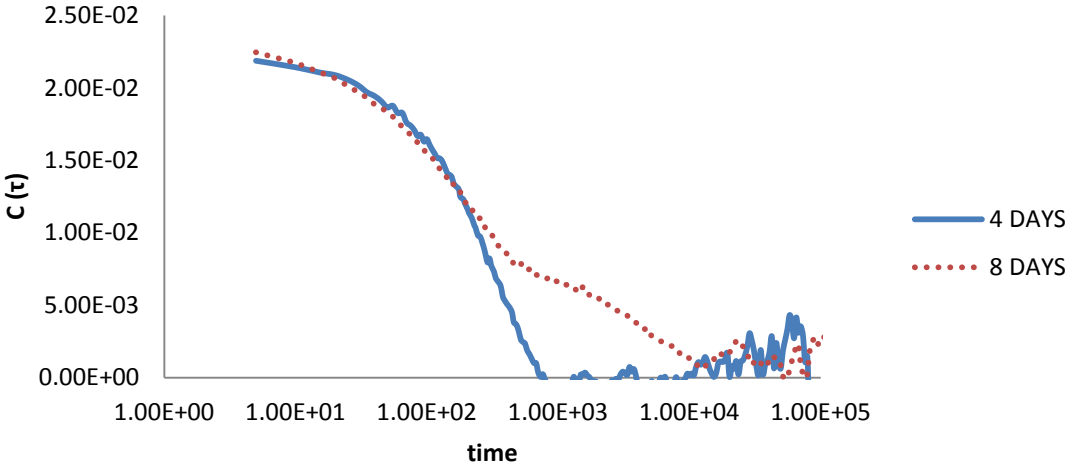

$(Lys)_{10}$-b-$(Ile)_{10}$ in 20%/80% (PC)/Cholesterol

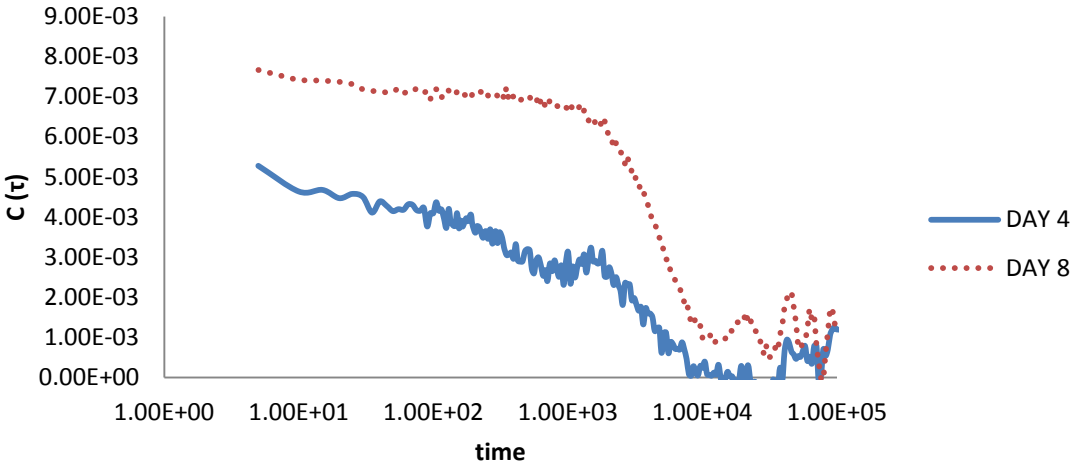

$(Lys)_{10}$-b-$(Ile)_{10}$ in 2:2:1:1 Cholesterol/PC/PG/PE

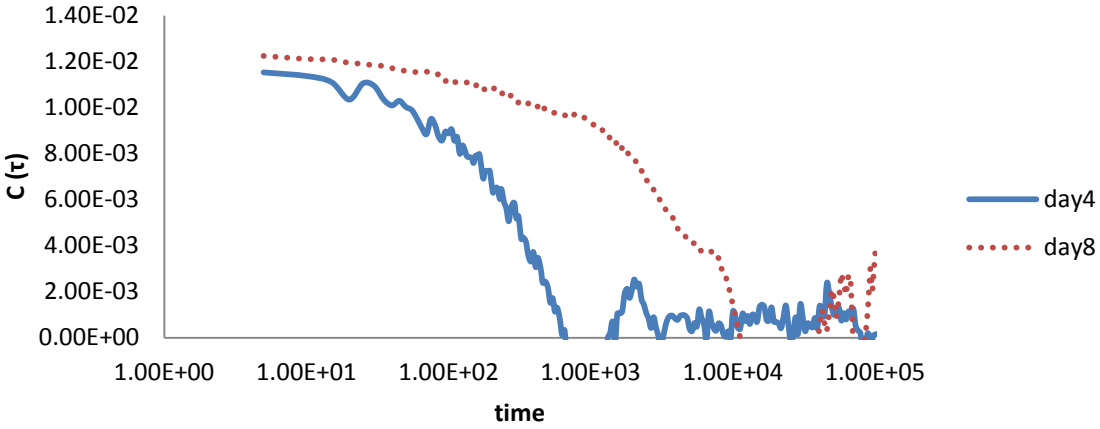

$(Lys)_{10}$-b-$(Ile)_{10}$ in 10/5/7.5/16 PC/PE/PS/Cholesterol

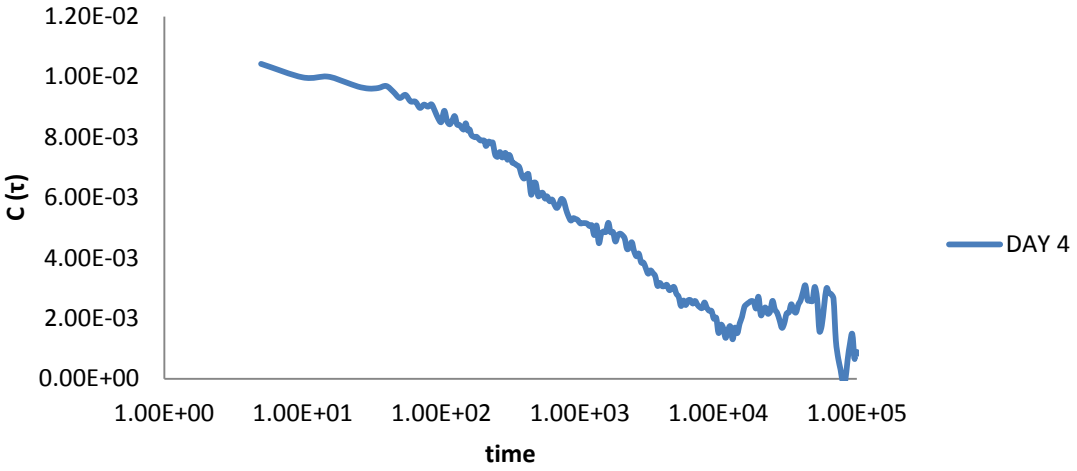

$(Ile)_5$-b-$(Lys)_5$

$(Ile)_5$-b-$(Lys)_5$ in PS

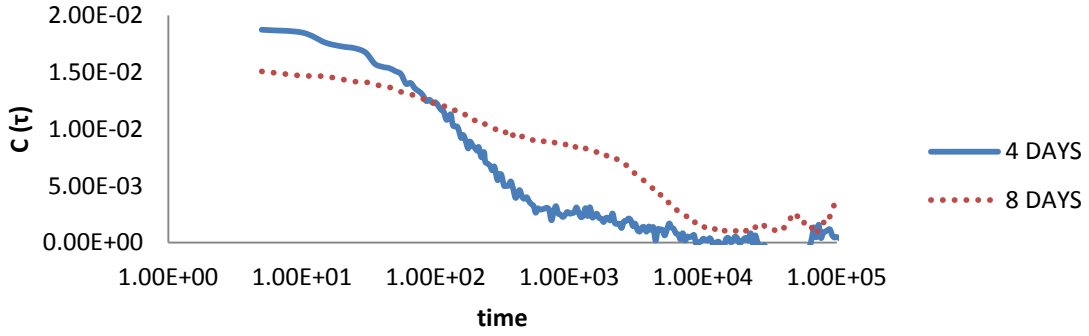

$(Ile)_5$-b-$(Lys)_5$ in 20%/80% (PC)/Cholesterol

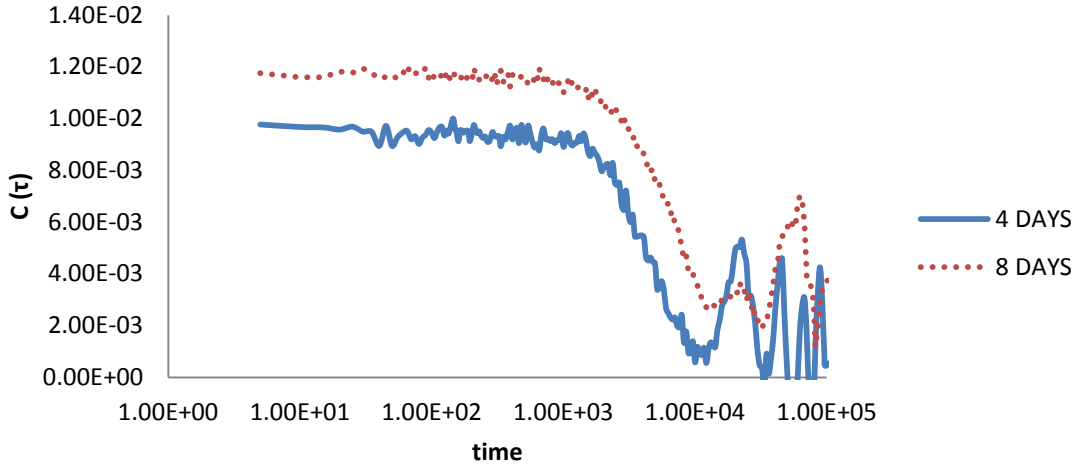

$(Ile)_5$-b-$(Lys)_5$ in bulk

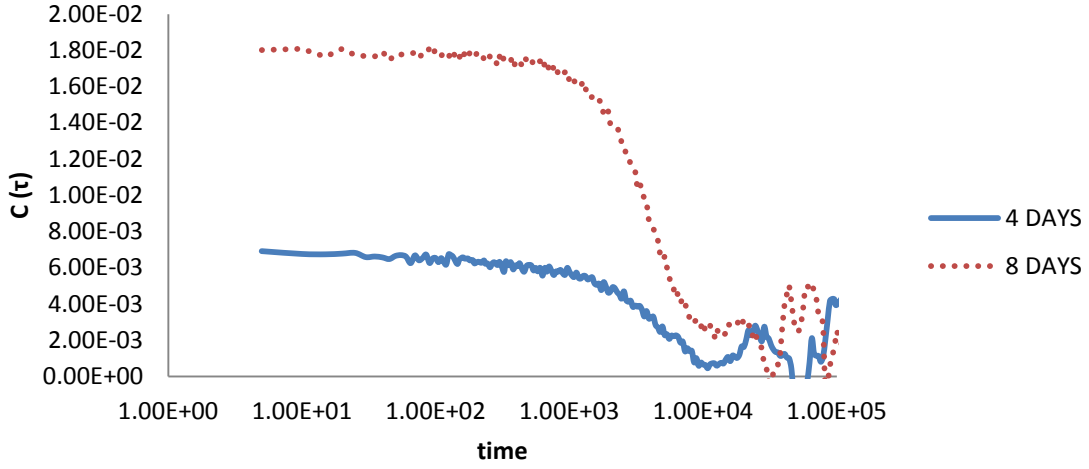

$(Ile)_5$-b-$(Lys)_5$ in 2:2:1:1 Cholesterol/PC/PG/PE

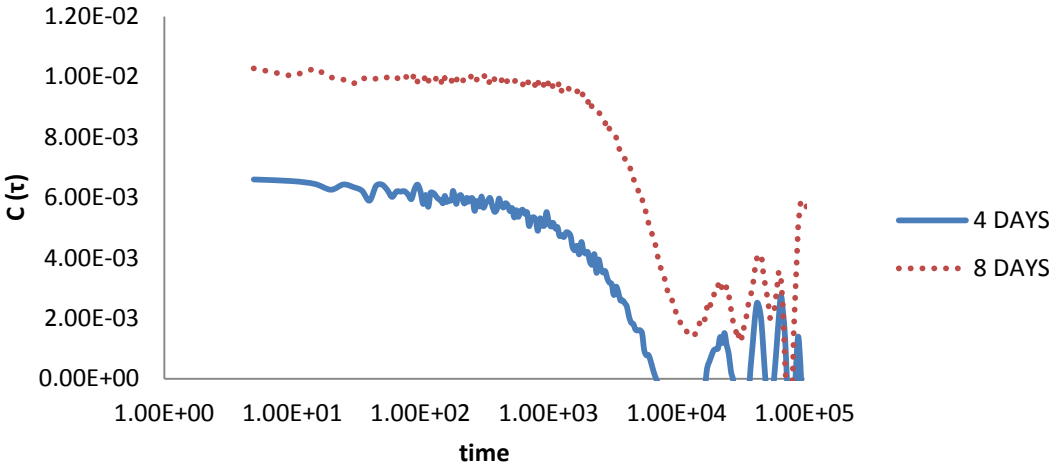

$(Ile)_5$-b-$(Lys)_5$ in 10/5/7.5/16 PC/PE/PS/Cholesterol

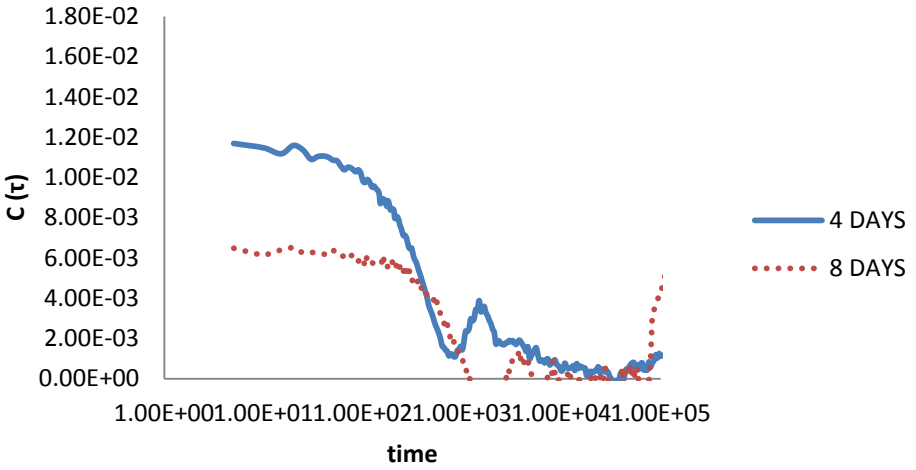

$(Ile)_6$-b-$(Lys)_4$

$(Ile)_6$-b-$(Lys)_4$ in PS

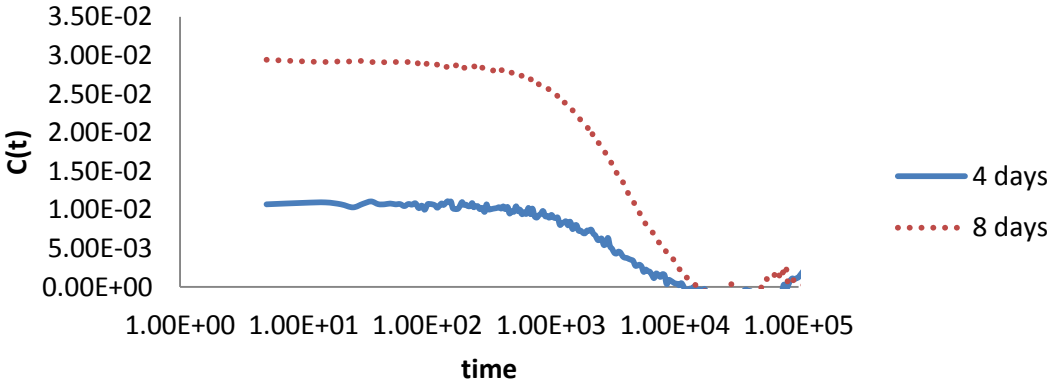

$(Ile)_6$-b-$(Lys)_4$ in PS-COOH (a)

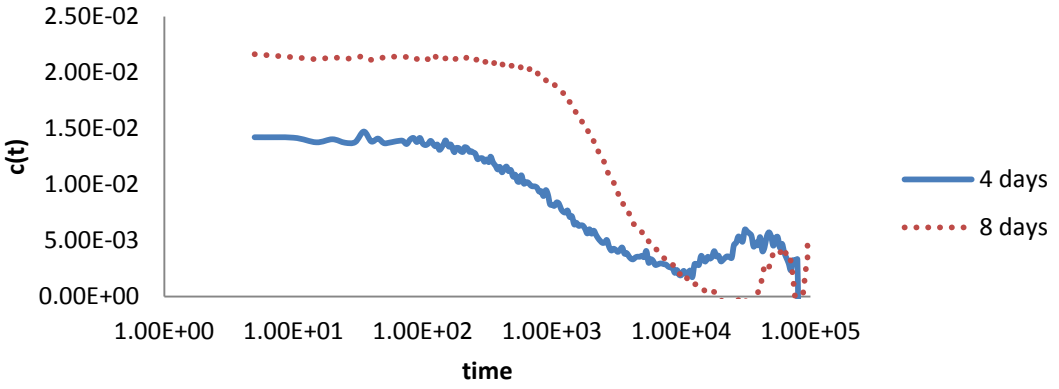

$(Ile)_6$-b-$(Lys)_4$ in 80%/20% PC /PS

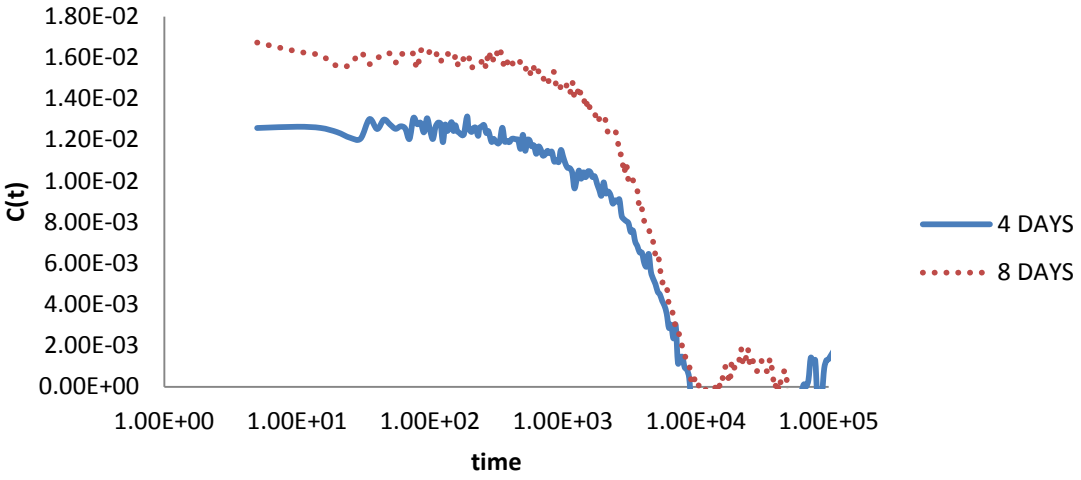

$(Ile)_6$-b-$(Lys)_4$ in 20%/80% (PC)/Cholesterol

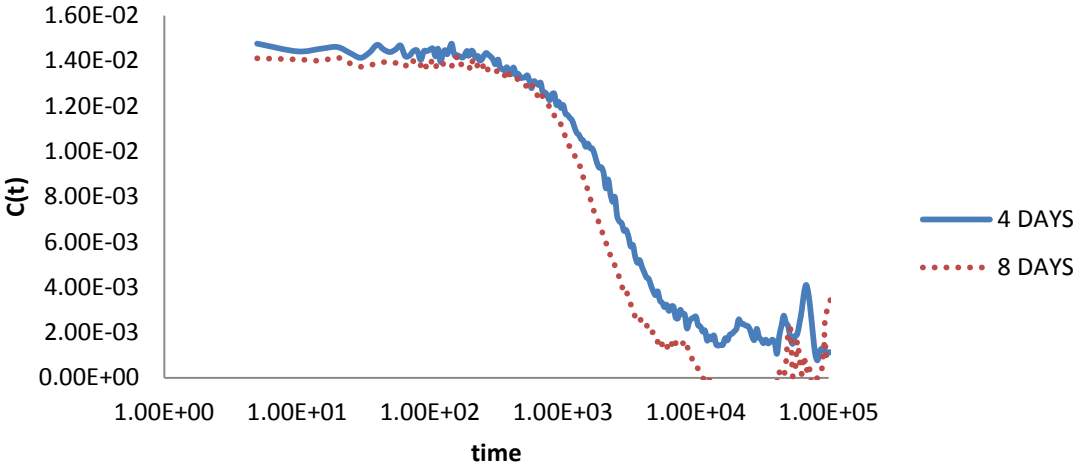

$(Ile)_6$-b-$(Lys)_4$ in PS-NH_2

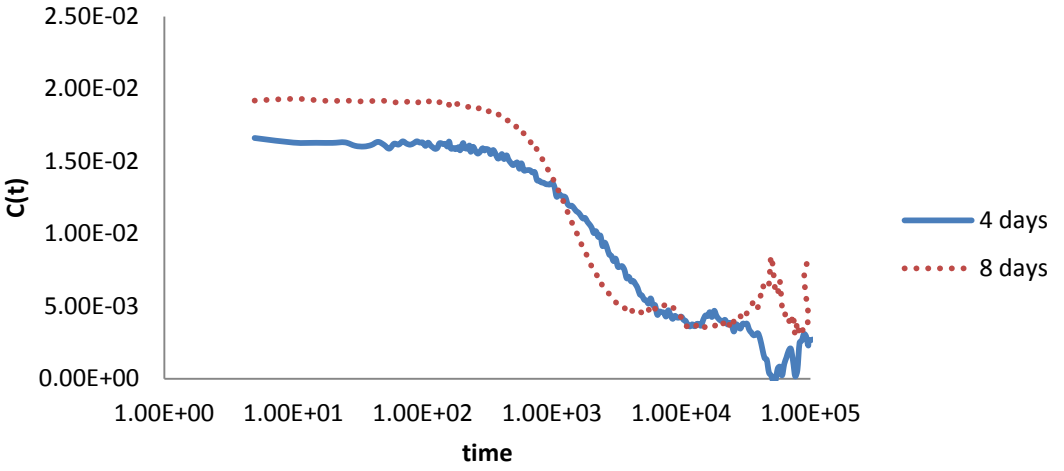

$(Ile)_6$-b-$(Lys)_4$ in PS-OH (a)

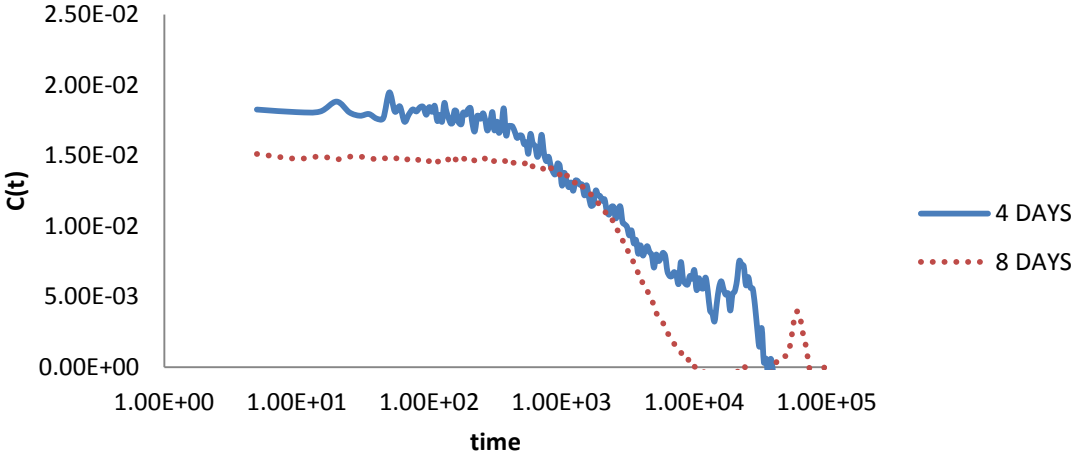

$(Ile)_6$-b-$(Lys)_4$ in 80%/20% PC /Cholesterol (a)

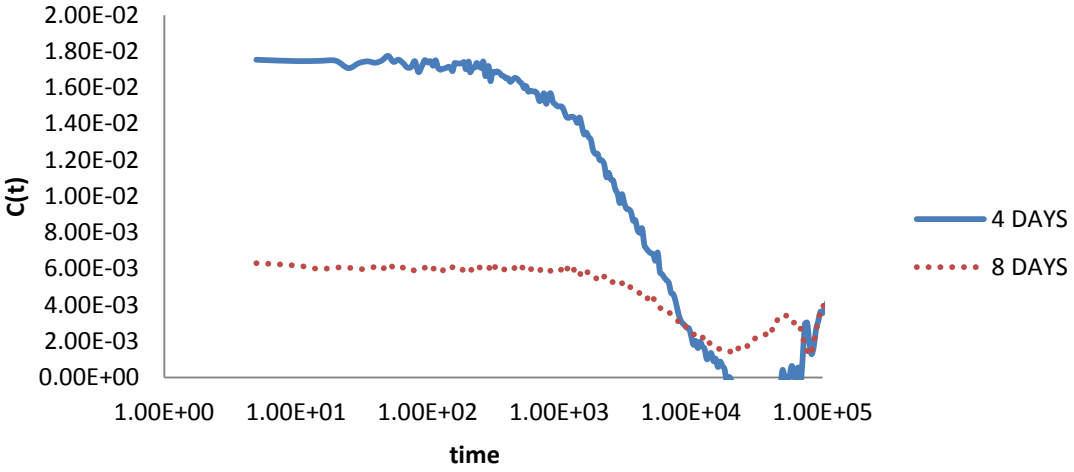

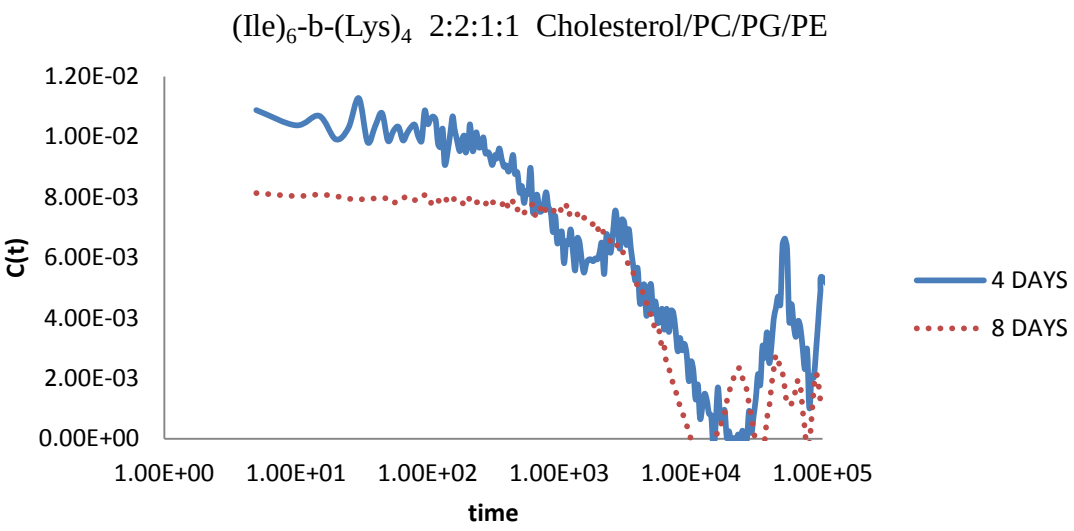
(Ile)6-b-(Lys)4 2:2:1:1 Cholesterol/PC/PG/PE
1.20E-02
1.00E-02
8.00E-03
6.00E-03
4.00E-03
2.00E-03
0.00E+00
C(t)
1.00E+00
1.00E+01
1.00E+02
1.00E+03
1.00E+04
1.00E+05
time
4 DAYS
8 DAYS

BIBLIOGRAPHY

1. Banerjee, A., Maji, S. K., Drew, M. G. B., Haldar, D., Das, A. K. and Banerjee, A. 2004. Hydrogen-bonded dimer can mediate supramolecular β-sheet formation and subsequent amyloid-like fibril formation: a model study. Tetrahedron, 60(28), 5935-5944.

2. Blake, C. C. F., Serpell, L. C., Sunde, M., Sandgren, O. and Lundgren, E. A. 1996. Molecular model of the amyloid fibril. Ciba Foundation Symposium, 199(Nature and Origin of Amyloid Fibrils), 6-12.

3. Blake, C. and Serpell, L. 1996. Synchrotron X-ray studies suggest that the core of the transthyretin amyloid fibril is a continuous β-sheet helix. Structure (London), 4(8), 989-998.

4. Blondelle, S.E., Forood, B., Houghten, R.A. and Perez-Paya, E. 1997. Polyalanine-based peptides as models for self-associated β-sheet complexes. Biochemistry, 36, 8393-8400.

5. Chiti, F, and Dobson C.M. 2006. Protein misfolding, functional amyloid and human disease. Annual Review in Biochemistry, 75, 333-366.

6. Come, J. H., Fraser, P. E. and Lansbury, P.T., Jr. 1993. A kinetic model for amyloid formation in the prion diseases: Importance of seeding. Proceedings of the National Academy of Sciences of the United States of America, 90(13), 5959-63.

7. Dentchev, T., Milam, A.H., Lee, V. M.-Y., Trojanowski, J. Q. and Dunaief, J. L. 2003. Amyloid-β is found in drusen from some age-related macular degeneration retinas, but not in drusen from normal retinas. Molecular Vision, 9, 184-190.

8. Deuther-Conrad, W., Loske, C., Schinzel, R., Dringen, R., Riederer, P. and Munch, G. 2001. Advanced glycation end products change glutathione redox status in SH-SY5Y human neuroblastoma cells by a hydrogen peroxide dependent mechanism. Neuroscience Letters, 312(1), 29-32.

9. Fandrich, M. and Dobson, C. M. 2002. The behavior of polyamino acids reveals an inverse side chain effect in amyloid structure formation. The EMBO Journal, l.21, 5682-5690.

10. Giacomelli, C.E. and Norde, W. 2003. Influence of hydrophobic Teflon particles on the structure of amyloid β-peptide. Biomacromolecules, 4, 1719-1726.

11. Giri K., Bhattacharyya N. P., and Basak S. 2007. pH-Dependent Self –Assembly of Polyalanine Peptides. Biophysical Journal, 92(1), 293-302.

12. Gorbenko, G.P. and Kinnunen P.K.J. 2006. The role of lipid–protein interactions in amyloid-type protein fibril formation, Chemistry and Physics of Lipids, 141(1-2), 72-82.

13. Hall, C.K. 2008. Thermodynamic and kinetic origins of Alzheimer's and related diseases: a chemical engineer's perspective, AIChE J., 54(8), 1956-1962.

14. Haywood, A.M. and Boyer, B.P. 1984. Effect of lipid composition upon fusion of liposomes with Sendai virus membranes. Biochemistry, 23 (18), 4161-4166.

15. Hong, Y., Legge R. L., Zhang S. and Chen P. 2003. Effect of amino acid and pH on nano fibril formation of self-assembling peptides. Biomacromolecules, 4(5), 1433-1442.

16. Inouye, H. and Kirschner, D. A. 1996. Refined fibril structures: the hydrophobic core in Alzheimer's amyloid β-protein and prion as revealed by X-ray diffraction. Ciba Foundation Symposium, 199(Nature and Origin of Amyloid Fibrils), 22-39.

17. Janek, K., Behlke, J., Zipper, J., Fabian, H., Georgalis, Y., Beyermann, M., Bienert, M. and Krause, E. 1999. Water-Soluble β-Sheet Models Which Self-Assemble into Fibrillar Structures. Biochemistry, 38(26), 8246-8252.

18. Klunk, W. E., Pettergrew, J. W. and Abraham, D. J. 1989. Quantitative Evaluation of Congo red binding to Amyloid like Protein with β-Pleated Sheet Conformation. J. Histcohem. Cytochem. 37, 1273-1281.

19. Koga, T., Taguchi, K., Kobuke, Y., Kinoshita, T. and Higuchi, M. 2003. Structural regulation of a peptide-conjugated graft copolymer: A simple model for amyloid formation. Chemistry -A European Journal, 9(5), 1146-1156.

20. Kong, J. and Yu, S. 2007. Fourier Transform Infrared Spectroscopic Analysis of Protein Secondary Structures, Acta Biochemica et Biophisica Sinica 39(8), 549-559.

21. Kortemme, T., Ramirez-Alvarado, M. and Serrano, L. 1998. Design of a 20-amino acid, three-stranded β-sheet protein. Science, 281(5374), 253-256.

22. Krebs, M. R. H., MacPhee, C. E., Miller, A. F., Dunlop, I. E., Dobson, C. M. and Donald, A. M. 2004. The formation of spherulites by amyloid fibrils of bovine insulin, Journal of Biophysics, 101(40), 14420–14424.

23. Lashuel, H. A., LaBrenz, S. R., Woo L., Serpell, L. C. and Kelly, J. W. 2000. Protofilaments, filaments, ribbons, and fibrils from peptidomimetic self-assembly: implications for amyloid fibril formation and materials science. Journal of the American Chemical Society, 122(22), 5262-5277.

24. Li, C. and Deng, Y. 2004. A novel method for the preparation of liposomes: Freeze drying of monophase solutions. Journal of Pharmaceutical Sciences, 93 (6) 1403-14.

25. Lienkamp, K., Kumar, K., Som, A., Nusslein, K. and Tew, G. N. 2009. Doubly selective anti-microbial polymers: how do they differentiate between Bacteria? Chemistry -A European Journal, 15(43), 11710-4.

26. Loske, C., Gerdemann, A., Schepl, W., Wycislo, M., Schinzel, R., Palm, D. and Riederer, P. 2000. Munch, G. Transition metal-mediated glycoxidation accelerates cross-linking of β-amyloid peptide. European Journal of Biochemistry, 267(13), 4171-4178.

27. MacRaild, C. A., Stewart, C. R., Mok, Y.-F., Gunzburg, M. J., Perugini, M.A., Lawrence, L.J., Tirtaatmadja, V., Cooper-White, J. J. and Howlett, G.J. 2004. Non-fibrillar Components of Amyloid Deposits Mediate the Self-association and Tangling of Amyloid Fibrils. Journal of Biological Chemistry, 279(20), 21038-21045.

28. Mahler, H.C., Friess, W., Grauschopf, U. and Kiese, S. 2008. Protein Aggregation: Pathways Induction Factors and Analysis, Journal of Pharmaceutical Sciences, 98, 9, 2909-2934.

29. Moores, B., Drolle, E., Attwood S.J., Simons, J. and Leonenko, Z. 2011. Effect of Surfaces on Amyloid Fibril Formation. Department of Biology, University of Waterloo, Waterloo, Ontario, Canada, 6(10), e25954.

30. Muench, G., Gasic-Milenkovic, J. and Arendt, T. 2003a. Effect of advanced glycation endproducts on cell cycle and their relevance for Alzheimer's disease. Advances in Research on Neurodegeneration , 10, 63-71.

31. Muench, G., Apelt, J., Kientsch-Engel, R., Stahl, P., Lueth, H. J.and Schliebs, R. 2003b. Advanced glycation end products and pro-inflammatory cytokines in transgenic Tg2576 mice with amyloid plaque pathology. Journal of Neurochemistry, 86(2), 283-289.

32. Mulder, C., Scheltens, P., Visser, J. J., Van Kamp, G.J. and Schutgens, R. B. H. 2000. Genetic and biochemical markers for Alzheimer's disease. Recent developments. Annals of Clinical Biochemistry, 37(5), 593-607.

33. Munch, G., Cunningham, A.M., Riederer, P., Braak, E. 1998. Advanced glycation end products are associated with Hirano bodies in Alzheimer's disease. Brain Research, 796(1-2), 307-310.

34. Nilsson, M. R. 2004. Techniques to study amyloid fibril formation in vitro. Methods, 34(1), 151-160.

35. Ruschak, A. and Miranker, A.D. 2007. Fibril-dependent amyloid formation as catalysis of an existing reaction pathway. Proceedings of the National Academy of Sciences of the United States of America, 104 (30) 12341-12346.

36. Som, A., Nusslein, K. and Tew, G. N. 2007. Influence of lipid composition on membrane activity of antimicrobial phenylene ethynylene, Journal. Phys. Chem., 3495-3502.

37. Sousa, M. M. and Saraiva, M. J. 2003. Neurodegeneration in familial amyloid polyneuropathy: from pathology to molecular signaling. Progress in Neurobiology (Amsterdam, Netherlands), 71(5), 385-400.

38. Sunde, M., and Blake, C. 1997. The structure of amyloid fibrils by electron microscopy and X-ray diffraction. Advances in Protein Chemistry, 50 (Protein Misassembly), 123-159, 2 plates.

39. Sunde, M., Serpell, L.C., Bartlam, M., Fraser, P.E., Pepys, M. B. and Blake, C. C. F. 1997. Common core structure of amyloid fibrils by synchrotron X-ray diffraction. Journal of Molecular Biology, 273(3), 729-739.

40. Symmons, M. F., Buchanan, S. G. St. C.; Clarke, D. T., Jones, G. and Gay, N. J. 1997. X-ray diffraction and far-UV CD studies of filaments formed by a leucine-rich repeat peptide: structural similarity to the amyloid fibrils of prions and Alzheimer's disease β-protein. FEBS Letters, 412(2), 397-403.

41. Tartablia, G.G., A. Cavalli, R. Pellarin and A. Caflisch. 2005. Prediction of aggregation rate and aggregation-prone segments in polypeptide sequences. Protein Science, 14, 2723-2734.

42. Tjernberg, L.O., Callaway, D.J., Tjernberg, A., Hahne, S., Lilliehook, C., Terenius, L., Thyberg, J. and Nordstedt. C. 1999. A molecular Model of Alzeimer amyloid β–peptide fibril formation. Journal of Biological Chemistry, 274 (18) 12619-12625.

VITA

Kunal Mukesh Naik was born in Mumbai, India. He graduated with a Bachelor of Chemical Engineering degree in June 2008 from University of Mumbai. He joined Missouri S&T in the fall of 2009 for his Master`s degree in Chemical Engineering. His area of focus is peptide synthesis and interaction of peptides with solid/ liquid surfaces. He received his M.S. degree in Chemical Engineering in May 2012.